How to Reach Us

We welcome letters to the editor; but, we reserve the right to edit for space, style, and clarity.
Include address and daytime phone number with your correspondence.
E-mail: sudhir.dixit@gmail.com

If you would like to submit an article, please visit our submission portal for details:
https://wireless-magazine.com/index.php/WWRT/about/submissions

Official Magazine of the
WIRELESS WORLD RESEARCH FORUM

2025 | Vol 2 | Issue 2
WWRT
Wireless World Research and Trends Magazine

EDITORIALS

EXPERTS COLUMN

PEER REVIEW ARTICLES

NEWS AND INFORMATION

River Publishers
Broagervej 10, 9260 Gistrup, Denmark
www.riverpublishers.com

From the Desk of the Editor-in-Chief

Dr Sudhir Dixit
Editor-in-Chief

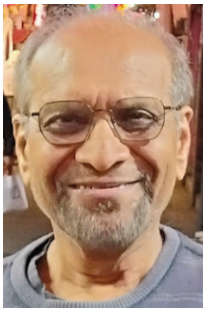

Welcome to the second issue of *Wireless World Research and Trends (WWRT)* magazine in 2025, and the fourth issue since the magazine's launch last year. WWRT has attracted significant interest from the research community, with several articles being accessed hundreds of times – thank you for your continued support. This issue features seven engaging articles covering some of the most active and impactful topics in the communications field. In addition, our lead Op-Ed article is authored by Prof. Gerhard Fetweiss, who shares insightful perspectives on 6G calling for pragmatism in its development.

The first article, by Avarino *et al.*, presents a comprehensive comparative study of two widely used channel modeling standards: 3GPP TR 38.901 and ITU-R M.2412. The authors analyze how these models predict real-world radio channel performance and demonstrate that, despite their widespread adoption, they exhibit notable technical differences – particularly in sub-6 GHz bands and millimeter-wave indoor scenarios. To the best of our knowledge, this is the first study of its kind.

In the second article, Hjalmarsson *et al.* address the challenge of integrating terrestrial and non-terrestrial networks to support in-flight broadband Internet access in 5G and beyond-5G (B5G) systems. The paper compares three architectural approaches: (i) a Distributed Unit/Centralized Unit (DU/CU) functional split with the DU located on the aircraft and the CU on the ground; (ii) an enhanced version of this split incorporating integrated access and backhaul to enable a flying ad-hoc network; and (iii) a novel architecture in which the aircraft functions as a mobile wireless access node, supported by backhaul nodes equipped with Mobile Edge Computing (MEC) capabilities to enable low-latency services and local breakout.

The third article focuses on reconfigurable intelligent surfaces (RIS), also known as intelligent reflecting surfaces (IRS), a key enabling technology for future wireless systems. In this contribution, Ramadevi *et al.* provide a broad overview of RIS technology and demonstrate that integrating RIS-assisted cooperative NOMA (C-NOMA) offers a transformative approach for 6G networks. Their analysis shows significant gains in spectral efficiency and signal reliability, along with reduced power consumption and extended network coverage.

With Unmanned Aerial Vehicles (UAVs) increasingly attracting public and industrial attention, reliable communication among UAVs and with ground control stations has become critically important. Accordingly, the fourth article, by Madhavi and Sahoo, presents an overview of UAV communication technologies, with a particular emphasis on multi-standard reconfigurable OFDM transceivers. These transceivers are shown to be highly efficient, reliable, and flexible, enabling robust communication even in challenging environments such as dense urban areas and long-distance links.

Addressing the urgent need to reduce road accidents, the fifth article by Mangroliya *et al.* proposes a proactive accident detection and prevention system based on Vehicular Ad-hoc Networks (VANETs) and Internet of Things (IoT) technologies. Unlike traditional reactive safety mechanisms such as airbags and ABS, the proposed solution relies on a smart onboard unit (OBU) capable of real-time communication with nearby vehicles and roadside units (RSUs). Using ultrasonic sensors and an Arduino-based microcontroller, the OBU detects potential collisions and broadcasts alerts via Dedicated Short-Range Communications (DSRC). The system supports both accident prevention and post-accident management through real-time vehicle-to-vehicle (V2V) and vehicle-to-infrastructure (V2I) communication, demonstrating reduced accident frequency and severity while improving traffic safety and response times.

In the sixth article, Maturi *et al.* focus on enhancing pedestrian safety at crosswalks through a vehicle-to-everything (V2X) communication framework operating in the 28 GHz band. The proposed approach enables collaborative communication between roadside infrastructure and pedestrians. The authors evaluate the performance of a linearly polarized antenna (LPA) array with and without the use of maximum ratio transmission (MRT), from the pedestrian's perspective. The results show that both techniques significantly improve signal reception for pedestrians near crosswalks.

The seventh and final article, by Altmayer *et al.*, introduces a machine-learning-based deep neural network (DNN) approach for predicting the performance of RIS-assisted systems in the low-frequency range. The authors demonstrate that DNN-based

models achieve superior estimation accuracy, particularly under complex channel conditions, and show strong potential for extension to millimeter-wave and terahertz frequency bands.

We hope you find the articles in this issue informative and inspiring. As always, your feedback and comments are most welcome.

Pragmatic 6G

Gerhard P. Fettweis,
Vodafone Chair Professor at TU Dresden, and Scientific Director & CEO at Barkhausen Institute (Dresden)

Cellular communication is the backbone of our digital society. Today's excitement around AI is a result of the whole planet having access to newest developments instantaneously via the mobile Internet. However, the cellular industry is currently not in a good shape. It therefore is time to wake-up and draw a picture of opportunities ahead that could make 6G a real game changer.

This paper is not about presenting math, or a technically detailed vision about technologies that might enter the 6G standard as e.g. [1]. It is about presenting a vision and roadmap towards a possibly amazing future of the cellular industry.

The Situation Room

Every generation of cellular communications has given us a chance to move ideas into reality, creating innovations that are the basis of our modern life. Now we are at the doorstep of defining 6G, which again poses the chance to write a new chapter of technology benefits for humankind.

However, the cellular world is in a mode of crisis, as can be seen by analyzing the stock charts of public companies involved. On a 20-year timeline, no operator and no equipment manufacturer is performing at the S&P 500 level, but all are well below. The market cap of publicly listed equipment manufacturers has even been trending negative in absolute numbers. As a generation of cellular technology has entered the market roughly every 10 years, this means that the industry has not overcome the Y2K bubble and remains in post-3G hangover. At the same time the world has become more and more dependent on the cellular infrastructure. We desperately need a new silver lining to revive the industry. Cellular is the backbone of our modern life.

5G was driven by three main needs:

1. Increasing bandwidth to address the traffic growth as seen during 4G
2. Reducing the latency, creating an ultra-reliable low-latency (URLLC) network slicing architecture, to address the "Tactile Internet" [2] requirements of motion control of real (robots) and virtual objects (XR)
3. Implementing massive machine type communications (mMTC) for an Internet-of-Things (IoT) use case envisioned

The reality has come to face the following.

1. Bandwidth is currently hardly increasing anymore, i.e. the assumption of an ever-increasing explosion of traffic bandwidth is false, at least as of now (2025/26). Growth is slow at 20% per year. Traffic volume has nearly come to a halt.
2. Each odd generation of cellular introduced a new service, namely 1G introduced mobile telephony, and 3G mobile Internet, respectively. These new services were initially successful for business customers. You might remember that 1G was a business phone, and 3G was either a Blackberry or Nokia Communicator, clearly addressing the business needs. In case of 5G, the new Tactile Internet service via URLLC was tried out by many businesses in so-called campus or private mobile networks (PMN); this, in many cases, turned out to be way too complex for running a PMN. The wide area applications, such as autonomous driving, have only been successful use cases in niche markets, e.g., for moving outdoor AGVs (automatic guided vehicles).
3. In 5G, the evolution of low-power massive IoT builds directly on 4G's NB-IoT and LTE-M. This is realized within 5G New Radio through the mMTC service class, while RedCap (Reduced Capability, also known as NR-Light) addresses medium-complexity IoT use cases. NB-IoT and LTE-M remain supported and continue to evolve within the 5G ecosystem. Rather than introducing a single new IoT technology, 5G integrates these approaches, with RedCap bridging the gap to more capable IoT devices. Neither was a truly low-power IoT system standardized nor was RedCap available soon enough to build-up momentum so far.

It is therefore time to revisit the 6G vision [3] and update this at a high level.

6G's Profit & Loss Approach

Every company has to publish its profit & loss statement (P&L). The top-line shows the revenue sources, the bottom-line the profit. Achieving higher profits can be done either by increasing the top line without dramatically increasing the costs, or by reducing the costs to improve the bottom-line.

Taking current cellular industry's situation, we desperately have to concentrate on the P&L. What are new sources of revenue, and what are possibilities to reduce cost? Reducing cost of an operator at the cost of reducing its infrastructure equipment expenses makes operators happy, but destroys the future of vendors. This sounds like a less promising idea for recreating a vibrant cellular industry.

In well-established industries as oil & gas, car manufacturing, retail, and construction, it's a margin game. Revenues are varying over time; profits can only be improved by reducing costs and therefore improving the profit margin on revenue. The cellular industry is also a "margin game" in mature markets, but for different reasons. It is characterized by:

- **High Competition:** Intense competition among providers in mature markets erodes margins as services become commoditized.
- **High Capital Expenditure (CapEx):** The industry requires continuous, massive investment in infrastructure (e.g., 5G and soon 6G networks) and technology upgrades, which impacts net profit margins.
- **Focus on Volume/Subscribers:** Historically, the business model focused on expanding the subscriber base; now the challenge is maintaining margins through diversification into new services (like gaming or data analytics) as core services face commoditization.

The cellular network operators have a difficult stance. They must continue investing to deliver services at the forefront of technological development, yet they have increasingly become a commodity infrastructure, often taken for granted like rail or road network. Due to the latter, leadership is torn between having to adhere with business school rules of a margin business but at the same time having to be at the forefront of understanding the new generations of technology coming, influencing them to their benefit, and planning for the future.

For us, as technologists, we therefore must understand this and deliver technology in a classical way of a margin business: increasing the top-line and bottom line of a profit-and-loss (P&L) statement. We must develop technology that addresses the P&L!

Pragmatic Bottom-Line Opportunity: Energy Efficiency, e.g. via Gearbox PHY

The bottom line can be improved by reducing the CapEx and hence the depreciation. As cellular technology evolves, this, however, would be equivalent to reducing the investment into the future. This is dangerous. On the other hand, an operational expenditure (OpEx) which does not add value is the line item due to energy consumption.

We have experienced a phenomenal improvement in terms of energy consumption per transmitted bit of the modem from 1G to 4G. The 1G analog modulation's induced power consumption was so high that initially the "handset" was conceived to be a car phone, less a portable device. The single-carrier modulation of 2G made it possible for exploiting the advancements of microelectronics via DSP (digital signal processing), however requiring a maximum-likelihood sequence estimator equalizer whose complexity grows exponential with the delay-spread of the channel, The code division multiple access (CDMA) spread-spectrum of 3G required for a RAKE receiver, whose complexity grows linearly with the number of channel paths taken into account. This grows linear with the delay spread of the channel. Finally, with 4G the OFDM modulation (orthogonal frequency division multiple access) was introduced into cellular. Its complexity is dominated by the FFT, whose size is chosen to grow linearly with the delay spread, however, whose complexity per processed sample grows only logarithmically with the FFT size. Hence, the equalizer of OFDM grows logarithmically with the delay spread.

This trend in equalization has been a factor in successfully driving data rates ever higher, without a major impact in power consumption of the DSP. As the bandwidth increased over time to support the increasing data rates, the effective delay spread increased as well, but not the DSP complexity due to innovations in modulation methods and accompanying required equalization techniques.

However, with 5G we have come to an end of new ideas, as we again are using OFDM. To support higher data rates the cardinality of the modulation was increased as well as the number of antennas supported in the MIMO transmission (multiple input multiple output). In consequence, microelectronic advances were not able to cover for this and as a consequence 5G networks have an increased power consumption compared to 4G.

A proposed solution named Gearbox PHY [4,5] is to capture the fact that networks are seldom fully loaded. On 24/7 average, the traffic is far below maximum capacity in every cell. Therefore, it makes sense to standardize multiple modulation techniques and implement their respective modems side-by-side as separate "gears", using extremely energy efficient modulation techniques on average and only switching to the high data-rate modem "gear" which has high energy consumption only during the short periods where peak traffic is needed.

Reducing the energy consumption and therefore improving the bottom-line of operators by 10x is a challenge. The Gearbox PHY seems to provide a viable solution.

Pragmatic Top-Line Opportunity: Coverage

Coverage remains to be a challenge, even 40 years into cellular network deployments. And, many people in the world live in rural areas without internet access today: ITU's current number is nearly 3 billion people still unconnected [6]!

To realize the ever-increasing demand in traffic, the data rate of the physical layer has been boosted via increasing the QAM cardinality and number of MIMO streams has, however, at the cost of lowering the receiver sensitivity and the link budget. This is one reason why the inter-site distance has been reduced, making it more and more difficult to cover rural areas without massive densification, which poses a financial challenge. Why shall one invest into an expensive infrastructure that has very low utilization?

In the days of 2G modulations with nearly constant-envelope were chosen to minimize the RF transceiver power. We experienced very good link budget and could operate with very good receiver sensitivity. This allows for GSM extended-range cells to cover 200 km radius, a reason why we remain having GSM in wide areas of South America and Africa today. However, the modem DSP per bit is complex due to the MLSE equalizer. In the meantime, we know that frequency-domain equalization [7] can also be applied if the signal packet were designed accordingly. Again, making the DSP a logarithmic effort in terms of channel delay spread. Impulse radio is even more energy efficient and the receiver sensitivity is even higher.

Therefore, to address the coverage challenge one could again use a Gearbox PHY approach. Urban and suburban cells would have all gears, supporting extremely high data rates as traffic

demand dominates the base station deployment. In rural areas base stations could be installed that only have the lower gears, supporting e.g. only up to 50Mb/s. These could be way more energy efficient, provide extreme coverage, and would be far less costly compared to a base station built to deliver rates in the multi-Gb/s range.

An alternative clearly is the use of non-terrestrial networks (NTN), in particular satellite networks. Due to the drop in satellite launch cost per kg weight, this can provide another viable solution. However, covering the nearly 3B nonconnected people will most likely not be possible with an ARPU (average revenue per user) far below $5/month, as required in many unconnected areas of the earth. A coverage-providing Gearbox PHY could be the more cost optimal solution, or as an intermediate step between an NTN and a full terrestrial rollout.

Connecting the unconnected and providing global seamless coverage is a goal. With the Gearbox PHY umbrella-cells a range of coverage radius of approximately 100 km becomes a viable way forward in achieving this.

Top-Line Opportunity: Consumer Robotics

5G introduced URLLC to support remote control of robotic devices. We have observed many use cases for industrial and business applications. Visible examples are cleaning robots in public spaces, 5G drones, logistics robots, agriculture robotics. All are professional business use cases, and all with cellular connectivity. The vacuum cleaner robots at home is reconnected with WiFi so far. We are at the verge of robotic helpers and companions at a large scale. Examples are:

1. Home cleaning
2. Kitchen helpers
3. White good robots doing the wash
4. Mobility (autonomous cars)
5. Local mobility (wheel chairs, exoskeletons)
6. Entertainment/Gaming
7. Gardening
8. Sports
9. Companions, e.g. robotic pets
10. Tools

Assume you bought one personal mobile robot (PMR) of every of the ten categories every 10 years. This would result in buying on average one PMR per year. The cell phone renewal rate is currently around one every 3 years. This would mean:

The PMR market is at least 3x larger than the mobile phone market

This is substantial, and provides a nice opportunity for cellular networks. And this does not account for drones and other professional logistics applications. They come on top!

And the opportunity becomes even larger when taking the following into account. Today's Waymo or Zoox autonomous cars are equipped with a very large number of sensors to enable driverless level-5 [8] performance. The cost markup over a car driven by humans is large, more than double. Assume the network was providing the missing sensing for a car equipped and capable of level-3 driving to achieve level-5. Then this would be way more cost effective. Take the following back-of-the-envelope calculation:

> *If the markup from level-3 to level-5 were $50k and the car was driven 250K km within its life time, this results in 20 cents per km additional costs, not taking interest into account. If the network provided the necessary sensing for 10c/km this would half the price!*
>
> *Now remember the many use cases for PMRs listed in the previous section. Assuming this pricing of 10c/km and 2000 km of PMR service provisioning per month. This would amount to $200/month additional ARPU.*

PMRs and professional robots are a great top-line opportunity for network operators. Their development will not happen overnight, but the prospects are great.

Pragmatic Top-Line Opportunity: Integrated Sensing & Communications at FR2

The above-mentioned service requires to install new infrastructure, e.g. LIDAR and RADAR at street crossings, and/or new integrated sensing within the licensed communications bands. A pragmatic approach could be to use the existing FR2 for sensing (cellular frequency range 2, typically between 24.25GHz and 30GHz. This band has not been heavily used for communication services, but is ideally suited for RADAR [9]. Installing RADAR at this band gives operators the chance to capture the static environment as well as the moving targets.

The most pragmatic way to implement this is to use an already standardized protocol. In case FR2 is used for communications the UE operates in dual connectivity with an FR1-anchored master cell group (MCG) handling control signaling and call management, while FR2 cells are used as a secondary cell group for high-rate user-plane transmission. Equivalently, FR2 radar can be scheduled and mastered and scheduled by an MCG at FR1, only using FR2 for sensing [9].

A mono-static, bi-static, or multi-static RADAR could enable positioning as well as RADAR imaging. For professional services, e.g. logistics delivery on ground or by drone, this capability is needed as well. Not only PMR but all professional applications require sensing.

Importantly, note that sensing data can be very personal and therefore privacy is a very important aspect to be taken into account. Operators are highly regulated concerning privacy of phone calls and Internet access. They are a natural for being the host of sensing data.

Integrated sensing and communications done right gives the operators the chance to monetize their most valuable asset, the sensing data. The future of operators is not only to deliver connectivity, but to provide access to data. At the age of AI this clearly is another interesting revenue opportunity.

Important Top-Line Differentiator: Trustworthiness

In the coming new world of robotics and XR, commencing with 6G but clearly developing over the next decades, privacy will

become a major concern. However, not only privacy is a characteristic of concern. When encountering PMRs and professional robots we must trust them at least as much as trusting people. It therefore is important to understand an overarching concept of trust and trustworthiness, as it has been developed in social sciences over the last half century, see in particular [10, 11].

The 5G and O-RAN standards were therefore analyzed in the study [12] concerning five characteristics:

1. Confidentiality
2. Integrity
3. Availability
4. Accountability
5. Privacy

An even more comprehensive list of objectively measurable characteristics to be analyzed in the future has been standardized in the meantime as [13] shows that current standards default dramatically. How can we make subjective decisions based on the situation encountering a robot when the network fails to be trustworthy?

The paper [14] conceptualizes trust and trustworthiness in communications as a first step. This is just a start. We must get going and develop finer models to tackle the world of robotics age ahead.

Trustworthiness and trust are key for human-human interaction. 6G must embrace this as this is the basis for monetizing most top-line opportunities ahead. And this starts at the basis, building the right chip architectures [15], see also [16].

Top-Line Opportunity: AI induced Traffic Growth

Formerly we were used to cellular data traffic to grow exponentially. Therefore, the radio access network also followed this trend to provide the bandwidth required to serve the appetite for data. It nearly followed Moore's law, doubling every 18 months which is the same as growing by 10-fold every 5 years.

Cellular traffic growth has been nearly flat in the last 4 years. It shows merely a 20% growth and the growth is continuing to be falling. When analyzing the published traffic growth in [17], it shows an exponential decay. This is due to the fact that in absolute numbers traffic has stopped growing exponentially by the end of 2021. Important to note: November 2021 was when LLM AI (large language model) hit the market. It might be that people were busy with interacting with AI and less with data-heavy video content.

Therefore, let us learn from the past and project the future: Cellular data usage exploded with 4G. It was less the cellular technology but video content being downloaded and uploaded while visiting social media sites that created this demand. In 2G data was dominated by SMS, text messaging. In 3G it was mainly email and attached files that created the demand for data. At the end of 3G and then with 4G, social media video clips hit the users by storm. We saw an explosion in data usage. Now where do we stand in AI prompting? At first, we were able to prompt simple text messages. Now we can upload files and in return receive files. Wide-scale video prompting is only expected to be ready for broad use in 2027. Then we will be able to upload reels and whole videos, or capture the input by camera, and in return receive fantastic animated video content.

And then come the PMRs. As we interact with them, AI is at work. Cameras and RADAR will capture the environment and our gestures. This will be uploaded to AI computing systems and in return the PMR needs to react, swiftly! This means the days when we are used to waiting 10s of seconds and minutes for the reply to a prompt will be over. Today we can average-put data transmission as real-time plays hardly any role. Tomorrow, when interacting with robots, peak data rates and latency matter. Will this wave influence the wireless roadmap of [18] and refreshed in [3]? And will it look as sketched in the update below?

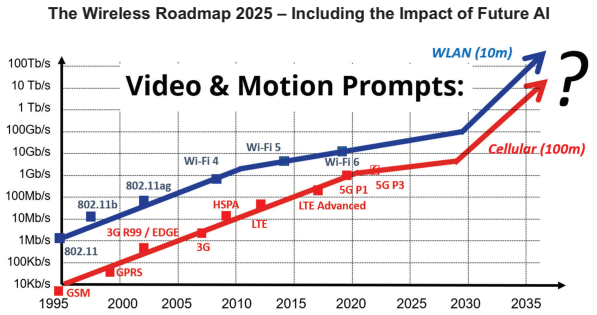

It is sensible to assume that we are at the verge of a large wave of increase in data traffic in cellular networks! We must get ready and have energy optimizations ready, as e.g. the Gearbox PHY. The days of slow growth will most likely be over soon 6G will be turned on when this wave hits the market. Only planning for low-growth is planning for failure?

Synthesis

The cellular industry is at the verge of an exciting new wave. Let us focus on the top-line and bottom-line opportunities ahead. Personal mobile robots and motion capture AI prompting are just two applications to mention that seem natural to project. They both create valuable growth opportunities for the industry and must be addressed by 6G. They require the development of many solutions to overcome technical challenges. A pragmatic approach seems most promising.

Operators have a new chance for revenue ahead. As robots require sensing, it seems more sensible to implement a vast amount of the sensing within the network and implement only basic sensing in robots, not overloading every robot with costly large sensing. At a meta-level this is equivalent to having compute power in terminals, but for many applications relying on data centers to provide additional performance. Making the network a source for sensing and its data makes this another exciting opportunity for networks of the future.

But we must not forget that trustworthiness and trust must be addressed at a very deeper level as done up to now in 1G-5G cellular standards. For the implementation we need trustworthy platform chips as an anchor for enabling this future [15].

References

[1] You, X., Wang, CX., Huang, J. *et al.* Towards 6G wireless communication networks: vision, enabling technologies, and new paradigm shifts. *Sci. China Inf. Sci.* 64, 110301 (2021). https://doi.org/10.1007/s11432-020-2955-6.

[2] G. P. Fettweis, "The Tactile Internet: Applications and Challenges," in *IEEE Veh. Technology Magazine*, vol. 9, no. 1, pp. 64–70, March 2014, doi: 10.1109/MVT.2013.2295069.

[3] G. P. Fettweis and H. Boche, "6G: The Personal Tactile Internet – And Open Questions for Information Theory," in *IEEE BITS the Information Theory Magazine*, vol. 1, no. 1, pp. 71–82, 1 Sept. 2021, doi: 10.1109/MBITS.2021.3118662.

[4] F. Gast, F. Roth, M. Dörpinghaus, P. Sen, S. Zeitz and G. P. Fettweis, "Energy Optimization using Joint Modulation Scheme and Front End Adaptation – the Gearbox-PHY," *2024 19th ISWCS*, Rio de Janeiro, Brazil, 2024, pp. 1–6, doi: 10.1109/ISWCS61526.2024.10639053.

[5] F. Gast, F. Roth, et al. "The Role of Oscillator Phase Noise in Maximizing Transceiver Energy Efficiency," *2025 IEEE Wireless Communications and Networking Conference (WCNC)*, Milan, Italy, 2025, pp. 1-6, doi: 10.1109/WCNC61545.2025.10978835.

[6] ITU Press Release, "Population of global offline continues steady decline to 2.6 billion people in 2023," https://www.itu.int/en/mediacentre/Pages/PR-2023-09-12-universal-and-meaningful-connectivity-by-2030.aspx?utm_source=chatgpt.com.

[7] D. Falconer, S. L. Ariyavisitakul, A. Benyamin-Seeyar and B. Eidson, "Frequency domain equalization for single-carrier broadband wireless systems," in *IEEE Communications Magazine*, vol. 40, no. 4, pp. 58–66, April 2002, doi: 10.1109/35.995852.

[8] SAE Standard J3016_202104 – Taxonomy and Definitions for Terms Related to Driving Automation Systems for On-Road Motor Vehicles, Issuing Committee: On-Road Automated Driving Committee, SAE, doi https://doi.org/10.4271/J3016_202104.

[9] G. Fettweis and F. Gast, "Radio Sensing Device Control," European Patent pending, P110669-GB (I001222) / P270594EP00, 2025 (Vodafone).

[10] N. Luhmann, *Vertrauen. Ein Mechanismus der Reduktion sozialer Komplexität*, Ferdinand Enke Verlag Stuttgart (original); UVK / Lucius & Lucius, 1968 (1973, 1989, 2000 reprints).

[11] R. C. Mayer, J. H. Davis, F. D. Schoorman, (1995), "An integrative model of organizational trust," *Academy of Management Review*, 20(3), 709–734.

[12] S. Koepsell et al, "Open RAN Risk Analysis," Study published by the BSI, February 2022, https://www.bsi.bund.de/SharedDocs/Downloads/EN/BSI/Publications/Studies/5G/5GRAN-Risk-Analysis.pdf?__blob=publicationFile&v=7.

[13] ISO/IEC Standard on "Trustworthiness," TS 5723:2022, July 2022.

[14] G. P. Fettweis, P. Grünberg, T. Hentschel and S. Köpsell, "Conceptualizing Trustworthiness and Trust in Communications," in *IEEE Communications Magazine*, vol. 63, no. 12, pp. 126–132, December 2025, doi: 10.1109/MCOM.001.2400383.

[15] S. Haas, C. Dunkel, F. Pauls, M. Hasler and Y. Verma, "Trustworthy Silicon: An MPSoC for a Secure Operating System," *2024 IEEE Nordic Circuits and Systems Conference (NorCAS)*, Lund, Sweden, 2024, pp. 1–7, doi: 10.1109/NorCAS64408.2024.10752473.

[16] EC CORE next project, Trustworthy 6G chips, https://corenext.eu/scientific-publications/.

[17] Ericsson Mobility Report, "During 2025, mobile network data traffic growth has been stable," November 2025, page 12.

[18] G. Fettweis and S. Alamouti, "5G: Personal mobile internet beyond what cellular did to telephony," in *IEEE Communications Magazine*, vol. 52, no. 2, pp. 140–145, February 2014, doi: 10.1109/MCOM.2014.6736754.

Acknowledgement

The vision presented in this paper would not have been possible without the daily interactions with my teams at TU Dresden and at the Barkhausen Institute. And, I thank my colleagues of the scientific community for all the discussions. The work is supported by Vodafone, the governments of Saxony, Germany, the European Commission, many industrial partners as well as the European Research Council and the German Science Foundation (Deutsche Forschungs-Gemeinschaft: DFG).Many parts of the vision have been presented at keynote talks at IEEE conferences.

Biography

Gerhard P. Fettweis, earned a Ph.D. under H. Meyr at RWTH Aachen (Germany) in 1990. After a postdoc at IBM Research, San Jose, he joined TCSI, Berkeley, USA. Since 1994 he is Vodafone Chair Professor at TU Dresden, Germany. Since 2018 he is also founding Scientific Director & CEO of the Barkhausen Institute. He researches wireless communications and chip design, coordinates 5G++Lab Germany and the German Cluster-for-Future SEMECO. His team spun-out 28 tech startups, and he initiated 6 platform entities. Gerhard is member of the US National Academy of Engineering, the German Academy of Sciences (Leopoldina), the German Academy of Engineering (Acatech), and Fellow of IEEE, VDE/ITG, National Academy of Inventors, EURASIP, WWRF, and DATE. He is active in organizing IEEE conferences.

DOI. No. 10.13052/2794-7254.021

A Comparative Analysis of 3GPP and ITU-R 5G Channel Models: Technical Divergence and Philosophical Implications

Nicolò Avarino, Christos Politis and Nuwan Weerasinghe*

Abstract: The design and validation of 5G systems rely heavily on standardized radio channel models to predict real-world performance. The 3GPP TR 38.901 and the ITU-R M.2412 reports are the industry's cornerstones for this purpose, yet they exhibit significant technical differences, particularly in the sub-6 GHz frequency band and millimeter-wave indoor scenarios. This paper presents a rigorous comparative study of these two standards, quantifying the performance impact of their divergences across canonical deployment scenarios. Using a unified simulation framework implemented in ns-3, we analyze pathloss and Signal-to-Noise Ratio (SNR) in Rural Macro (RMa), Urban Macro (UMa), Urban Micro (UMi), and Indoor Hotspot (InH) environments.

Our results reveal that while the models align in rural scenarios, they diverge fundamentally in complex urban environments. The ITU-R model proves to be a more conservative benchmark in UMa NLOS, predicting a median SNR up to 9.5 dB lower than 3GPP. Conversely, in UMi NLOS, the 3GPP model describes a significantly more volatile channel (higher shadow fading variance), making it a risky predictor for Ultra-Reliable Low-Latency Communications (URLLC). Furthermore, our analysis of the indoor 28 GHz scenario exposes a dramatic discrepancy: the ITU-R's optional model is exceptionally optimistic, showing a performance gap of up to 34 dB compared to the standard 3GPP model. We conclude that these technical divergences reflect differing design philosophies – optimistic prediction vs. conservative benchmarking – dictating that model selection must be strategically aligned with the specific 5G service pillar (eMBB or URLLC) under evaluation.

Keywords: 5G, channel modeling, 3GPP TR 38.901, ITU-R M.2412, ns-3, pathloss, SNR, URLLC, eMBB.

1. Introduction

The fifth generation of mobile communications (5G), categorized under the IMT-2020 vision, marks a paradigm shift from traditional mobile broadband to a diverse ecosystem of services. As defined by ITU-R Recommendation M.2083 [1], 5G is built upon three distinct pillars: Enhanced Mobile Broadband (eMBB), focusing on high data rates (up to 20 Gbit/s) and mobility; Massive Machine-Type Communications (mMTC), targeting high-density IoT connectivity; and Ultra-Reliable and Low-Latency Communications (URLLC), enabling mission-critical applications with sub-millisecond latency and 99.999% reliability.

Designing networks that meet these varied and stringent requirements necessitates highly accurate channel modeling. The adoption of millimeter-wave (mmWave) frequency bands introduces complex propagation characteristics, such as high free-space path loss, extreme sensitivity to blockage, and sparse scattering, which challenge conventional sub-6 GHz modeling approaches [2]. Accurate simulation tools are therefore vital for predicting key metrics like coverage, throughput, and reliability before physical deployment [3].

Currently, the two industry-standard frameworks for 5G channel modeling are the 3GPP TR 38.901 [4] and the ITU-R M.2412 [5] reports. While the ITU-R model builds upon the 3GPP specification, it introduces significant modifications, particularly in pathloss formulations for the sub-6 GHz band and new statistical distributions for angular spreads. However, the practical impact of these technical divergences on system-level performance is not always fully quantified. Model selection is often treated as a minor configuration detail, yet it can fundamentally alter simulation outcomes and, consequently, network design decisions.

This paper presents a rigorous comparative study of the 3GPP and ITU-R channel models. We implement the ITU-R M.2412 model within the ns-3 network simulator, creating a unified framework to benchmark it against the established 3GPP implementation. We analyze performance across four canonical scenarios: Rural Macro (RMa), Urban Macro (UMa), Urban Micro (UMi), and Indoor Hotspot (InH). Our primary objective is to quantify the differences in pathloss and Signal-to-Noise Ratio (SNR) and to interpret these divergences through the lens of the different service requirements (eMBB vs. URLLC).

The remainder of this paper is organized as follows: Section 2 details the technical differences between the two channel models. Section 3 describes our simulation framework in ns-3. Section 4 presents the comparative analysis of pathloss and SNR. Section 5 discusses the philosophical implications of the results for 5G service pillars, and Section 6 concludes the paper.

School of Computer Science and Engineering, Kingston University, London, UK
E-mail: nicoloavarino@icloud.com
*Corresponding Author
Manuscript received 21 November 2025, accepted 05 December 2025, and ready for publication 31 December 2025.

2. Overview of Channel Models

The relationship between the 3GPP TR 38.901 [4] and ITU-R M.2412 [5] channel models is one of foundation and refinement. The 3GPP model provides a comprehensive baseline for frequencies from 0.5 to 100 GHz. The ITU-R model adopts this baseline but introduces a bifurcated architecture based on frequency, along with specific modifications for indoor millimeter-wave scenarios.

2.1. Architectural Framework: Model A vs. Model B

While 3GPP defines a single, continuous framework across the frequency spectrum, ITU-R M.2412 introduces a distinction:

- **Model B (6–100 GHz):** For frequencies above 6 GHz, the ITU-R explicitly aligns with the 3GPP specification. Pathloss formulas, line-of-sight (LOS) probabilities, and fast-fading parameters are identical.
- **Model A (0.5–6 GHz):** For the lower frequency bands, which are critical for wide-area 5G coverage (e.g., 700 MHz, 3.5 GHz), ITU-R introduces distinct formulations.

2.2. Scenarios of Consensus and Alignment

Before analyzing the divergences, it is crucial to identify where the standards harmonize.

2.2.1. *Rural macro (RMa)*

For the Rural Macro scenario, the ITU-R does not introduce a unique formulation. It explicitly adopts the pathloss equations and fading parameters defined in 3GPP TR 38.901 for both LOS and NLOS conditions. The only minor distinction is the applicability range: ITU-R extends the validity distance up to 21 km, whereas 3GPP typically defines it up to 10 km. Mathematically, however, the models are identical.

2.2.2. *Standard indoor hotspot (InH)*

For standard office environments in the sub-6 GHz band, the ITU-R introduces specific "InH-A" formulas. While technically distinct from the generic 3GPP equations, they are designed to yield functionally equivalent results. The mean pathloss trends and shadow fading parameters (e.g., $\sigma_{SF} \approx 3-4$ dB) are largely harmonized, reflecting a consensus on the propagation physics within standard buildings.

2.3. Critical Pathloss Divergences

The most impactful technical differences arise in urban environments and specific mmWave use cases.

2.3.1. *Urban Macro (UMa) NLOS*

The 3GPP model employs a generalized distance-dependent formula. In contrast, the ITU-R Model A incorporates specific environmental geometry. The 3GPP formula relies primarily on 3D distance (d_{3D}), carrier frequency (f_c), and user terminal height (h_{UT}):

$$PL_{3GPP} = 13.54 + 39.08\log_{10}(d_{3D}) + 20\log_{10}(f_c) - 0.6(h_{UT} - 1.5) \quad (1)$$

The ITU-R formula is significantly more complex, introducing sensitivity to the average building height (h) and street width (W):

$$\begin{aligned} PL_{ITU} = {} & 161.04 - 7.1\log_{10}(W) + 7.5\log_{10}(h) \\ & - (24.37 - 3.7(h/h_{BS})^2)\log_{10}(h_{BS}) \\ & + (43.42 - 3.1\log_{10}(h_{BS}))(\log_{10}(d_{3D}) - 3) \\ & + 20\log_{10}(f_c) - (3.2(\log_{10}(17.625))^2 - 4.97) \end{aligned} \quad (2)$$

This complexity aims to model diffraction loss over rooftops more explicitly than the regression-based 3GPP approach.

2.3.2. *Urban micro (UMi) NLOS*

In the street canyon environment, the models diverge in their regression coefficients and, crucially, in their statistical variance. The mean pathloss formulas differ in slope and intercept:

$$PL_{3GPP} = 22.4 + 35.3\log_{10}(d_{3D}) + 21.3\log_{10}(f_c) \quad (3)$$

$$PL_{ITU} = 36.7\log_{10}(d_{3D}) + 22.7 + 26\log_{10}(f_c) \quad (4)$$

However, the most significant difference for system reliability is the **Shadow Fading (SF)** standard deviation (σ_{SF}). The 3GPP standard specifies a high $\sigma_{SF} = 7.82$ dB, implying a highly volatile channel. The ITU-R standard specifies a much lower $\sigma_{SF} = 4.0$ dB, describing a more stable environment.

2.3.3. *Indoor 28 GHz optional model*

For indoor mmWave scenarios, ITU-R introduces "Optional Model I", a simplified deterministic model based on 2D distance (d_{2D}):

$$PL_{ITU,Opt} = 22.0\log_{10}(d_{2D}) + 61.2 \quad (\sigma_{SF} = 3.3\text{ dB}) \quad (5)$$

This model ignores the height component (d_{3D}) and assumes a very low shadow fading variance compared to the full 3GPP stochastic model, representing an idealized propagation environment.

2.4. Small-Scale Fading and Angular Distributions

Beyond pathloss, the models differ in how they generate multipath components (Fast Fading). Small-scale fading is typically modeled according to classical distributions, as described in [6].

2.4.1. *The Laplacian innovation*

A major novelty in ITU-R M.2412 is the mandate to use the **Laplacian distribution** for the Power Angular Spectrum (PAS) of zenith angles (ZOD/ZOA) in sub-6 GHz scenarios, whereas 3GPP exclusively uses the Wrapped Gaussian distribution [7].

Table 1.

Summary of technical characteristics (sub-6 GHz)		
Feature	**3GPP TR 38.901**	**ITU-R M.2412**
RMa and InH LOS	Baseline	Identical Aligned
UMa NLOS	Simplified Formula	Complex Formula
UMi NLOS σ_{SF}	High (7.82 dB)	Low (4.0 dB)
Zenith Angles	Wrapped Gaussian	Laplacian
Indoor mmWave	Full Stochastic	Optional Simplified (2D)

- **Gaussian (3GPP):** Symmetric, thin tails. Assuming scattering clusters are concentrated around a mean direction.
- **Laplacian (ITU-R):** Sharper peak, heavier tails. This models environments where strong reflections can occur at angles significantly offset from the main direction.

Table 1 summarizes these key technical characteristics.

3. Simulation Methodology

To conduct a fair and rigorous comparison, we developed a unified simulation framework within the Network Simulator 3 (ns-3) environment. ns-3 is a discrete-event network simulator widely used in academia and industry for 5G research. While ns-3 natively includes a robust implementation of the 3GPP TR 38.901 channel model, it lacks the specific modifications introduced by ITU-R M.2412. Therefore, our primary methodological contribution was the extension of the ns-3 propagation module to incorporate the ITU-R specifications.[1]

3.1. Framework Architecture

Our implementation extends the existing ns-3 architecture by introducing new classes that inherit from the core `PropagationLossModel` and `ChannelConditionModel`. Our simulation framework was informed by the WWRF-IEG evaluation of IMT-2020 candidate technologies [8]. This modular approach ensures that the only variable in our comparative study is the channel model definition itself; the underlying simulation engine, mobility models, and antenna arrays remain consistent.

Key features implemented include:

- **Dual-Mode Pathloss Engine:** A logic switch that applies either "Model A" (ITU-R sub-6 GHz formulas) or "Model B" (standard 3GPP formulas) based on the carrier frequency and scenario.
- **Laplacian Angular Distribution:** We modified the channel generation procedure to support the Laplacian distribution for zenith angles (ZOD/ZOA) as mandated by ITU-R, alongside the standard Wrapped Gaussian distribution.
- **Scenario-Specific Parameters:** We integrated the complete set of fast-fading parameters (delay spread, angular spread, cross-correlations) from the ITU-R M.2412 report.

[1] The complete source code developed for this study is available at: https://github.com/simultelco/ns-3-itu

Table 2.

Simulation configuration parameters (ITU-R M.2412)				
Parameter	**InH**	**UMi**	**RMa**	**UMa**
Carrier Freq.	4 GHz	4 GHz	700 MHz	700 MHz
BS Height	3 m	25 m	35 m	25 m
UE Height	1.5 m	1.5 m	1.5 m	1.5 m
Tx Power	24 dBm	44 dBm	49 dBm	49 dBm
UE Noise Fig.	7 dB	7 dB	7 dB	7 dB
Thermal Noise	–174 dBm/Hz			

3.2. Simulation Configuration

All simulations were configured according to the "Evaluation configurations for test environments" specified in ITU-R M.2412. We simulated single-link performance with a channel bandwidth of 20 MHz. The key parameters for each of the four scenarios are summarized in Table 2.

3.3. Evaluation Scenarios and Metrics

We evaluated performance in two distinct propagation conditions for each scenario:

- **Line-of-Sight (LOS):** The receiver moves away from the transmitter in a straight line (10 m to 100 m) with a clear optical path.
- **Non-Line-of-Sight (NLOS):** The receiver is positioned at a distance where the LOS probability is negligible (e.g., >900 m for UMa), ensuring that the channel is dominated by multipath and obstructions. Shadow fading is enabled to capture large-scale signal variations.

Our comparison relies on two primary metrics:

1. **Pathloss vs. Distance:** This validates the correctness of the large-scale attenuation models and visualizes the mean signal decay predicted by each standard.
2. **Signal-to-Noise Ratio (SNR) CDF:** The Cumulative Distribution Function of the SNR captures the combined effect of pathloss, shadow fading, and fast fading. It allows us to quantify link reliability (outage probability at the tail) and ergodic capacity (median SNR).

3.4. Limitations

To focus on the fundamental differences in channel modeling, certain complexities were simplified. Specifically, dynamic blockage (e.g., by moving vehicles) was not modeled, and isotropic antennas were used to isolate channel propagation effects from beamforming gains.

4. Results and Comparative Analysis

This section presents the comprehensive simulation results across four canonical deployment scenarios: Rural Macro (RMa), Urban Macro (UMa), Urban Micro (UMi), and Indoor Hotspot (InH). For each scenario, we first validate the pathloss models by comparing theoretical formulas against simulated data, and then

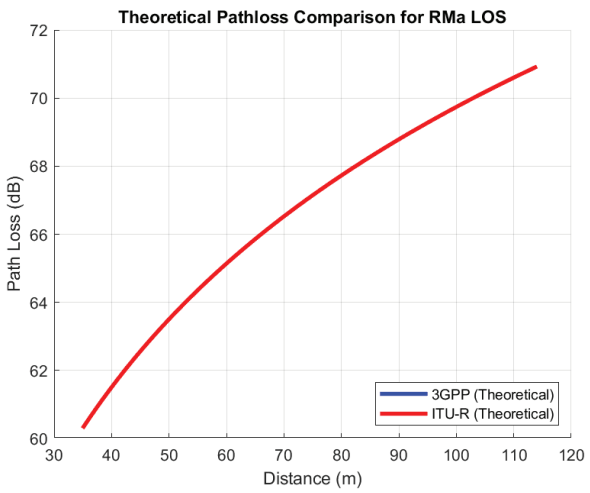

Figure 1.
RMa LOS theoretical pathloss.

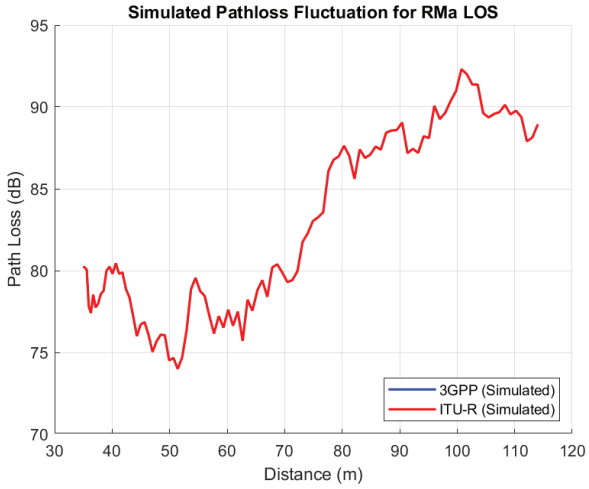

Figure 2.
RMa LOS simulated data.

analyze the Signal-to-Noise Ratio (SNR) Cumulative Distribution Functions (CDFs) to quantify system performance.

4.1. Rural Macro (RMa) Scenario

The RMa scenario serves as the validation baseline. Since ITU-R M.2412 explicitly adopts the 3GPP TR 38.901 formulas for rural environments at 700 MHz, we expect identical performance.

4.1.1. *Pathloss Validation*

As shown in Figure 1, the theoretical curves for 3GPP and ITU-R are perfectly superimposed for both Line-of-Sight (LOS) and Non-Line-of-Sight (NLOS) conditions. The simulated data points (Figure 2) align flawlessly with the theoretical predictions, confirming the correctness of the simulation framework implementation.

4.1.2. *SNR analysis*

Consequently, the SNR performance is identical. Figure 3 and 4 show a perfect overlap of the CDF curves. In LOS, the median SNR is approximately 68 dB, dropping to 19 dB in NLOS. This scenario confirms that where standards converge, the models yield indistinguishable results.

4.2. Urban Macro (UMa) Scenario

In the UMa scenario, divergences appear due to the ITU-R's specific "Model A" formulations for the sub-6 GHz band.

4.2.1. *Pathloss validation*

In LOS conditions, the models remain identical (Figures omitted for brevity as they mirror the RMa consensus). However, in NLOS conditions, a significant gap emerges. Figure 5 shows that the

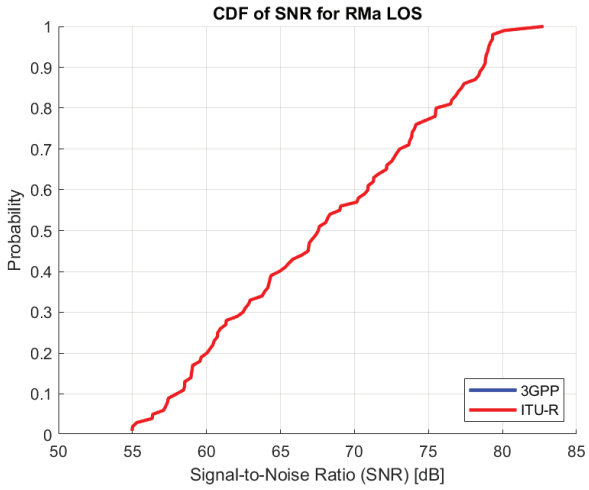

Figure 3.
RMa LOS SNR CDF.

ITU-R model (red) predicts consistently higher pathloss than the 3GPP model (blue). While the simplified formulas might suggest a minimal difference, the full implementation reveals a gap often exceeding 10 dB due to environmental parameters like building heights incorporated in the ITU-R model.

4.2.2. *SNR analysis*

In the LOS condition, the performance curves for 3GPP and ITU-R are practically identical (Figure 6). It is important to note that any minor behavioral variations observed in this state are not due to signal attenuation, but are solely attributable to slight differences in the fast-fading parameters (small-scale fading) defined by the two standards.

In contrast, the NLOS condition shows a dramatic divergence where pathloss dominates. The higher attenuation predicted by ITU-R directly degrades link quality. The SNR CDF in Figure 7

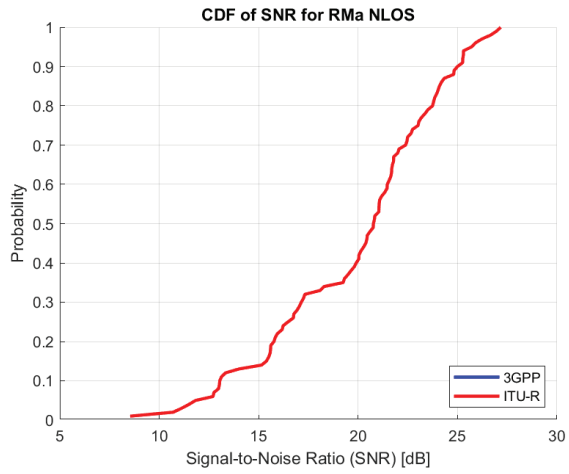

Figure 4.
RMa NLOS SNR CDF.

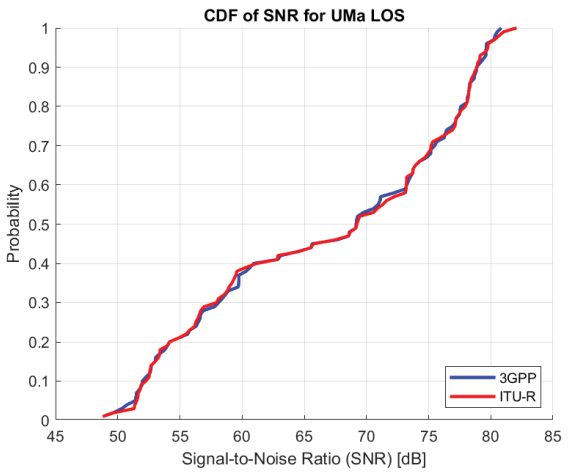

Figure 6.
UMa LOS SNR CDF (identical).

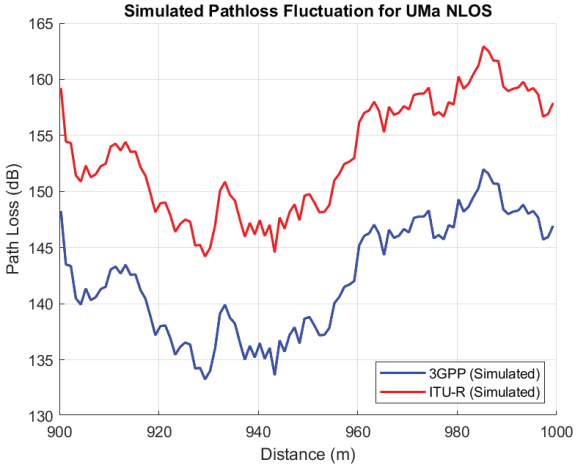

Figure 5.
UMa NLOS simulated pathloss.

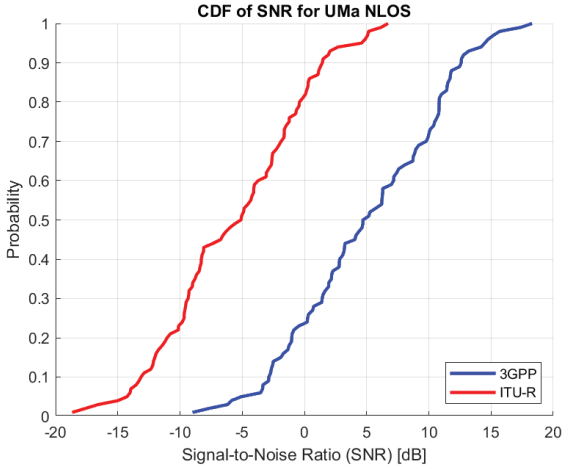

Figure 7.
UMa NLOS SNR CDF (divergent).

reveals a clear horizontal shift. The 3GPP model predicts a median SNR of +4.5 dB, whereas the ITU-R model predicts −5 dB. This **9.5 dB deficit** in the ITU-R model implies a much higher outage probability, positioning it as a significantly more conservative benchmark for urban coverage compared to the 3GPP baseline.

4.3. Urban Micro (UMi) Scenario

The UMi "Street Canyon" scenario at 4 GHz exhibits the most complex behavior, with model superiority flipping between LOS and NLOS.

4.3.1. *Pathloss validation*

In LOS (Figure 8), the ITU-R model is more optimistic, predicting 2–3 dB lower pathloss than 3GPP. However, in NLOS (Figure 9), the relationship inverts: the ITU-R model becomes more pessimistic, predicting 5–7 dB higher pathloss. The simulation data confirms these trends.

4.3.2. *SNR analysis and the capacity-reliability trade-off*

The SNR analysis for the UMi scenario provides the most critical insight of this comparative study. While the LOS condition follows the pathloss trend (ITU-R slightly better), the NLOS condition reveals a fundamental trade-off driven by the statistical properties of the channel.

Figure 10 confirms the inversion observed in the pathloss analysis, but a closer examination of the Cumulative Distribution Function (CDF) shape reveals a complex behavior that can be analyzed in three distinct regions:

1. **The Low-SNR Tail (Deep Fades):** In the lower probability region (e.g., below 10%), the 3GPP curve (blue) exhibits a significantly shallower slope compared to the ITU-R curve

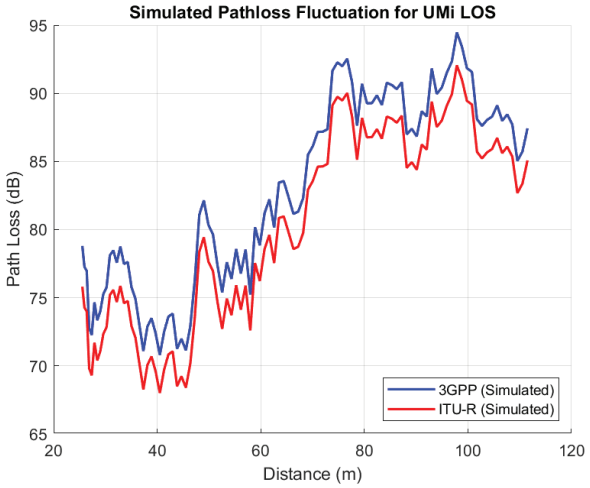

Figure 8.
UMi LOS simulated pathloss.

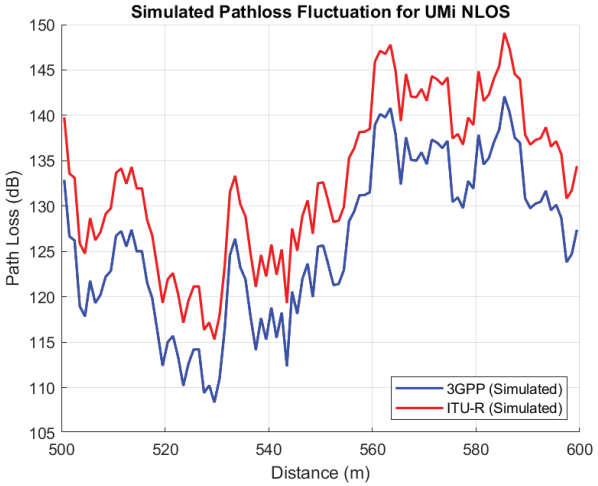

Figure 9.
UMi NLOS simulated pathloss.

(red). This "heavy tail" indicates a much higher probability of experiencing severe deep fades. For URLLC applications where reliability is paramount, this tail behavior is critical: the 3GPP model predicts that the link is more prone to catastrophic drops in quality, making it a more volatile environment.

2. **The Median Region (Average Capacity):** In the central portion of the distribution (probability between 20% and 80%), the 3GPP curve is shifted horizontally to the right. Specifically, the 3GPP model predicts a median SNR of approximately **13 dB**, compared to **8 dB** for the ITU-R model. This **5 dB advantage** implies that for standard eMBB services, which rely on ergodic capacity and retransmissions, the 3GPP model is decidedly more optimistic.

3. **The High-SNR Tail (Signal Peaks):** At the upper end of the distribution (above 90%), the 3GPP curve extends much further to the right. This suggests a higher likelihood of encountering exceptionally strong signal peaks, which opportunistic scheduling algorithms could exploit to maximize throughput.

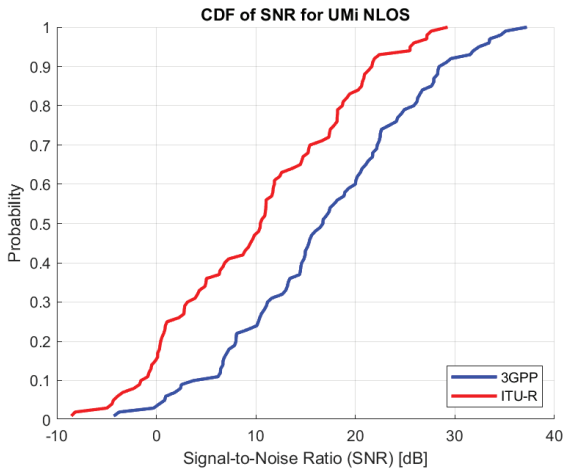

Figure 10.
UMi NLOS SNR CDF. 3GPP shows higher median capacity but higher volatility (shallower slope) compared to ITU-R.

The Root Cause: This distinct three-part behavior is a direct mathematical consequence of the different coefficients in their respective pathloss formulas:

$$PL_{3GPP} = 22.4 + 35.3\log_{10}(d_{3D}) + 21.3\log_{10}(f_c) - 0.3(h_{UT} - 1.5) \quad (6)$$

$$PL_{ITU-R} = 36.7\log_{10}(d_{3D}) + 22.7 + 26\log_{10}(f_c) - 0.3(h_{UT} - 1.5) \quad (7)$$

However, the most critical finding here lies in the link reliability, which is governed by the shadow fading standard deviation, σ_{SF} [9]. The 3GPP model specifies an extremely high value of 7.82 dB, compared to the moderate ITU-R value of 4.0 dB. This higher variance in the 3GPP model makes the channel fundamentally more volatile.

The SNR CDF in Figure 10 visualizes this trade-off. We can analyze its shape in three distinct regions:

1. **The Low-SNR Tail (Deep Fades):** In the region below approximately 8 dB, the 3GPP curve has a much shallower slope. This indicates a significantly higher probability of experiencing severe deep fades, a critical vulnerability for URLLC services.
2. **The Median Region (Average Capacity):** Between roughly 20% and 80% probability, the 3GPP curve is shifted to the right, reflecting its 5 dB advantage in median SNR and thus its higher ergodic capacity, favorable for eMBB.
3. **The High-SNR Tail (Signal Peaks):** Above approximately 27 dB, the 3GPP curve is again shallower. This means a higher probability of exceptionally strong signal peaks, which opportunistic eMBB services can exploit.

This three-part behavior is a direct mathematical consequence of the higher σ_{SF} in the 3GPP model.

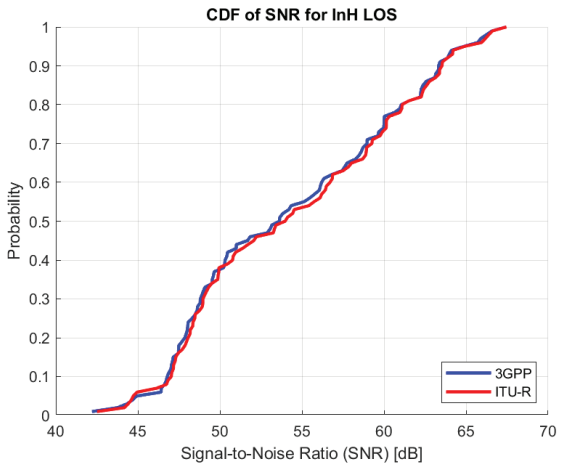

Figure 11.
InH LOS SNR CDF (4 GHz).

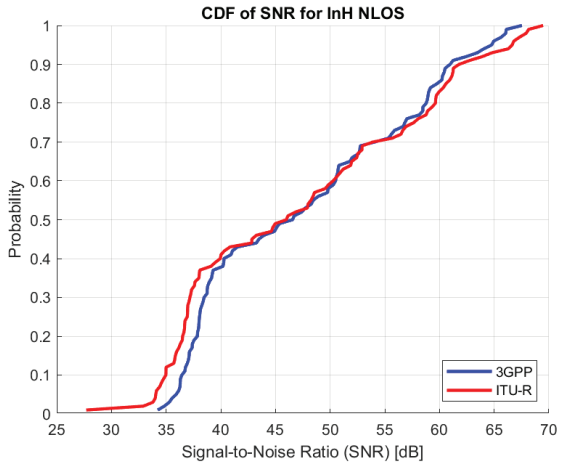

Figure 12.
InH NLOS SNR CDF (4 GHz).

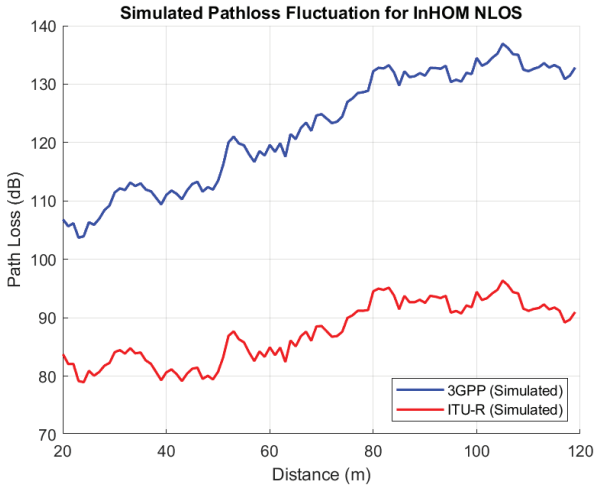

Figure 13.
InH 28 GHz simulated pathloss.

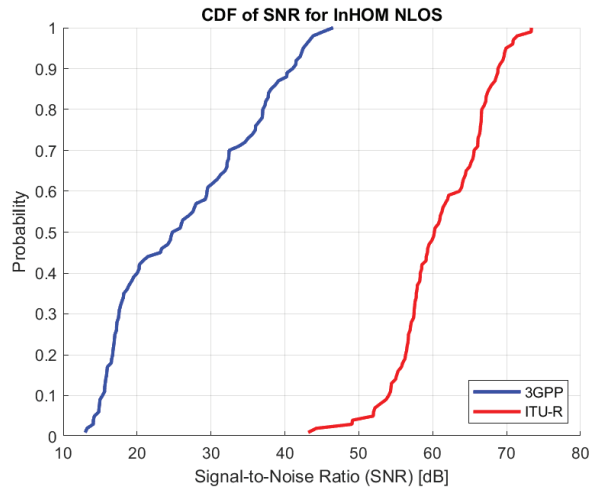

Figure 14.
InH 28GHz SNR CDF.

4.4. Indoor Hotspot (InH) Scenario

We analyzed the InH scenario in two configurations: standard sub-6 GHz (4 GHz) and the optional mmWave model (28 GHz).

4.4.1. *Standard InH (4 GHz)*

At 4 GHz, the models show only minor nuances. In LOS, ITU-R is marginally more optimistic (<1 dB)(Figure 11). In NLOS, despite a theoretical crossover point in the pathloss formula, the simulated SNR performance is functionally identical (median SNR ≈43 dB), as shown in Figure 12.

4.4.2. *Optional model (28 GHz)*

The contrast at 28 GHz is dramatic. We compared the standard 3GPP model against the ITU-R "Optional Model I". Figure 13 demonstrates a massive divergence. The ITU-R optional model predicts significantly lower pathloss. This translates to the SNR CDFs in Figure 14. In NLOS, the ITU-R optional model predicts a median SNR of 58 dB, while the standard 3GPP model predicts only 24 dB. This **34 dB gap** confirms that the ITU-R Optional Model is an idealized baseline that effectively ignores severe mmWave blockage effects.

5. Philosophical Implications for 5G Services

The comprehensive scenario-by-scenario analysis presented in Section 4 allows us to synthesize a broader conclusion regarding the design intent behind these standards.

It is crucial to frame this discussion within the genealogical relationship of the models. Since ITU-R M.2412 is explicitly derived from 3GPP TR 38.901, the differences we observed –

especially the variance in σ_{SF} and the resulting SNR slope – are not merely statistical curiosities. They embody two distinct philosophies of system design. Consequently, the terms "optimistic" and "conservative" used here are relational characterizations, describing how ITU-R deliberately deviates from the 3GPP baseline.

5.1. Areas of Consensus: The Baseline Validation

The perfect alignment in the **Rural Macro (RMa)** scenario and the functional equivalence in the **Standard Indoor (InH)** scenario confirm that the ITU-R accepts the 3GPP baseline as valid for "well-understood" environments. In these contexts, the standardization bodies agree on the physics, and model selection has negligible impact on simulation outcomes.

5.2. 3GPP: The Philosophy of Optimism (Trusting the System)

Relative to the ITU-R modifications, the foundational 3GPP model tends to yield results favorable for capacity-oriented services. This reflects an **optimistic philosophy**: it assumes that communication systems can adapt dynamically, exploit high-SNR moments, and recover from deep fades.

- **Capacity Optimism:** In UMi NLOS, despite high volatility, 3GPP predicts a higher median SNR (+5 dB).
- **Alignment with eMBB:** This mindset fits naturally with **Enhanced Mobile Broadband (eMBB)**. In scenarios like video streaming, maximizing ergodic throughput is more important than guaranteeing every single packet. The "heavy tails" of the 3GPP model are acceptable because mechanisms like Hybrid ARQ (HARQ) and adaptive coding can bridge the gaps caused by deep fades [10].

Essentially, **3GPP trusts the system** to mitigate channel volatility, making it the appropriate choice for dimensioning maximum network capacity.

5.3. ITU-R: The Philosophy of Discipline (Testing the System)

In contrast, the specific formulas introduced by ITU-R (Model A) act as a rigorous benchmark, adopting a **conservative philosophy**. By introducing complex environmental variables in UMa and deliberately limiting variability in UMi (lower σ_{SF}), it ensures steadier and more predictable channel behavior.

- **Stability in Reliability:** The lower variance in UMi (σ_{SF} = 4.0 dB vs 7.82 dB) describes a stable channel. The "heavy tail" of the 3GPP model represents a non-negligible probability of catastrophic packet loss (outage), which is unacceptable for autonomous systems [11].
- **Alignment with URLLC:** This approach aligns directly with **Ultra-Reliable Low-Latency Communications (URLLC)**, where stability matters far more than peak capacity [12]. A high average SNR is useless if the link is prone to unpredictable fades.

Thus, **ITU-R tests the system**: it provides the stable baseline needed to verify "five-nines" reliability (99.999%), ensuring that a successful simulation implies robustness in real-world deployment.

5.4. The Outlier: The 28 GHz Trap

Our analysis of the **Indoor 28 GHz** scenario highlights a unique case where the ITU-R deviates in the opposite direction. Here, the ITU-R "Optional Model I" exhibits extreme optimism (34 dB gap) compared to the 3GPP stochastic baseline. This reflects a trade-off between computational simplicity and physical realism. Researchers must be aware that this specific ITU-R model is an idealized simplification. Using it to validate indoor URLLC would be dangerous, as it hides the blockage dynamics that are the main adversary at 28 GHz.

5.5. Strategic Model Selection

The choice of channel model acts as a silent "gain" or "loss" knob in system simulations. In short, channel-model selection is not a detail – it is a strategic modeling decision.

1. **Use 3GPP TR 38.901** for eMBB capacity evaluation, where the system is expected to exploit signal peaks.
2. **Use ITU-R M.2412 (Standard)** for URLLC reliability benchmarking, where the model's conservative nature provides a necessary stress test.
3. **Avoid ITU-R Optional Models** for realistic deployment planning at mmWave frequencies.

6. Conclusion

This paper presented a comprehensive comparative study of the 3GPP TR 38.901 and ITU-R M.2412 channel models, implemented within a unified ns-3 framework. By analyzing four canonical deployment scenarios, we quantified the practical impact of technical divergences in pathloss formulas and fading parameters.

Our results demonstrate that while the models converge in simple rural and standard indoor settings, they diverge sharply in complex urban environments. In UMa NLOS, the ITU-R model proves to be significantly more pessimistic (9.5 dB median SNR deficit). In UMi NLOS, a critical trade-off was identified: 3GPP predicts higher capacity but higher volatility, while ITU-R describes a more stable, lower-capacity channel. Furthermore, we exposed a massive 34 dB discrepancy in indoor mmWave modeling, identifying the ITU-R Optional Model as an idealized outlier.

We conclude that these divergences represent distinct simulation philosophies. The 3GPP model is an optimistic predictor suitable for eMBB capacity planning, whereas the standard ITU-R model serves as a conservative benchmark ideal for stress-testing URLLC reliability. Together, they form the two necessary ends of the 5G design spectrum.

Suggestions for Future Research

Looking forward, there are several meaningful ways to expand this research to refine how we evaluate next-generation networks:

- **MIMO Beamforming:** Incorporating massive MIMO and spatial selectivity might either magnify or mitigate the divergences seen in our SISO analysis.
- **Hybrid & AI Models:** A promising direction is to explore hybrid models or AI/ML-based site-specific models **Alkhateeb2021** to bridge the gap between stochastic estimation and physical reality.
- **Extension to sub-THz:** Validating these models against measurements in the 100-300 GHz range will be essential as the industry moves towards 6G networks **6GFlagship2020**.

References

[1] International Telecommunication Union, "IMT Vision – Framework and overall objectives of the future development of IMT for 2020 and beyond," ITU-R, Recommendation M.2083-0, 2015. [Online]. Available: https://www.itu.int/rec/R-REC-M.2083-0-201509-I/en.

[2] C.-X. Wang, J. Bian, J. Sun, W. Zhang, and M. Zhang, "A survey of 5g channel measurements and models," *IEEE Communications Surveys and Tutorials*, vol. 20, no. 4, pp. 3142–3168, 2018. DOI: 10.1109/COMST.2018.2862141.

[3] T. S. Rappaport, *Wireless Communications: Principles and Practice*, 2nd. Upper Saddle River, NJ, USA: Prentice Hall, 2002.

[4] 3GPP, "Study on channel model for frequencies from 0.5 to 100 GHz," 3rd Generation Partnership Project (3GPP), Technical Report TR 38.901, version V17.0.0, 2023. [Online]. Available: https://www.3gpp.org/ftp/Specs/archive/38_series/38.901/.

[5] International Telecommunication Union, "Guidelines for Evaluation of Radio Interface Technologies for IMT-2020," ITU-R, Report M.2412-0, 2017. [Online]. Available: https://www.itu.int/rec/R-REP-M.2412/en.

[6] D. Tse and P. Viswanath, *Fundamentals of Wireless Communication*. Cambridge, UK: Cambridge University Press, 2005.

[7] S. Kotz, T. J. Kozubowski, and K. Podgórski, *The Laplace Distribution and Generalizations*. Springer, 2001.

[8] C. Politis, M. A. Usman, and N. Weerasinghe, "OUTLOOK: Visions and research directions for the Wireless World – WWRF-IEG's Evaluation of IMT-2020 Candidate Technology Enhanced Ultra High Throughput 5G (EUHT-5G) revised submission from NUFRONT," Wireless World Research Forum (WWRF), White Paper, version 3.1, 2023. [Online]. Available: https://wwrf.ch/wp-content/uploads/2023/04/Outlook31-EUHT-5G_V3.2_AU.pdf.

[9] J.-M. Kelif et al., "Statistical characterization of shadow fading in urban environments," *IEEE Transactions on Vehicular Technology*, vol. 59, no. 3, pp. 1025–1034, 2010. DOI: 10.1109/TVT.2010.2041234.

[10] E. Dahlman, S. Parkvall, and J. Skold, *5G NR: The Next Generation Wireless Access*. Academic Press, 2018, Discusses HARQ and dynamic adaptation mechanisms in 5G.

[11] X. Ge et al., "Ultra-reliable low-latency communications in autonomous vehicular networks," arXiv preprint arXiv:1903.01863, 2019. [Online]. Available: https://arxiv.org/abs/1903.01863.

[12] P. Popovski et al., "Wireless access for ultra-reliable low-latency communication: Principles and building blocks," *IEEE Network*, 2019, Defines reliability and stability as primary KPIs over capacity.

Biographies

Nicolò Avarino received his B.Sc. in Computer Engineering from Politecnico di Milano and his M.Sc. in Networking and Data Communications from Kingston University London, where his thesis focused on the comparison of wireless communication channel models. He is currently working as a Cybersecurity Engineer, with interests in secure network architectures, wireless communication systems, and emerging technologies in digital infrastructure.

Nuwan Weerasinghe is an experienced researcher and technologist with over two decades of work in artificial intelligence, machine learning, data analytics, telecommunications, and digital health. He received his B.Sc. in Electrical and Information Engineering from the University of Ruhuna, Sri Lanka, and a Ph.D. from Kingston University London, where his doctoral research focused on enhancing security and reliability in future multi-hop wireless networks. He is currently a Consultant at the World Health Organization (WHO) Regional Office for Europe, leading AI-driven initiatives in digital health innovation, cloud infrastructure, and public health data monitoring, and has co-authored WHO publications on food environments and digital marketing practices. He is also the Founder and CEO of Simultelco Ltd., developing cloud-based network simulation technologies for 5G/6G research. Since 2020, he actively contributes to the WWRF Independent Evaluation Group on IMT-2020 (5G) technologies, with focus on cloud-native simulation and AI-integrated telecom architectures. His academic interests include digital health, future communication networks, V2X systems, and responsible AI in public sector innovation. He also serves as a Visiting Lecturer at Kingston University London and has published extensively in journals, conferences, and policy-focused publications.

Christos Politis Professor (Chair) of Digital Technologies at Kingston University London (KU), School of Computer Science (CS), where I am currently a senior member of the Cyber, Engineering and Digital Technologies KERI. Upon joining KU, I founded and led a research group on Wireless Multimedia and Networking (WMN). I teach modules on wireless systems, networks and protocols. Prior to this post, I worked for Ofcom, the UK Regulator and Competition Authority, as an R and D Team Leader. While at the University of Surrey, UK, I was a PostDoc Researcher (PDRA) working on virtual distributed testbeds in the Centre for Communication Systems Research (now the Institute for Communication Systems, 6G Innovation Centre). This was preceded by engineering positions with Intracom-Telecom SA and Maroussi 2004 SA in Athens, Greece. I have managed to raise sustained funding from the EU and UK research and technology frameworks under the ICT and Security programmes (FP5/6/7, H2020, Horizon Europe, EPSRC and Innovate UK). I hold two patents and have published over 230 papers in international journals and conferences and chapters in ten books. In parallel to my academic career, I am heavily involved in building and managing technology start-ups. At the same time to the above, I am the Founder and one of the Directors of Ubitech Ltd. Ubitech has recently launched its first product called UbiTheraPlay, which is a gaming platform for the rehabilitation of neurodivergent people. I also advise and consult for several governments, Universities and commercial organisations on their research programmes/agendas, policies and portfolios in EU, UK, Canada, Greece, Qatar, China, Malaysia to mention a few. I hold a PhD and MSc from the University of Surrey, UK and a BEng from the University of Athens, Greece, all in Electrical/Electronic Engineering. I am senior member of the IEEE and UK/Greece chartered engineer.

DOI. No. 10.13052/2794-7254.022

Robust and Resilient Terrestrial–Non-Terrestrial Connectivity for In-Flight Connectivity in the Beyond-5G/6G Era

Christoffer Hjalmarsson, Tasos Dagiuklas, Brahim El Boudani and Jonathan Rodriuguez*

Abstract: The integration of terrestrial and non-terrestrial networks is essential for reliable, secure, and ubiquitous connectivity with QoS guarantees, and is a key enabler for supporting emerging applications like in-flight broadband connectivity and mission-critical operations, though several challenges remain. This paper compares three architectural options for providing in-flight broadband connectivity: a DU/CU functional split with the DU on the aircraft and the CU on the ground; a similar split enhanced with integrated access and backhauling to enable 3GPP-compliant flying ad-hoc networks; and a novel architecture in which aircraft act as mobile wireless access and backhaul nodes hosting MEC capabilities for low-latency services and local breakout, a flexible approach that requires sophisticated SON functions and optimised routing.

Keywords: IAB, in-flight broadband connectivity, network automation, SATCOM, TN/NTN integration, WAB.

1. Introduction

The 5G mobile business case extends towards the air, where in-flight broadband connectivity (IFBC) is an emerging reality. A study by the London School of Economics and Political Science in association with Inmarsat showed 2015, that in-flight broadband connectivity had the potential to create a $130 billion global market within the next 20 years, resulting in $30 billion of additional revenue for airlines by 2035 [1]. There has already been some market penetration in this area, with legacy in-flight systems relying on satellite communications complemented by on-board Wi-Fi access. More recently, the market has introduced direct air-to-ground (DA2G) mobile services, such as the European Aviation Network (EAN), which delivers 4G-LTE connectivity and employs a single GEO satellite as a backup link when the higher-throughput DA2G connection degrades [2].

Department of Computer Science and Digital Technologies, London South Bank University, London, SE1 0AA, UK
E-mail: s4436857@lsbu.ac.uk; tdagiuklas@lsbu.ac.uk; elboudani@lsbu.ac.uk; e412038@lsbu.ac.uk
*Corresponding Author
Manuscript received 03 December 2025, accepted 04 December 2025, and ready for publication 31 December 2025.

In response to aviation stakeholders' requirements for IFBC services, the Next Generation Mobile Network Alliance (NGMN) has proposed key performance indicators (KPIs) for 5G use cases targeting mobile backhauling for aircraft in their 5G white paper [3]. Given their estimations, each user will have 15/(7.5) Mb/s download/(upload), so that 1.2/(0.6) Gb/s download/(upload) speed is required per aircraft, assuming 20% active users per aircraft and 400 passengers in each aircraft. These values significantly exceed the capacity of current DA2G systems, which typically achieve only a few hundred megabits per second per aircraft [4]. To meet such anticipated data rates, further integration of satellite systems within the evolving 5G standard is clearly required.

5G-satellite integration has already been playing a pivotal role in 5G standardisation. Initial studies on requirements for TN/NTN integration was captured in 3GPP (3rd Generation Partnership Project) Release 14 (R14), highlighting the added value that satellite coverage brings, as a complementary network forming part of the 5G paradigm, especially for mission-critical and industrial applications. 3GPP R15 was the first specification for 5G, and it introduced a study on New Radio (NR) support for non-terrestrial networks (NTN), examining potential architecture options and deployment scenarios. These included, for example, providing NTN-based broadband connectivity between the core network and cells located on board moving platforms such as aircraft or trains. R17, in contrast to earlier releases, was the first release to include normative specifications for NTN. It encompassed both Stage 1 requirements for defining what NTN services the 5G system should provide, as well as Stage 2 and Stage 3 protocol specifications detailing initial NTN functionalities. For example, R17 included normative Stage 3 requirements for UE initial attach procedures to NTN. It also included handovers between TN and NTN nodes, when satellites operate in transparent mode (bent-pipe architecture), meaning the satellite functions as a simple repeater, with all baseband processing functions remaining on the ground. R18 addressed further satellite integration under the new 5G-Advanced marker, including investigation of NTN backhauling, veryfing UE location information, and placing a UPF as satellite payloads. R19 still has satellite architecture evolution as a priority topic, and whilst previous releases focused on transparent payloads, R19 focuses on regenerative payloads where the NTN vehicle hosts 5G system functions. R19 also considers NR-NTN coexistence and functionalities such as store and forward (S&F) for increased resilience against NTN link

failures, mobility management, and a study item for user equipment (UE) multi-connectivity over NTN and TN nodes. Flexible integration and backhauling between TN and NTN is still under discussion, but will possibly build on 5G integrated access and backhaul (IAB) technology [5], evolving towards wireless access backhaul (WAB) nodes [6]. While both IAB and WAB nodes provide RAN access to UEs and perform wireless data forwarding for backhauling, IAB requires tight coupling between the IAB node and the IAB donor because the gNB functionality is split between the two entities. WAB nodes, in contrast, host the entire gNB stack and therefore offer a more flexible architecture, which could be beneficial in rapidly changing, dynamic networks, such as aerial networks. R20 is expected to be stabilised in 2027 and will include further upgrades for satellite networks, such as reduced UE dependency on the Global Navigation Satellite System (GNSS) when connected to NR-NTN for enhanced reliability, continued work on multi-connectivity over NTN, and improvements on narrowband IoT (NB-IOT) over NTN. In particular, R20 aims to enable NB-IoT voice services over GEO satellites, which could be used for emergency notifications. The R20 will be the last major release for 5G-Advanced and will also include study items for 6G networks (ITU-R's IMT-2030), which will start with R21. R21 is expected to natively integrate TN/NTN from the outset and not treat NTN as an add-on [7].

1.1. Structure of the Paper

This paper outlines different architecture options for integrated TN/NTN supporting IFBC services, as well as highlighting research challenges in this area.

The structure of the paper is as follows; Section 2 presents the state-of-the-art in TN/NTN integration, Section 3 presents three different TN/NTN architectures for IFBC, and research challenges to support IFBC in 5G/6G are outlined in Section 4.

2. State-of-the-Art in TN/NTN Integration

The requirements for 6G are specified by the International Telecommunication Union (ITU) in the ITU-R's IMT-2030 vision for 6G systems [8], which 3GPP R21 aims to satisfy. Of particular interest for this paper is the ambitious target of ubiquitous connectivity. Achieving this requires a complex, multi-layered architecture where both TN and NTN components operate cohesively as a single unified network. Traditional single-orbit satellite communication (SATCOM) systems such as Low Earth Orbit (LEO), Medium Earth Orbit (MEO), and Geostationary Orbit (GEO), offer distinct performance trade-offs: GEO provides high throughput and wide coverage but suffers from latency; LEO delivers low latency but requires frequent handovers and dense ground segment infrastructure; MEO provides intermediate performance but with limited flexibility. These constraints are well documented in ITU-R S.1716 and 3GPP R17 NTN specifications, which highlight the performance and interoperability challenges across orbital regimes.

2.1. Handovers

To reap the benefits of differentiated latencies, throughput, and coverage in an integrated TN/NTN network, efficient handover procedures are essential. 3G networks already introduced seamless mobility, allowing UEs to transition between cells without call drops. Over successive generations, handover performance has been continually optimised to the point of being almost imperceptible to the user. However, handovers either between NTN nodes or between TN and NTN nodes present additional challenges due to long satellite link delays, rapidly changing topologies that demand frequent handovers, unreliable feeder links, and limited processing capabilities on satellite payloads [9]. In 5G, R16 standardised conditional handovers (CHO) [10] for TN and R17 introduced a study item for CHO in NTN networks, which would address some of these challenges. CHO for NTN was later standardised in R18. Unlike traditional handovers, where the source gNB makes decisions based on periodic UE measurement reports, CHO works by having the gNB pre-configure rules for handovers, which the UE then executes autonomously. CHO reduces the NR Uu measurement traffic and shortens handover delays, which is particularly important when channel conditions degrade rapidly in highly dynamic networks. The trade-offs are additional complexity on the UE and reduced network control over resource management. CHO still relies on either the Xn or the N2 interface for the actual handover. In the case of satellites operating in regenerative mode the N2 handover procedure seems to be preferred since Xn communication is a challenge for multi-orbit satellite systems because of additional delays and mobility [11].

2.2. Multi-connectivity (MC)

Multi-connectivity (MC) enables concurrent connections across multiple carriers. Building on its success in terrestrial networks, the 3GPP introduced study items on MC support for satellite and integrated TN/NTN already in R16 and R17 (TR 38.821 and TR 23.737), but without any normative requirements. MC can be implemented at different layers of the protocol stack; carrier aggregation (CA) at the medium access control (MAC) layer and dual connectivity (DC) at the packet data convergence protocol (PDCP) layer, facilitating dynamic splitting and duplication of user traffic. This approach provides rapid adaptation to changing link qualities in real time, making CA and DC well-suited to address the challenges of multi-band multi-orbit (MBMO) satellite architecture. Theoretical analysis and experimental trials have demonstrated that MC significantly enhances data throughput, spectral efficiency, coverage, and reliability while lowering latency in NTNs [12]. This foundation has been primarily applied to networks limited to a single orbit or band.

3GPP R18 and the future R19 and R20 aim to enable seamless handovers and MC across LEO, MEO, and GEO assets, though it is still not clear if R20 will include any normative requirements for NTN MC. Introducing MC across TN and different satellite orbits adds spatial macro-diversity to the radio connection, which enhances resilience against both hardware failure and radio-link degradation [13]. Since the different radio links can operate over different frequencies and experience distinct radio channels, MC has the potential to enhance mission continuity under contested or degraded environments.

2.3. Multi-orbit SATCOM

Seamless integration between TN and NTN will allow global coverage and spectral efficiency in 3D space. Multi-orbit

SATCOM represents not only a technical evolution, but also a strategic necessity to safeguard decision advantage in multi-domain operations.

Multi-orbit SATCOM can offer a resilient, flexible, and globally available connectivity layer that can be integrated into NATO's Federated Mission Networking (FMN), which is an initiative to increase interoperability between coalition partners to enhance mission effectiveness. By leveraging LEO, MEO, and GEO systems in combination, FMN participants can benefit from assured communications that adapt to operational requirements, whether low-latency links for tactical edge operations or high-capacity GEO/MEO backhaul for strategic command. The integration of multi-orbit with FMN can be mapped to specific spiral specifications as follows:

- Core Mission Services & Interoperability: Multi-orbit SATCOM can provide mission-essential services (voice, data, video, etc.) over standardised interfaces to allow interoperability between national systems. Standardised SATCOM gateways and cross-domain solutions could allow seamless communication between coalition partners using heterogeneous systems even in bandwidth-constrained or denied areas where TN are unavailable.
- Cloud-Enabled Command and Control (C2) & Federated Services: By integrating software-defined networking (SDN) and network function virtualisation (NFV), multi-orbit SATCOM can provide adaptive routing and bandwidth-on-demand to support federated cloud-based mission services. This ensures reliable access to C2 applications, ISR (intelligence, surveillance, and reconnaissance) data, and coalition services hosted on FMN mission clouds.
- Mobility, Agility, and Mission Resilience: Multi-orbit SATCOM enhances secure mobile networking by enabling low-latency LEO links for tactical edge users, complemented by MEO/GEO for strategic backhaul. Seamless handovers and orbit diversity improve continuity of operations in highly mobile scenarios (e.g., maritime task groups, air operations, rapid deployment). Its inherent redundancy across orbits and bands also supports mission assurance in contested or denied environments.

Multi-orbit satellite communication systems rely on highly agile and adaptive hardware architectures capable of interfacing between GEO, MEO, and LEO satellites. One key enabler is the Multi-Layered Satellite System (MLSS) approach, where different orbital layers are tightly integrated to exploit their complementary strengths; GEO for wide coverage and stability; LEO/MEO for lower latency and higher link margins. These MLSS architectures have been demonstrated in systems that combine GEO and LEO capabilities to increase service resilience, latency performance, and coverage continuity [14].

Inter-satellite links (ISLs) and emerging inter-orbit links (IOLs) play pivotal roles in connecting satellites across orbits, thereby forming space information networks (SINs) [15]. SIN architectures incorporate ISLs and IOLs for in-space backhauling and enable real-time, high-throughput relay among satellites, reducing reliance on ground stations. Similar to how routing between RAN and core for TNs is outside the scope of 3GPP, routing over ISLs is also not standardised by 3GPP. Possible routing schemes include dynamic shortest path routing or predictive routing using the fact that aircraft and satellites move in a predictable path.

Multi-orbit SATCOM hardware must integrate advanced antenna and RF front-end technologies to support seamless communication across LEO, MEO, and GEO. Electronically steerable phased-array antennas and flat-panel designs (e.g., Kymeta u8, Intellian v240MT) replace bulky parabolic dishes, enabling agile beam steering, multi-band support (Ku/Ka/Ka-Q/V), and orbit diversity. Hardware integration also extends to RF front-end modules, which must accommodate multi-chain processing for concurrent links, and baseband chipsets that handle dual or multiple protocol stacks. Antenna miniaturisation, low-power amplifiers, and ruggedised designs are critical for defence and mobility scenarios. These architectures are evolving in line with 3GPP NTN standards (TR 38.811, TR 38.821), which define RF requirements and mobility support for NGSO systems.

2.4. QoS-aware Routing

Traditionally, user-plane traffic between the gNB and UPF, as well as between the DU and CU in O-RAN deployments, is transported inside a GTP-U tunnel. The GTP-U header is at least 8 bytes long and always contains a TEID (Tunnel Endpoint Identifier), which the receiver uses to map packets to the correct bearer or flow. The transport network between sender and receiver (midhaul or backhaul) has no visibility into the GTP-U payload, since it is encapsulated by UDP and IP headers. Intermediate routers forward packets solely based on the outer IP header, using routing protocols such as OSPF or IS-IS for IPv6. In static terrestrial networks dimensioned to carry all QoS flows without differentiation, this design works effectively and GTP-U was suitable for legacy, homogeneous, ground-based networks under the full control of the mobile operator. In dynamic and heterogeneous transport networks with limited capacity, such as integrated TN/NTN systems, GTP-U provides limited control and flexibility. SRv6 is being investigated as a programmable alternative that enables fine-grained flow steering and network visibility [16]. SRv6 integrates naturally with SDN controllers, which can compute routing paths centrally. The optimal placement and coordination of SDN controllers in TN/NTN deployments remains an open question. Furthermore, little research has been done on SRv6 for satellite-air-ground networks with wireless backhauling using either IAB or WAB technologies.

Replacing all network equipment and network functions from using GTP-U encapsulation to, for instance, SRv6 cannot be expected to be done quickly, and in the meantime, the Virtual Network Functions (VNFs) must be able to translate between encapsulations on a flow basis. Furthermore, in a diverse network, it might not even be desirable to enforce a single encapsulation scheme. [17] proposes the design of a polymorphic UPF which can serve different flows with different encapsulations by separating the data plane and control plane of the UPF, and implementing the user plane as a network of UPFs with one I-UPF (Intermediate-UPF) acting as a uplink classifier (UL-CL) diverting the traffic to different PSA-UPF (PDU Session Anchor-UPF) based on the encapsulation scheme.

2.5. Traffic Prediction

Although traffic prediction for individual gNBs and UPFs has been widely studied, approaches that model or predict traffic patterns across multiple interconnected entities are still limited. The authors in [18] propose an ML framework for predicting traffic for multiple UPFs simultaneously using Multi-Task Learning (MTL) and Multi-Core Parallel Computing (MCPC), where data from 91 consecutive days was used for learning traffic patterns. Obviously, this assumes a static topology with predictable traffic. In the case of TN/NTN integrated networks, there are few studies for predicting traffic per UPF.

3. Discussion of Different Architecture Options for Providing an Integrated TN/NTN Resilient Network for IFBC

This section examines different architecture options for providing seamless IFBC through TN/NTN integration within the 3GPP framework. First, background requirements are discussed as to what the architecture must support. After this, three different architectures are analysed, and they are also compared to each other in Table 1.

3.1. Requirements

The architecture solution must be able to provide IFBC to a wide variety of UEs ranging from different phones to wearables and smart flight sensors. For this reason, an on-board 5G radio is essential, as this will make the NR Uu interface identical to the terrestrial situation, and no modifications are needed for the UEs. Further, the architecture should preferably be able to cater to diverse use cases, some of which are listed below:

- Passenger connectivity to the ground network for services such as video streaming, voice calls, or telehealth monitoring. Premium access may be offered.
- While safety-critical air traffic control (ATC) communication is currently based on dedicated radio systems [19], future 5G-Advanced or 6G systems could support integration under stringent isolation and reliability guarantees.
- On-board IoT networks with local processing before sending aggregated data to ground networks. The NFV-orchestrator (NFVO) would need to deploy a lightweight on-board UPF for local breakout while maintaining control-plane synchronisation with ground-based core functions.
- On-board entertainment systems delivered over 5G. Similar to the previous case, this requires orchestration between an on-board UPF and the ground network.

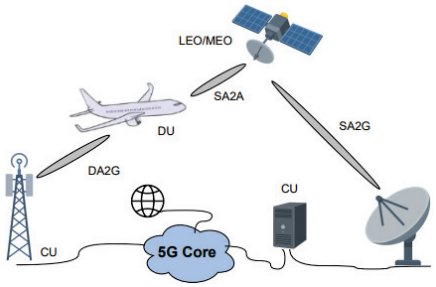

Figure 1.
In-flight connectivity, AO1. Note that the DA2G, SA2A, and SA2G could be propriatary interfaces.

Clearly, the above use cases show diverse requirements regarding link reliability, throughput, and latency. Using the unique characteristics of a TN/NTN integrated network, each traffic flow needs optimal and flow-dedicated routing to meet the required SLAs. The routing needs to make use of the diverse characteristics of the different links (A2A, SA2G, ISL, IOL, etc.) when it comes to reliability, throughput, and latency.

3.2. Architecture Option 1 (AO1) -- DU/CU-split

One alternative for providing IFBC would be to split the gNB between a DU and a CU, where the DU is placed on the aircraft and provides connectivity within the plane, as shown in Fig. 1. There are eight different split options (SO) but one of the strongest contenders for NTN is SO 2 [20]. SO 2 places the RRC and PDCP in the CU whereas RLC and lower-layer RAN functions are placed on the DU. The SO 2 interface between the DU and CU is named the F1 interface and is standardised within 3GPP. This SO is also one of the SO advocated by the O-RAN Alliance in their 7-2x split for TN. SO 2 is a reasonable option because it allows IP-based connectivity between the DU and CU, and the interface is less time-sensitive than other higher-level SO. Although there is no 3GPP-specified time constraint for the F1 interface between the CU and DU, this interface was not designed for large delays, and [21] asserts the delay over the F1 interface should be within 10 ms in a TN setting. The delay sensitivity makes the network very sensitive to radio-link failures and intermittent connectivity.

Although a longer delay between CU and DU in SO 2 might be possible by adjusting timing parameters, it seems unreasonable that a GEO satellite could be used either in transparent mode or in regenerative mode using the CU/DU split since the one-way delay between aircraft and GEO already may exceed 200 ms. Using this split, the CU would most likely have to reside on the ground, and

Table 1.

Comparison of IFBC connectivity architectures: CU/DU, IAB, and WAB							
Architecture	**On-board Code Complexity**	**3GPP-Specified Node-to-Node Communication**	**Max Intermediate Hops**	**Delay Tolerance**	**Local UPF Breakout**	**Mobility Support**	**Resilience to Link Failure**
CU/DU (AO1)	Low	No	0	Low	No	Low	Low
IAB (AO2)	Medium	Yes	Multiple	Low	No	Medium	Medium
WAB (AO3)	High	Yes	0 (R19)	High	Yes	High	High

the onboard DU would communicate with it either via a DA2G link or via LEO/MEO satellites operating in transparent mode.

The IP-based midhaul between the DU and CU is not defined by 3GPP, and in the case of DU on board an aircraft and CU on the ground, this link will be vendor dependent. Additionally, because of the separation of DU and CU, all user traffic must leave the aircraft. This means that although the aircraft could host an on-board entertainment portal or other services, traffic must still pass through the ground CU and ground core before being routed back to the on-board server. This introduces extensive delays and defeats the purpose of on-board hosting.

3.3. Architecture Option 2 (AO2) -- IAB

Integrated access and backhauling (IAB) was first specified by 3GPP in R16 for terrestrial deployment as an extension of LTE relay nodes from R10. The technology was aimed at rapidly expanding 5G coverage by enabling wireless backhauling between an IAB donor and one or multiple IAB nodes. The IAB-node consists of an IAB-DU providing connectivity to UEs and an IAB-MT which wirelessly connects to the IAB parent node over the standard NR Uu interface. 3GPP R17 has further developed IAB, allowing for IAB-donor handovers using the XnAP IAB protocol, which enables IAB mobility. However, it must be noted that inter-IAB handovers are significantly more complicated than a normal UE handover, and no implementation has been commercially deployed on a large scale.

IAB could potentially be used in NTN settings, as presented in [5]. One IAB node must be placed within the aircraft to provide IFBC, and the IAB donor containing the CU would probably be best situated on the ground for the same reasons as in Architecture Option 1 (AO1). The main difference between this option and AO1 is that IAB allows for multi-hop routing between IAB nodes, and the interface between IAB nodes and the IAB donor is the 3GPP NR Uu interface. Reusing the Uu interface for routing reduces the risk for a plethora of vendor-specific solutions forcing vendor lock-in.

Using IAB with multi-hopping, aircraft could potentially route traffic to the donor through satellites, other aircraft, or ground-based IAB nodes, as illustrated in Fig. 2. The additional routing freedom stemming from multi-hopping, increases redundancy and resilience to link failures. However, due to latencies, the number of hops must be limited, and using GEO satellites should be avoided. Furthermore, the rapidly changing topology would incur substantial signalling overhead and frequent inter-IAB-donor handovers. As in AO1, all traffic must go through the ground core, which does not allow local breakout to an on-board MEC cloud, for instance, used to provide an in-flight entertainment portal.

3.4. Architecture Option 3 (AO3) -- WAB and MEC

Whereas both AO1 and AO2 deploy a DU on the aircraft, this option investigates placing the entire gNB stack on the aircraft. This option removes the problem of F1 delays at the expense of additional computational complexity needed on board the aircraft. The gNB communicates with the core via the N2 (gNB-AMF) and N3 (gNB-UPF) interfaces, which are not as sensitive to delays as

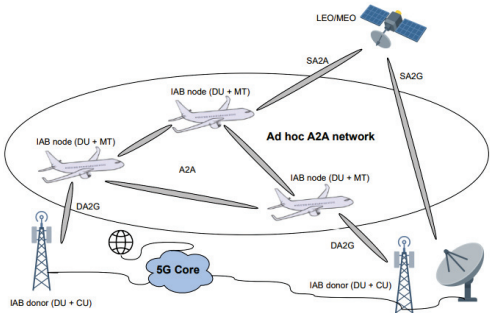

Figure 2.
In-flight connectivity, AO2. Note that the A2A, SA2A, and DA2G interfaces are 3GPP standardised.

the F1 interface. This opens up additional possibilities, where, for instance, GEO satellites could be used. The technology that allows for placing a complete gNB on the aircraft and routing traffic through different nodes is wireless access and backhauling (WAB). WAB is introduced in 3GPP R19 and is an extension of IAB. A WAB node consists of two parts: the WAB-gNB and the WAB-MT. The WAB-gNB connects to UEs over the NR Uu interface, and the WAB-MT connects to an upstream gNB over the NR Uu interface as well. The WAB-MT opens a new PDU session carrying both user data and NG/Xn signalling. This PDU session terminates at a PDU session anchor UPF (PSA-UPF), and the UE user data is forwarded to the serving UPF from the PSA-UPF. The fact that the WAB-MT attaches to the upstream gNB as a UE with a dedicated UPF allows for buffering both at the WAB-MT and at the UPF. This, together with less strict latencies over the N2/N3 interface, should make this architecture more robust to link failures and intermittent connectivity. Although R19 only considers single-hop WAB, it is probable that future releases will investigate multi-hop WAB as well.

As long as the PSA-UPF remains the same, a handover between the WAB-MT and a source and target gNB would be the same as a normal UE handover. However, if the PSA-UPF has to change, a new PDU session must be established, which is time-consuming and adds delay.

Since this architecture places an entire gNB on the plane, MEC clouds could be placed on board in either the aircraft or satellite, and traffic could be routed to the cloud through an on-board lightweight UPF. This would enable, for instance, an on-board entertainment portal with very low latencies or local processing of flight sensor data. The on-board UPF could potentially use UL-CL to apply differentiated routing in uplink. Some traffic could exit the 5GS directly on the plane and route to a DN, for instance, the Internet using Starlink. Other traffic could still route to the ground UPF. Additionally, the on-board UL-CL UPF could also enable store and forwarding (S&F) capabilities to increase resilience against intermittent connectivity [22].

When deploying an on-board UPF, N2/N4 signalling would still need to be routed to the ground core. It must be noted that AMF handover events would be very rare, and the Xn interface would probably also not be frequently used in the given scenario. Combining an on-board UPF with WAB would increase redundancy for user traffic and also enforce signalling to stay within the 3GPP framework.

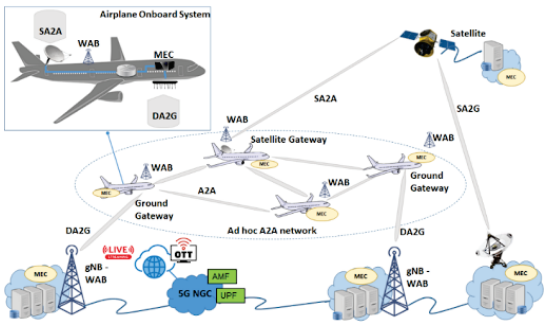

Figure 3.
In-flight connectivity, AO3.

A potential future architecture based on WAB with MEC is illustrated in Fig. 3. The 5G services can be delivered either through the 5G direct air-to-ground (DA2G) service or through the satellite air-to-ground (SA2G) service when there is no option to connect to a ground station, for instance, when flying over the sea. Moreover, the proposed architecture enables aircraft-to-aircraft (A2A) connectivity, which can be used when the aircraft is flying in airspace above land borders where terrestrial coverage starts to diminish and can benefit from backhauling through other aircraft.

3.5. Comparison Between the Three Architecture Options

The three different architecture options are compared in Table 1, where the following fields were used for the comparison:

- *On-Board Code Complexity*: The software running on an aircraft should be kept as simple as possible due to strict constraints on energy, cooling, and weight, each of which affects fuel consumption.
- *3GPP-Specified Node-to-Node Communication*: As the telecommunications industry moves toward open interfaces to avoid vendor lock-in and improve transparency, it is advantageous for air–satellite–ground wireless links to use open, standardised interfaces such as those defined by 3GPP.
- *Max Intermediate Hops*: To extend coverage, nodes may route traffic through intermediate airborne nodes, enabling concepts such as ad-hoc A2A networks.
- *Delay Tolerance*: Highly dynamic environments lead to intermittent connectivity and fluctuating throughput. The architecture should tolerate link outages and variable delays without degrading essential services.
- *Local UPF Breakout*: Support for a local on-board UPF enables delay-sensitive or mission-critical applications to run directly on the aircraft, avoiding unnecessary routing through ground-based core networks.
- *Mobility Support*: Given the rapidly changing network topology, the architecture should support fast and seamless reconfiguration to maintain service continuity during movement.
- *Resilience to Link Failures*: Air-to-air, air-to-satellite, and air-to-ground links can change or fail unexpectedly. A resilient architecture must enable rapid rerouting and robust handling of link disruptions.

4. Research Challenges

This section outlines some research challenges that must be addressed for IFBC.

4.1. Antenna Design

In-flight 5G services will require antenna designs that operate at 5G NR-NTN frequencies used by both 5G NR A2G and NTN satellite bands (FR1, FR2) and adopt a proactive stance to maintaining beam-locking and synchronisation, given the challenging atmospheric environment and the changing position of the aircraft. Smart localisation based on angle of arrival (AoA) is a proven beam-management technique. Moreover, contemporary aircraft can include up to 25 protruding antennas, which not only disrupt the aircraft's aesthetics but also result in significant aerodynamic drag and increased fuel consumption, introducing the need for antennas to be conformal to the body of the aircraft [23]. How to provide conformal designs for aircraft applications that operate at mmWave (millimetre-wave) frequencies with adaptive multibeam formation based on intelligent localisation to achieve high-throughput transmission while maintaining beam-locking and synchronisation is an open issue, but could be based on planar leaky-wave and surface-wave technologies [24]. The compact and conformal design must offer low dielectric losses and moisture resistance to ensure reliable performance in harsh environments. Future antenna systems should support spatial beam scanning for DA2G (Direct Air-to-Ground) and inter-aircraft links exceeding current multi-beam capabilities to support both static and dynamic beam formation.

4.2. WAB-routing

Although R19 introduces WAB, WAB has not been examined for NTN scenarios, and further investigations are needed to see if a WAB-MT could backhaul via a satellite using NR-NTN. As of R19, WAB is also limited to a single hop, which would exclude ad-hoc meshes from being formed between aircraft using WAB. Future research on WAB for NTN and ad-hoc A2A networks is needed.

4.3. Transport Network Routing

In current and legacy mobile networks, the transport network between the RAN and the core has typically been static and homogeneous, supporting conventional dynamic routing protocols such as OSPF or slice-dedicated transport using MPLS. In future TN/NTN integrations, where gNBs may reside on moving platforms, transport-level slice management becomes significantly more complex and critical. This calls for intelligent and adaptive routing strategies that account for real-time topology changes and the intermittent nature of aerial network connectivity, where

feeder links to the ground infrastructure may not always be available.

4.4. Self-organising Networks

Self-organising networks (SON) functionalities are being standardised in order to ensure automatic management procedures in 5G systems, and several studies are being pursued in order to have an autonomously managed network [25]. ML technology in 5G and beyond is having widespread adoption for intelligent decision-making solutions, such as automatic systems for managing network slices [26]. Going a step further, there are a limited number of studies that demonstrate how intelligence and SON can be applied to network slicing to ensure effective and autonomous resource reservation in integrated TN-NTNs within the ETSI frameworks ZSM (Zero-touch network and Service Management), GANA (Generic Autonomic Networking Architecture), and ENI (Experiential Network Intelligence). Considering the Architecture Option 3 (AO3) with an on-board MEC hosting a local UL-CL UPF and connected to the ground core via an ad-hoc A2A network, optimal routing, NF orchestration, and life management are necessary. How to best implement the SON logic in such a dynamic network is an open research question.

5. Conclusion

The telecommunication industry is clearly moving towards native integration between TN and NTN to meet the demand for reliable, secure, and ubiquitous coverage with guaranteed QoS. Native integration will enable applications such as IFBC and mission-critical services, yet several barriers remain before large-scale deployment can be achieved. In particular, aircraft antenna design must advance to reduce drag and enable robust connectivity across LEO, MEO, and GEO systems, and intelligent handover mechanisms are needed to manage mobility across TN/NTN environments with minimal overhead and interference. Cognitive and slice-aware routing over the transport network is needed and has to be synchronised with the VNFO to ensure SLAs are met for all traffic flows.

The paper compared different architecture options for providing IFBC. In particular, a novel architecture where aircraft and satellites are mobile WAB nodes capable of acting as both access and backhaul nodes was proposed. Each node could potentially host MEC for latency-sensitive services, where a lightweight UPF could be deployed for local breakout. Whereas this architecture offers high flexibility and the potential to support a broad range of applications, its success will depend on the development of advanced SON functionalities, AI-driven network optimisation, and proactive handover solutions. Future research should therefore focus on predictive mobility management, cross-layer optimisation, and adaptive resource allocation to fully realise the vision of seamless TN/NTN integration for IFBC.

Acknowledgement

This research has been financed by the European Commission HORIZON-MSCA-2024-SE-01-01 under grant agreement no. 101236523 (AeroNet project).

References

[1] LSE Consulting, "Sky High Economics: Chapter One," Research report, London School of Economics and Political Science (LSE), n.d, accessed: 24 September 2025.
[2] D. T. AG.
[3] NGMN Alliance, "5G White Paper," 2015, accessed: 2025-09-25.
[4] S. Hoppe, "High-Throughput Air-to-Ground Connectivity for Aircraft," 2021.
[5] D. Pugliese, M. Quadrini, D. Striccoli, C. Roseti, F. Zampognaro, G. Piro, L. A. Grieco, and G. Boggia, "Integrating terrestrial and non-terrestrial networks via IAB technology: System-level design and evaluation," *Computer Networks*, vol. 253, p. 110726, 2024.
[6] X. Lin, "The Bridge Toward 6G: 5G-Advanced Evolution in 3GPP Release I9," *IEEE Communications Standards Magazine*, vol. 9, no. 1, pp. 28–35, 2025.
[7] X. Lin, "A Tale of Two Mobile Generations: 5G-Advanced and 6G in 3GPP Release 20," *arXiv preprint arXiv:2506.11828*, 2025.
[8] ITU 2025, "IMT towards 2030 and beyond (IMT-2030)," Accessed: 2025-09-25.
[9] A. A. Alsaeedy, M. K. Mohsen, and E. K. Chong, "5G/6G TN-NTN Coexistence: Perspectives on Seamless Service and Handover Management," *IEEE Network*, 2025.
[10] J. Stanczak, U. Karabulut, and A. Awada, "Conditional handover in 5G-principles, future use cases and FR2 performance," in *2022 International Wireless Communications and Mobile Computing (IWCMC)*, pp. 660–665, IEEE, 2022.
[11] 5G Americas, "5G and Non-terrestrial networks, White paper," 2022, accessed: 2025-10-29.
[12] B. Shang, X. Li, Z. Li, J. Ma, X. Chu, and P. Fan, "Multi-connectivity between terrestrial and non-terrestrial mimo systems," *IEEE Open Journal of the Communications Society*, vol. 5, pp. 3245–3262, 2024.
[13] R.-J. Reifert, Y. Karacora, C. Chaccour, A. Sezgin, and W. Saad, "Resilience and criticality: Brothers in arms for 6G," *arXiv preprint arXiv:2412.03661*, 2024.
[14] M. Höyhtyä, A. Anttonen, M. Majanen, A. Yastrebova-Castillo, M. Varga, L. Lodigiani, M. Corici, and H. Zope, "Multi-Layered Satellite Communications Systems for Ultra-High Availability and Resilience," *Electronics*, vol. 13, no. 7, 2024.
[15] H. Al-Hraishawi, M. Minardi, H. Chougrani, O. Kodheli, and J. Montoya, "Multi-layer Space Information Networks: Access Design and Softwarization," 10 2021.
[16] Z. Mo and B. Long, "An Overview of SRv6 Standardization and Application towards 5G-Advanced and 6G," in *2022 IEEE 5th International Conference on Computer and Communication Engineering Technology (CCET)*, pp. 266–270, 2022.
[17] Y. Zhao, X. Liao, and M. Wang, "Multi-UPF: A Multi-Protocol Forwarding UPF towards 6G," in *2023 International Conference on Future Communications and Networks, FCN 2023 – Proceedings*, Institute of Electrical and Electronics Engineers Inc., 2023.
[18] Y. Su, H. Ma, B. Chen, Z. Ma, T. Wang, D. Ge, Z. Li, and S. Wang, "Multi-UPF Traffic Prediction of 5G Core Network With Multi-Task Learning and Multi-core Parallel Computing," in *Proceedings of the IEEE International Conference on Computer and Communications, ICCC*, pp. 2260–2264, Institute of Electrical and Electronics Engineers Inc., 2024, this article proposes a machine learning approach for predicting UPF traffic of multiple UPFs simultaneously instead of only focusing on one UPF at a time. They proposed a framework of how to utilise multiple cores for the predictions.
[19] L. Ren and M. Castillo-Effen, "Air Traffic Management (ATM) operations: a review," *Report 2017GRC0222*, 2017.
[20] A. Daurembekova and H. D. Schotten, "Unified 3D Networks: Dynamic RAN Functions Placement and Link Challenges," in *2024*

International Symposium on Networks, Computers and Communications (ISNCC), pp. 1–6, IEEE, 2024.

[21] E. Municio, G. Garcia-Aviles, A. Garcia-Saavedra, and X. Costa-Pérez, "O-ran: Analysis of latency-critical interfaces and overview of time sensitive networking solutions," *IEEE Communications Standards Magazine*, vol. 7, no. 3, pp. 82–89, 2023.

[22] H. Yoo, M. Park, and N. Ko, "A Mobile System Architecture for Store-and-Forward Operation in Non-Terrestrial Networks," in *2025 Sixteenth International Conference on Ubiquitous and Future Networks (ICUFN)*, pp. 709–712, IEEE, 2025.

[23] A. V. SE, S. J, and T. Kavitha, "Conformal Antenna for Aircraft Applications," in *2023 7th International Conference on Computation System and Information Technology for Sustainable Solutions (CSITSS)*, pp. 1–7, 2023.

[24] Y. Ma, X. Shi, J. Wang, Y. Zhang, F. Sun, and F. Wu, "Millimeter-Wave Conformal Directional Leaky-Wave Antenna Based on Substrate-Integrated Waveguide," *Electronics*, vol. 12, no. 14, 2023.

[25] A. G. Papidas and G. C. Polyzos, "Self-Organizing Networks for 5G and Beyond: A View from the Top," *Future Internet*, vol. 14, no. 3, 2022.

[26] H. O. Otieno, B. Malila, and J. Mwangama, "Deployment and Management of Intelligent End-to-End Network Slicing in 5G and Beyond 5G Networks: A Systematic Review," *IEEE Access*, vol. 12, pp. 190411–190433, 2024.

Biographies

Christoffer Hjalmarsson holds a Bachelor's degree in Physics from Chalmers University of Technology and two Masters' degrees in System and Control Theory from Chalmers University of Technology and the University of Stuttgart. He previously worked as a software engineer at Ericsson and is now pursuing a PhD at London South Bank University since October 2025, focusing on TN/NTN integration and IFBC.

Tasos Dagiuklas is a Professor in the Computer Science and Informatics Division at London South Bank University and Head of the Cognitive Systems Research Centre. His research spans cloud computing, 5G/O-RAN, network automation, edge/fog computing, and intelligent systems for smart cities, health, and manufacturing. He holds a PhD from the University of Essex and an MSc from the University of Patras. He has secured over £10 million in UK and EU research funding, collaborated widely with academia and industry, published extensively in IEEE, and serves on editorial boards of several international journals.

Brahim El Boudani is a Lecturer in Applied Artificial Intelligence and Computer Science at London South Bank University (LSBU). He holds a PhD in 3D Indoor Localisation for 5G Networks and is a researcher within the Smart Internet Technologies Hub (SITHub) group, focusing on programmable networks, intelligent routing, and other AI applications to next-generation networking technologies (6G and beyond). He has extensive industry experience from working with organisations in Cyprus, Portugal, and across Europe.

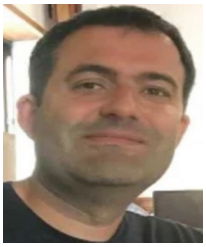

Jonathan Rodriuguez is a Professor of Mobile Communications at the University of South Wales and is an Honorary Senior Researcher at the University of Bradford. His area of expertise includes: 5G mobile systems, Terahertz communications, 2D system level simulation methodologies, and beamforming. His research work have resulted in over 500 published scientific works and 4000 citations. Professor Rodriguez is an IET Fellow and a Charted Engineer with advisory roles on FP7, and CSIM as well as being the founding member of IEEE Technical Subcommittee on Green Communications and Computing.

DOI. No. 10.13052/2794-7254.023

Reconfigurable Intelligent Surfaces in Cooperative NOMA: A Review of Key Concepts and Applications

M. Ramadevi, Manuuru Naga Sree Lekha, V. Phanitha Sree and Madha Sai Prashanth Goud*

Abstract: The purpose of this survey paper is to provide an overview of the different multiple access techniques, the reason for integrating Reconfigurable Intelligent Surfaces (RIS) with Cooperative Non-Orthogonal Multiple Access (C-NOMA) and the system model of RIS-aided C-NOMA with mathematical equations. The study discusses other 6G technologies and contributes to understanding how RIS-aided C-NOMA together with the other 6G technologies comes close to realizing the goals 6G wireless networks. The paper presents the real-world applications of RIS-aided C-NOMA along with challenges and possible solutions on which upcoming researchers can focus on.

Keywords: 6G wireless communication, cooperative NOMA, energy efficiency, reconfigurable intelligent surface (RIS), successive interference cancellation (SIC).

1. Introduction

Each generation of wireless communication has introduced a new multiple access paradigm – from Frequency Division Multiple Access (FDMA) in 1G and Time Division Multiple Access (TDMA) / Code Division Multiple Access (CDMA) in 2G and 3G, to Orthogonal Frequency Division Multiple Access (OFDMA) in 4G. Although these techniques have progressively improved performance, they fundamentally rely on orthogonality, which inherently limits spectral efficiency and user connectivity. To overcome these constraints, Non-Orthogonal Multiple Access (NOMA) was introduced in 5G systems, allowing multiple users to share the same frequency resources through power-domain multiplexing [1].

While NOMA improves spectral efficiency and supports massive connectivity, its performance is still limited due to far users' poor channel conditions. In order to address it, Cooperative NOMA extends NOMA by allowing the near users to become relays, which forward the signal to far users, improving coverage and fairness [2]. However, the performance of these C-NOMA systems still degrades under severe channel fading [3], which is addressed by the integration of C-NOMA with RIS. It can dynamically adjust the signal properties to reconfigure the wireless environment, capable of converting non-line-of-sight links into constructive reflective paths [4]. This capability has significantly enhanced the reliability and energy efficiency of cooperative transmissions.

Hence, through this paper, we discuss the basic model of RIS-aided C-NOMA system and explore the different researches on it (see Section 2), see how this technology fits along with other 6G enabling technologies (see Section 3) and the applications of the technology in real world (see Section 4). The conclusion of this paper summarizes the finding and highlights the practical challenges in realizing the system and also suggest potential solutions for future researches to mitigate the challenges (see Section 5). To improve clarity and ease of reading, Table 1 presents the full forms of abbreviations used throughout this paper.

2. The System Model

2.1. RIS and C-NOMA

2.1.1. *RIS*

RIS is a 2D surface made of an array of programmable reflecting units called meta-atoms which reconfigure the environment properties by adjusting the reflecting signal's phase, amplitude, frequency and polarization as required. The principle of RIS can be explained via two approaches: physics-based and communication-based. According to physics, beamforming and reflections can be achieved by electrical, thermal or mechanical tuning of surface impedance. In communication terms, a virtual LoS path is created between the base station and the receiving user by the RIS [4]. RIS can be easily installed on walls, advertisement boards and even on moving vehicles. Figure 1 shows the picture of an RIS of order (3×3).

RIS is broadly of two types: passive RIS, which does not provide amplification and is used for comparatively shorter distances due to the decrease in capacity gain in certain conditions because of multiplicative fading effect, and active RIS, which amplifies the reflected signal and is best suited for long distance communication, though it consumes more power and introduces noise [5]. Next, we discuss about C-NOMA.

2.1.2. *C-NOMA*

C-NOMA enhances spectral and energy efficiencies by incorporating relays that help in forwarding the information from the

Department of Electronics and Communication Engineering, VNR VJIET, Hyderabad, Telangana, India – 500090
E-mail: ramadevi_ece@vnrvjiet.in; mnslekha@gmail.com; phanithavemulapalli1111@gmail.com; madhasaiprashanth@gmail.com
*Corresponding Author
Manuscript received 06 April 2025, accepted 20 November 2025, and ready for publication 31 December 2025.

Table 1.

Full forms of abbreviations used in the paper			
Abbreviation	**Full Form**	**Abbreviation**	**Full Form**
RIS	Reconfigurable Intelligent Surface	C-NOMA	Cooperative Non-Orthogonal Multiple Access
FDMA, OFDMA	Frequency Division Multiple Access, Orthogonal Frequency Division Multiple Access	TDMA, CDMA	Time Division Multiple Access, Code Division Multiple Access
DF, AF	Decode-and-Forward, Amplify-and-Forward	SIC	Successive Interference Cancellation
AWGN	Additive White Gaussian Noise	MIMO	Multiple Input Multiple Output
HD, FD	Half Duplex, Full Duplex	SE, EE	Spectral Efficiency, Energy Efficiency

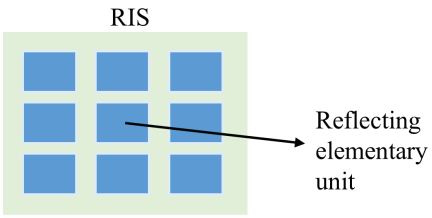

Figure 1.
RIS of Order (3×3), $M = 9$.

source to the far users. C-NOMA systems are classified as user-relaying based C-NOMA systems, where the near user—the strong user—acts as a relay for the far user—the weak user—and, relay-assisted C-NOMA systems where a dedicated relay node is used in place of the near user to forward the signal to the far user. Relays are much suited for scenarios where the user distribution is asymmetric or unpredictable [6].

Relaying of information can be done in two ways: decode-and-forward (DF), where the near user separates far user's signal using Successive Interference Cancellation (SIC) and relays the decoded signal after encoding it to the far user and, amplify-and-forward (AF), where the near user just amplifies the signal it receives from the source and forwards it to the far user. The noise accumulation is less in DF while the complexity of the process is less in AF. In the next subsection, we will discuss how RIS is incorporated in C-NOMA, about the system architecture, channel coefficients, phase shift matrices and performance metrics.

2.2. RIS-aided C-NOMA

We consider a downlink RIS-aided C-NOMA system consisting of a Base Station (BS), an RIS with M passive reflecting elements, and two users: the near user, U_N (acting as a DF relay), and the far user, U_F (see Fig. 2(b)). Notions used in this paper are describes in Table 2.

The channel coefficient between any two nodes i and j is represented by h_{ij}, defined by $h_{ij} = \sqrt{L_{ij}} g_{ij}$, where L_{ij} is the deterministic path loss and g_{ij} is the small-scale fading component. For paths involving the RIS, channels are modeled as vectors. We denote the channel vector from the BS to the RIS as $\mathbf{h}_{BR} \in \mathbb{C}^{M\times 1}$, the channel vector from the RIS to U_N as $\mathbf{h}_{RN} \in \mathbb{C}^{M\times 1}$, and similarly for the channel vector from U_N to the RIS, $\mathbf{h}_{NR}$ and the

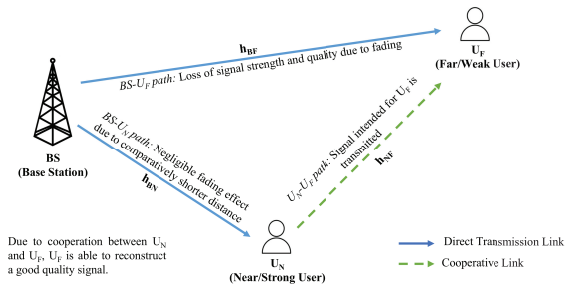

(a) Cooperative NOMA system with a single Base Station (BS) and two users: U_N and U_F.

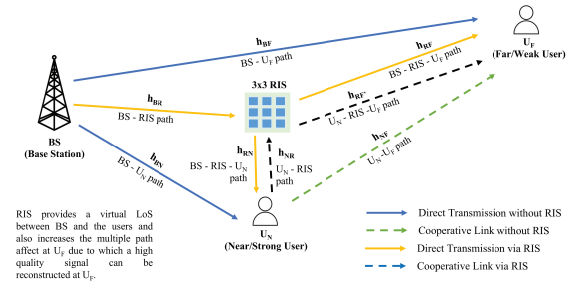

(b) RIS-aided C-NOMA System with a single Base Station (BS), two users: U_N and U_F and RIS with $M = 9$.

Figure 2.
System model comparison.

channel vectors associated with the link from the RIS to U_F, $\mathbf{h}_{RF}$ and $\mathbf{h}_{RF'}$. The direct channels are denoted by scalars h_{BN} (channel coefficient from BS to U_N), h_{BF} (channel coefficient from BS to U_F), and h_{NF} (channel coefficient from U_N to U_F) [4, 7, 8].

The RIS applies a diagonal phase-shift matrix $\mathbf{\Phi} \in \mathbb{C}^{M\times M}$ [9],

$$\mathbf{\Phi} = \text{diag}(e^{j\phi_1}, e^{j\phi_2}, \ldots, e^{j\phi_M}) \tag{1}$$

We consider the total transmit power at the BS as P_T. The superimposed signal X is given by [10]

$$X = \sqrt{\alpha P_T} x_N + \sqrt{(1-\alpha) P_T} x_F \tag{2}$$

where α is the power allocation factor for the near user U_N. According to the standard NOMA power allocation constraint,

Table 2.

Notations used in the paper			
Notation	**Description**	**Notation**	**Description**
BS	Base Station	U_N, U_F	Near/Strong User, Far/Weak User
L	Deterministic Path Loss	g	Small-scale Fading Component
X	Superimposed signal of x_N and x_F	x_N, x_F	Signal to be sent to U_N, Signal to be sent to U_F
P_T	Total Power with which X is transmitted from BS	M	Number of reflecting units in RIS
Φ	Diagonal Phase-Shift Matrix	h_{BN}	Channel Coefficient from BS to U_N
h_{BF}	Channel Coefficient from BS to U_F	h_{NF}	Channel Coefficient from U_N to U_F
h_{BR}	Channel Vector from BS to RIS	h_{RN}	Channel Vector from RIS to U_N
$h_{RF}, h_{RF'}$	Channel Vector from RIS to U_F during direct transmission phase, Channel Vector from RIS to U_F during cooperaton phase	h_{NR}	Channel Vector from U_N to RIS
y_N	Signal received by U_N from BS	w_N	AWGN during transmission of signal through BS-U_N path
y_{F1}	Signal received by U_F from BS	w_{F1}	AWGN during transmission of signal through *BS-U_F* path
y_{F2}	Signal received by U_F from U_N	w_{F2}	AWGN during transmission of signal through U_N-U_F path

the user with the better channel receives less power, meaning $1-\alpha > \alpha$ since U_F is the weak user. Thus, we assume $\alpha < 0.5$ [11].

In general, there are two channel modes that can be used: half duplex (HD) and full duplex (FD) [12]. We adopt half duplex (HD) channels and divide the transmission of information into two stages: direct transmission phase and cooperation phase. Hence, transmission of information is considered to be done in two time slots. In the first time slot, which is the direct transmission phase, BS transmits X to both U_N and U_F. In the second time slot, U_N transmits the decoded information x_F to U_F [10]. Note that $\mathbf{h}_{RF'} = \sqrt{L_{RF'}} g_{RF'}$, where $L_{RF'}$ and $g_{RF'}$ are the deterministic path loss and the small-scale fading component respectively for RIS-U_F path during the cooperation phase.

2.2.1. *Direct transmission phase*

The BS transmits X. The RIS applies phase shifts $\mathbf{\Phi}_N$ to optimize the link to U_N, where $\mathbf{\Phi}_N$ is the phase-shift matrix for BS-U_N communication. The effective channel gain from the BS to U_N, $h_{eff,N}$, accounts for both the direct and reflected paths [4,10,13]:

$$h_{eff,N} = h_{BN} + \mathbf{h}_{RN}^T \mathbf{\Phi}_N \mathbf{h}_{BR} \tag{3}$$

Without RIS, $h_{eff,N}$ remains as h_{BN} only. The difference in the channel links can be clearly seen in Fig. 2.

The received signal at U_N is

$$y_N = h_{eff,N} X + w_N \tag{4}$$

where $w_N \sim \mathcal{CN}(0, \sigma_N^2)$ is AWGN and σ_N^2 is the noise power at U_N.

U_N performs SIC: it first decodes x_F, treating x_N as interference. The SINR for decoding x_F at U_N is:

$$\gamma_{F \to N} = \frac{|h_{eff,N}|^2 (1-\alpha) P_T}{|h_{eff,N}|^2 \alpha P_T + \sigma_N^2} \tag{5}$$

Assuming successful decoding, U_N removes x_F and then decodes its own signal x_N. The SINR for decoding x_N at U_N is:

$$\gamma_{N \to N} = \frac{|h_{eff,N}|^2 \alpha P_T}{\sigma_N^2} \tag{6}$$

Similarly, U_F receives X from BS via RIS. The RIS applies $\mathbf{\Phi}_{F1}$. The effective channel $h_{eff,F1}$ is given as,

$$h_{eff,F1} = h_{BF} + \mathbf{h}_{RF}^T \mathbf{\Phi}_{F1} \mathbf{h}_{BR} \tag{7}$$

Without RIS, $h_{eff,F}$ remains as h_{BF} only.

The SINR for x_F is:

$$\gamma_{F1} = \frac{|h_{eff,F1}|^2 (1-\alpha) P_T}{|h_{eff,F1}|^2 \alpha P_T + \sigma_{f1}^2} \tag{8}$$

where $w_{F1} \sim \mathcal{CN}(0, \sigma_{F1}^2)$ is AWGN and σ_{F1}^2 is the noise power at U_F during direct transmission phase.

2.2.2. *Cooperation phase*

U_N re-encodes the decoded x_F and forwards it with transmit power to U_F via RIS. The RIS applies $\mathbf{\Phi}_{F2}$. The effective channel $h_{eff,F2}$ is given as,

$$h_{eff,F2} = h_{NF} + \mathbf{h}_{RF}^H \mathbf{\Phi}_{F2} \mathbf{h}_{NR}. \tag{9}$$

Without RIS, $h_{eff,F2}$ remains as h_{NF} only.

The received signal at U_F is

$$y_{F2} = h_{eff,F2} X + w_{F2} \tag{10}$$

where $w_{F2} \sim \mathcal{CN}(0, \sigma_{F2}^2)$ is AWGN and σ_{F2}^2 is the noise power at U_F during cooperation phase.

The SINR for x_F is:

$$\gamma_{F2} = \frac{|h_{eff,F2}|^2 P_R}{\sigma_{f2}^2} \tag{11}$$

Table 3.

Comparison of review papers on RIS-aided cooperative NOMA				
Authors	**Year**	**Title**	**Strengths**	**Limitations**
Zhu et al.	2024	A review of RIS-assisted wireless communication research	Details the comparison of active and passive RIS approaches, discusses energy efficiency challenges	Lack of C-NOMA specific optimization strategies
Gu et al.	2023	On the performance of cooperative NOMA downlink: A RIS-aided D2D perspective	Analytical performance bounds, extensive simulation analysis, highlights effects of RIS in cooperative NOMA	Assumes perfect CSI, limited focus on relay diversity
Zhang et al.	2021	Reconfigurable intelligent surfaces aided multi-cell NOMA networks: A stochastic geometry model	Rigorous system modeling, stochastic geometry framework, explores large-scale deployments	Limited real-world validation, no hardware implementation results

2.2.3. *Final SINR at U_F*

U_F uses the simplest joint decoding technique, Selection Combining (SC), which chooses the signal with the best quality [4]:

$$\gamma_F = \max(\gamma_{F1}, \gamma_{F2}) \tag{12}$$

2.3. Performance Metrics

To comprehensively evaluate the system performance, the following metrics are used throughout various research papers, the comparison of which is given in Table 3:

- **Sum Rate (R_{sum}):** The total achievable throughput of both users, defined as $R_{sum} = R_N + R_F$. Higher the sum rate, better is the system performance [14].
- **Outage Probability (OP):** Defined as the probability that a user's instantaneous SINR falls below a predefined threshold γ_{th}: $P_{out,i} = \Pr(\gamma_i < \gamma_{th,i}), \quad i \in \{N, F\}$. Lower the outage probability, better is the system performance. Outage analysis is crucial in cooperative systems to quantify reliability under fading conditions [10].
- **Energy Efficiency (EE):** Given by the ratio of the sum rate to the total consumed power: EE $= \frac{R_{sum}}{P_T + P_R + P_{RIS}}$, where P_{RIS} denotes the power consumed by the RIS control circuitry. Higher the energy efficiency, better is the system performance [15].

3. Other 6G Enabling Technologies

6G aims to deliver unprecedented performance, characterized by peak data rates up to 1 Terabit per second (Tb/s) and ultra-low latency in the range of 0.1 to 1 millisecond (ms) for demanding real-time applications [16]. To achieve the goals, 6G development is driven by the exploration of several critical technological enablers across various domains. The New Spectrum Frontier is defined by the necessary transition to Terahertz (THz) Communication, which utilizes the extremely wide spectrum above 100 GHz to facilitate Tb/s data rates [17]. Cell-Free Massive MIMO (CF-mMIMO), for improved uniform coverage and simplified interference management [18], alongside the integration of Non-Terrestrial Networks (NTNs) [19] (such as satellites and High-Altitude Platforms (HAPs)) guarantees ubiquitous Global Coverage. Furthermore, the functions of communication and sensing are converged into Integrated Sensing and Communication (ISAC) to enable highly accurate environmental detection and localization [20]. Finally, all these architectural and functional enhancements are unified and optimized through the pervasive Integration of Artificial Intelligence (AI), moving the network toward self-management and native intelligence [21].

The focus of our paper, RIS-aided C-NOMA, operates as a critical spectral efficiency and energy efficiency layer, but its true potential is unlocked when integrated with other 6G enablers that address different facets of network performance. For example, in Terahertz (THz) communications, RIS enables focused and redirected highly directional beams, mitigating blockage issues and real-time optimization of RIS phase shifts and dynamic resource allocation in C-NOMA environments, the use of AI/ML reduces .the computational complexity and enables adaptive system performance under varying network conditions.

4. Applications of RIS-Aided C-NOMA

4.1. Massive Machine-Type Communications (mMTC)

mMTC targets connectivity for massive numbers of low-rate, sporadically active devices (sensors, smart meters) with stringent energy and overhead constraints. RIS can boost uplink SNR for cell-edge and shadowed devices, while C-NOMA enables many devices to share the same resource block and exploit cooperative relaying for reliability [22].

4.2. SWIPT and Wireless Energy Harvesting

Simultaneous wireless information and power transfer (SWIPT) is essential for batteryless or energy-constrained IoT devices. RIS can focus and steer RF energy toward energy harvesters, increasing harvested power without extra transmit power, while C-NOMA

allows simultaneous energy and information delivery to multiple receivers and cooperative forwarding by stronger devices [23].

4.3. Autonomous Vehicles and V2X

Connected and autonomous vehicles require ultra-reliable, low-latency V2X communications for safety messages and cooperative perception in highly dynamic, often obstructed environments. Roadside RIS (gantries, poles) and vehicle-mounted RIS can redirect mmWave/THz beams to occluded vehicles and improve link reliability; C-NOMA supports prioritized multiplexing of safety (high priority) and non-safety traffic while cooperative relaying helps reach occluded nodes [24].

4.4. UAV/Drone Networks and Aerial Relaying

UAVs function as flexible aerial access points or relays for temporary events, disaster response, and remote coverage. UAV-mounted RIS (or ground RIS directed by UAVs) can dynamically form favorable reflection paths to reach clusters of users; combined with C-NOMA, UAVs can serve multiple users simultaneously with cooperative relaying to extend coverage [25].

4.5. Smart Cities (Dense Urban IoT and Infrastructure)

Smart city deployments mix heterogeneous devices—environmental sensors, traffic cameras, public-safety sensors—operating in urban canyons with frequent blockage and interference. Strategically deployed RIS panels on lampposts, façades, and bus stops can create controllable reflective links to mitigate dead zones; C-NOMA enables heterogeneous devices to share scarce spectrum and cooperatively forward traffic for disadvantaged nodes [26].

5. Conclusion and Future Works

The integration of RIS-aided C-NOMA provides a transformative approach to 6G, significantly enhancing spectral efficiency and signal reliability while reducing power consumption and extending network coverage. Despite the advantages, there are major critical research challenges that include:

- Difficulty of Channel Estimation and handling Imperfect CSI,
- The complex Joint Non-Convex Optimization of power, pairing, and RIS phases,
- Hardware Constraints (like quantized phase shifts) and Modeling Gaps limit theoretical gains.

We outline promising potential solutions and research directions in order to mitigate these challenges. Potential solutions identified in the literature include advanced channel estimation methods, such as compressive sensing and deep learning techniques that could efficiently exploit channel sparsity and reduce pilot overhead [8, 27]. Typically, optimization of RIS-aided C-NOMA systems is addressed by alternating optimization and successive convex approximation [9, 10], besides deep reinforcement learning for adaptive resource allocation in dynamic environments [26]. In order to bridge the gap between theoretical models and their practical deployment, several recent contributions underline the importance of quantized phase shift optimization and detailed hardware modeling [5], while very low-complexity and scalable RIS architectures have been evaluated for practical scenarios [4].

References

[1] M. Abd-Elnaby, G. G. Sedhom, E.-S. M. El-Rabaie, and M. Elwekeil, "NOMA for 5G and beyond: literature review and novel trends," *Wireless Networks*, vol. 29, no. 4, pp. 1629–1653, 2023.

[2] A. Amhaz, M. Elhattab, C. Assi, and S. Sharafeddine, "Integrated sensing and communication: NOMA vs cooperative NOMA," in *GLOBECOM 2023-2023 IEEE Global Communications Conference*, pp. 407–412, IEEE, 2023.

[3] U. Mushtaq and S. Baig, "Resource Allocation in Cooperative NOMA: Opportunities and Challenges," in *2024 3rd International Conference on Emerging Trends in Electrical, Control, and Telecommunication Engineering (ETECTE)*, pp. 1–6, IEEE, 2024.

[4] X. Gu, G. Zhang, B. Zhuo, W. Duan, J. Wang, M. Wen, and P.-H. Ho, "On the performance of cooperative NOMA downlink: A RIS-aided D2D perspective," *IEEE Transactions on Cognitive Communications and Networking*, vol. 9, no. 6, pp. 1610–1624, 2023.

[5] Z. Zhu, "A review of RIS-assisted wireless communication research," *Applied and Computational Engineering*, vol. 88, pp. 158–165, 2024.

[6] S. Sharma, A. K. Mishra, M. H. Kumar, K. Deka, and V. Bhatia, "Intelligent reflecting surfaces (IRS)-enhanced cooperative NOMA: A contemporary review," *IEEE Access*, vol. 12, pp. 82168–82191, 2024.

[7] L. Wei, C. Huang, G. C. Alexandropoulos, C. Yuen, Z. Zhang, and M. Debbah, "Channel estimation for RIS-empowered multi-user MISO wireless communications," *IEEE Transactions on Communications*, vol. 69, no. 6, pp. 4144–4157, 2021.

[8] A. Taha, M. Alrabeiah, and A. Alkhateeb, "Enabling large intelligent surfaces with compressive sensing and deep learning," *IEEE access*, vol. 9, pp. 44304–44321, 2021.

[9] T. Bai, C. Pan, Y. Deng, M. Elkashlan, A. Nallanathan, and L. Hanzo, "Latency minimization for intelligent reflecting surface aided mobile edge computing," *IEEE Journal on Selected Areas in Communications*, vol. 38, no. 11, pp. 2666–2682, 2020.

[10] K.-T. Nguyen, T.-H. Vu, and S. Kim, "A unified framework analysis for reconfigurable intelligent surface-aided coordinated NOMA systems," *IEEE Transactions on Vehicular Technology*, vol. 72, no. 11, pp. 15115–15120, 2023.

[11] J. A. Oviedo and H. R. Sadjadpour, "A fair power allocation approach to NOMA in multiuser SISO systems," *IEEE Transactions on Vehicular Technology*, vol. 66, no. 9, pp. 7974–7985, 2017.

[12] A. Muhammad, M. Elhattab, M. A. Arfaoui, and C. Assi, "Optimizing age of information in RIS-empowered uplink cooperative NOMA networks," *IEEE Transactions on Network and Service Management*, vol. 21, no. 1, pp. 897–907, 2023.

[13] J. Ren, X. Lei, Z. Peng, X. Tang, and O. A. Dobre, "RIS-assisted cooperative NOMA with SWIPT," *IEEE Wireless Communications Letters*, vol. 12, no. 3, pp. 446–450, 2022.

[14] P. Dinh, M. A. Arfaoui, S. Sharafeddine, C. Assi, and A. Ghrayeb, "A low-complexity approach for sum-rate maximization in cooperative NOMA enhanced cellular networks," in *2020 IEEE international conference on communications workshops (ICC Workshops)*, pp. 1–7, IEEE, 2020.

[15] Q. Zhai, L. Dong, C. Liu, Y. Li, and W. Cheng, "Resource management for active RIS aided multi-cluster SWIPT cooperative NOMA networks," *IEEE Transactions on Network and Service Management*, vol. 21, no. 4, pp. 4421–4434, 2024.

[16] V. K. Quy, A. Chehri, N. M. Quy, N. D. Han, and N. T. Ban, "Innovative trends in the 6G era: A comprehensive survey of architecture, applications, technologies, and challenges," *IEEE Access*, vol. 11, pp. 39824–39844, 2023.
[17] W. Jiang, Q. Zhou, J. He, M. A. Habibi, S. Melnyk, M. El-Absi, B. Han, M. Di Renzo, H. D. Schotten, F.-L. Luo, et al., "Terahertz communications and sensing for 6G and beyond: A comprehensive review," *IEEE Communications Surveys & Tutorials*, vol. 26, no. 4, pp. 2326–2381, 2024.
[18] N. Ahmadi and G. Akbarizadeh, "Optimizing Power Control in Cellular and Cell-Free Massive MIMO Systems: A SVM/RBF Approach," *IEEE Access*, 2025.
[19] A. Guidotti, A. Vanelli-Coralli, M. El Jaafari, N. Chuberre, J. Puttonen, V. Schena, G. Rinelli, and S. Cioni, "Role and evolution of non-terrestrial networks toward 6G systems," *IEEE Access*, vol. 12, pp. 55945–55963, 2024.
[20] A. Cengiz and Y. Kabalci, "Towards Unified Wireless Systems: ISAC Technologies in the 6G Era," in *2025 7th Global Power, Energy and Communication Conference (GPECOM)*, pp. 1026–1031, IEEE, 2025.
[21] A. Alhammadi, I. Shayea, A. A. El-Saleh, M. H. Azmi, Z. H. Ismail, L. Kouhalvandi, and S. A. Saad, "Artificial intelligence in 6G wireless networks: Opportunities, applications, and challenges," *International Journal of Intelligent Systems*, vol. 2024, no. 1, p. 8845070, 2024.
[22] S. Liesegang, A. Zappone, O. Munoz, and A. Pascual-Iserte, "Rate optimization for RIS-aided mMTC networks in the finite block-length regime," *IEEE Communications Letters*, vol. 27, no. 3, pp. 921–925, 2022.
[23] Z. Yang, L. Xia, J. Cui, Z. Dong, and Z. Ding, "Delay and energy minimization for cooperative NOMA-MEC networks with SWIPT aided by RIS," *IEEE Transactions on Vehicular Technology*, vol. 73, no. 4, pp. 5321–5334, 2023.
[24] M. Deng, M. Ahmed, A. Wahid, A. A. Soofi, W. U. Khan, F. Xu, M. Asif, and Z. Han, "Reconfigurable intelligent surfaces enabled vehicular communications: A comprehensive survey of recent advances and future challenges," *IEEE Transactions on Intelligent Vehicles*, 2024.
[25] N. Rahmatov and H. Baek, "RIS-carried UAV communication: Current research, challenges, and future trends," *ICT express*, vol. 9, no. 5, pp. 961–973, 2023.
[26] Y. Zou, Y. Liu, X. Mu, X. Zhang, Y. Liu, and C. Yuen, "Machine learning in RIS-assisted NOMA IoT networks," *IEEE Internet of Things Journal*, vol. 10, no. 22, pp. 19427–19440, 2023.
[27] Y. Cao, C. Xing, Y. Wu, J. An, D. W. K. Ng, and X.-G. Xia, "RIS-Assisted Massive Access With Semi-Passive Elements," *IEEE Transactions on Wireless Communications*, vol. 23, no. 9, pp. 10546–10561, 2024.

Biographies

M. Ramadevi received the B.Tech degree in ECE from JNTUH and M. Tech degree in Embedded Systems from VNRVJIET. Currently, an Assistant Professor in VNRVJIET, Hyderabad. and Ph.D. candidate at NIT Warangal. Research interests: cooperative NOMA, wireless communications.

Manunuru Naga Sree Lekha is a B.Tech ECE student at VNR VJIET, Hyderabad. Interest in communication systems and space science; member of IEEE, IUCEE, and IETE student chapters. Published a paper in January 2025.

V. Phanitha Sree is a B.Tech ECE student at VNR VJIET, Hyderabad. Proficient in programming and technical tools; participated in hackathons and team projects; Chair of IEEE MTT-S division of the college.

Madha Sai Prashanth Goud is a B.Tech ECE student at VNR VJIET, Hyderabad. Skilled in C, Python, MATLAB, VLSI/PCB design, and signal processing; completed internship in CNN optimization.

DOI. No. 10.13052/2794-7254.024

Reconfigurable OFDM Transceivers for UAVs: A Survey of Technologies and Design Strategies

V. C. Madhavi and Subhendu Kumar Sahoo*

Abstract: Unmanned Aerial Vehicles (UAVs), commonly known as drones, are becoming an integral part of modern life. They are increasingly used in communication, surveillance, photography and filmmaking, military operations and commercial applications. As drones take on more diverse roles, their communication systems must be highly efficient, reliable, and flexible. One promising way to meet these demands is through Orthogonal Frequency Division Multiplexing (OFDM) transceivers. OFDM is a popular communication technology known for its ability to transmit data effectively, even in challenging environments such as cities or over long distances. It excels at mitigating signal interference caused by reflections (multipath propagation) and efficiently using the available frequency spectrum. These features make OFDM an excellent choice for drone communication. However, UAVs often need to operate across a variety of environments and support multiple communication standards, such as 5G, Wi-Fi, and IoT. This creates a need for transceivers that can adapt to these varied requirements. A reconfigurable OFDM transceiver addresses this need by supporting multiple communication standards and adjusting its parameters in real-time, enabling seamless communication across different networks. This is especially important for drones, as they frequently switch between tasks and environments. For instance, a drone may need high-speed connections for streaming video in one scenario and low-power connections for transmitting sensor data in another. This survey paper focuses on the design, development, and challenges associated with building multi-standard reconfigurable OFDM transceivers for drone applications. It reviews key technologies, recent advancements, and future possibilities.

Keywords: Adaptive wireless systems, drone networking, multi-standard transceiver, OFDM for UAVs, reconfigurable OFDM, UAV communication, 5G integration.

1. Introduction

Unmanned Aerial Vehicles (UAVs), commonly known as drones, are increasingly used in military, commercial, and industrial sectors. Their growing popularity is mainly due to their flexibility, mobility, and ability to access remote areas. To function efficiently, UAVs require reliable and high-speed communication systems that can handle fast movement, changing signal conditions, and interference [1–3]. Orthogonal Frequency Division Multiplexing (OFDM) is one of the most widely adopted modulation techniques in modern wireless communication systems. It offers high spectral efficiency and strong resistance to multipath fading, which makes it well-suited for UAV-based applications [4–8]. However, UAVs often need to operate in dynamic and diverse environments where different wireless standards such as Wi-Fi, LTE, 5G, and future 6G networks are used [9–11]. This diversity presents a challenge for maintaining consistent and reliable communication links. To overcome this, a reconfigurable OFDM transceiver can be employed. Such a transceiver can adjust its parameters, such as subcarrier spacing, modulation scheme, and coding rate, based on the operating conditions and the required wireless standard [4, 5, 12]. This adaptability ensures better connectivity, reduced latency, and improved communication quality, even in highly dynamic scenarios. Recent research has also explored additional enhancements such as integration with MIMO, NOMA, and mmWave technologies [1, 7, 13, 14], and the use of intelligent algorithms like machine learning to optimize performance [2,6,10, 15]. Moreover, newer methods such as Reconfigurable Intelligent Surfaces (RIS) and joint radar-communication frameworks further enhance UAV communication systems by improving coverage and reliability [8,16].

2. Literature Review

Several studies have explored using different wireless technologies to improve UAV communication systems. For instance, a flexible FPGA-based transceiver was proposed for cognitive radios, enabling seamless switching between Wi-Fi, WiMAX, and WRAN standards. This design reduces reconfiguration time and enhances synchronization accuracy in multi-standard environments [4]. Full-duplex communication for UAVs using millimeter-wave (mmWave) frequencies has also been studied to increase data throughput and reduce latency. The integration of non-orthogonal multiple access (NOMA) further improves spectral efficiency, making these systems suitable for high-capacity UAV networks [1, 13]. Another line of research has focused on Cognitive UAVs (CUAVs), where energy efficiency and low-latency transmission are achieved using adaptive NOMA techniques and dynamic spectrum access strategies [2, 14]. Reconfigurable Intelligent Surfaces (RIS) have recently gained attention for UAV-based wireless systems. RIS enhances signal coverage by enabling passive beamforming and reflection control, especially in urban or

Department of Electrical & Electronics Engineering, BITS-Pilani, Hyderabad Campus, Hyderabad-500078, India
E-mail: p20240069@hyderabad.bits-pilani.ac.in; sahoo@hyderabad.bits-pilani.ac.in
*Corresponding Author
Manuscript received 06 April 2025, accepted 28 November 2025, and ready for publication 31 December 2025.

complex environments with physical obstructions [7, 16]. Moreover, combining RIS with MIMO and OFDM technologies offers better performance in beamforming, interference management, and adaptability [8, 16]. These works collectively highlight the need for communication systems to adapt to different wireless standards, channels, and network demands. Building on these insights, this paper envisions a conceptual design for a flexible, multi-standard, reconfigurable OFDM transceiver tailored for UAV applications. The envisioned system would dynamically adjust transmission parameters—such as subcarrier spacing, modulation schemes, and coding rates—in real-time to accommodate varying environments and communication requirements. This adaptability is expected to enable improved connectivity, lower latency, and enhanced compatibility with both existing and emerging wireless technologies.

3. Overview of OFDM and UAV with Multi-Standards

3.1. What is OFDM?

Orthogonal Frequency Division Multiplexing (OFDM) is a widely used multi-carrier modulation technique adopted in modern communication systems, including 4G LTE, 5G NR, Wi-Fi (IEEE 802.11), DVB, and ADSL [4, 5, 7, 10]. OFDM works by dividing a high-speed data stream into several lower-speed streams that are transmitted in parallel over orthogonal subcarriers. These subcarriers are closely spaced in frequency but remain mathematically orthogonal to prevent intercarrier interference. Figure 1 depicts a typical OFDM transceiver architecture, while Figure 2 illustrates how a UAV can dynamically switch between these wireless standards in real-time.

In an OFDM transmitter, data bits are mapped onto symbols using modulation schemes such as QPSK, 16-QAM, or 64-QAM. The symbols are then transformed to the time domain using an Inverse Fast Fourier Transform (IFFT). To mitigate inter-symbol interference (ISI) caused by multipath propagation, a cyclic prefix (CP) is added to each OFDM symbol. At the receiver side, the reverse process is performed using a Fast Fourier Transform (FFT) to recover the transmitted data. Mathematically, the time-domain

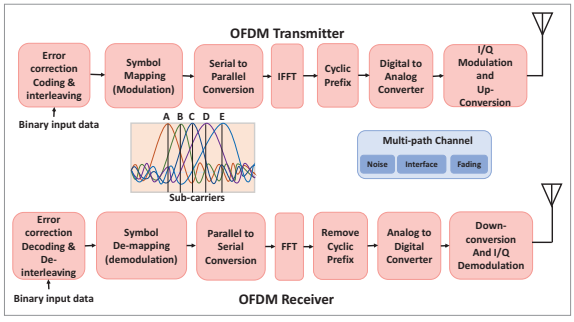

Figure 1.
Basic OFDM Transceiver

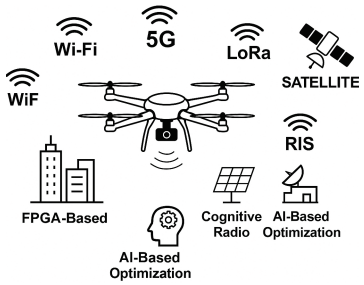

Figure 2.
Illustration of a multi-standard OFDM UAV dynamically switching between 5G, Wi-Fi, IoT, and THz communication in different environments.

OFDM signal is expressed as:

$$x[n] = \frac{1}{\sqrt{N}} \sum_{k=0}^{N-1} X_k \cdot e^{j\frac{2\pi kn}{N}}, \quad 0 \le n < N \tag{1}$$

where X_k represents the data symbol on subcarrier k, and N is the number of subcarriers. To mitigate inter-symbol interference, a cyclic prefix of length L_{CP} is appended:

$$x_{cp}[n] = x[n + N - L_{CP}], \quad -L_{CP} \le n < 0 \tag{2}$$

The transmitted OFDM signal becomes:

$$x_{tx}[n] = \begin{cases} x[n + N - L_{CP}], & -L_{CP} \le n < 0 \\ x[n], & 0 \le n < N \end{cases} \tag{3}$$

The UAV wireless communication channel is modeled as a discrete-time multipath fading channel:

$$h[n] = \sum_{\ell=0}^{L-1} h_\ell \cdot \delta(n - \tau_\ell) \tag{4}$$

The received signal is the convolution of the transmitted signal with the channel impulse response, plus additive white Gaussian noise:

$$y[n] = (x_{tx} * h)[n] + w[n] \tag{5}$$

At the receiver, after removing the cyclic prefix and applying FFT, the received subcarrier value is:

$$Y_k = H_k \cdot X_k + W_k, \quad k = 0, 1, \ldots, N-1 \tag{6}$$

The symbol can be recovered via equalization:

$$\hat{X}_k = \frac{Y_k}{H_k} \tag{7}$$

3.2. Performance Metrics and Adaptation

OFDM supports adaptive modulation. The bit error rate (BER) for an M-QAM signal in an AWGN channel is approximated by:

$$P_b \approx \frac{4}{\log_2 M} \left(1 - \frac{1}{\sqrt{M}}\right) Q\left(\sqrt{\frac{3 \log_2 M \cdot \text{SNR}}{M - 1}}\right) \tag{8}$$

Table 1.

Comparison of wireless communication standards					
Standard	**Frequency Band**	**Max Data Rate**	**Range**	**Primary Applications**	**References**
Wi-Fi 6 (IEEE 802.11ax)	2.4 GHz, 5 GHz	Up to 9.6 Gbps	Upto 35 m (indoor)	High-speed internet, video streaming, online gaming	[4, 9, 10]
Wi-Fi 7 (IEEE 802.11be)	2.4 GHz, 5 GHz, 6 GHz	Upto 46 Gbps	Similar to Wi-Fi 6	UHD streaming, virtual and augmented reality	[10]
Bluetooth (IEEE 802.15.1)	2.4 GHz	Upto 3 Mbps	Upto 100 m	Wireless peripherals, audio devices, short-range data exchange	[7]
Zigbee (IEEE 802.15.4)	2.4 GHz, 900 MHz, 868 MHz	20–250 Kbps	10–100 m	Home automation, industrial control, sensor networks	[2, 3, 6]
Cellular (5G)	Sub-6 GHz, mmWave (24–100 GHz)	Upto 10 Gbps	500 m (mmWave), several km (Sub-6)	Mobile broadband, IoT, autonomous vehicles	[1, 5, 6, 13, 16]
WiMAX (IEEE 802.16)	2.3 GHz, 2.5 GHz, 3.5 GHz	Upto 70 Mbps	Upto 50 km	Broadband wireless access, last-mile connectivity	[4, 9]

with the Q-function as:

$$Q(x) = \frac{1}{\sqrt{2\pi}} \int_x^\infty e^{-t^2/2} dt \tag{9}$$

Spectral efficiency η in bits/sec/Hz is given by:

$$\eta = R \cdot \log_2 M \cdot \left(1 - \frac{L_{CP}}{N + L_{CP}}\right) \tag{10}$$

where R is the coding rate. To optimize link performance, the system can switch modulation orders based on SNR:

$$M = \begin{cases} \text{BPSK}, & \gamma < \gamma_1 \\ \text{QPSK}, & \gamma_1 \le \gamma < \gamma_2 \\ \text{16-QAM}, & \gamma_2 \le \gamma < \gamma_3 \\ \text{64-QAM}, & \gamma \ge \gamma_3 \end{cases} \tag{11}$$

In reconfigurable systems, the delay for switching between standards is modeled as:

$$T_{\text{switch}} = T_{\text{detect}} + T_{\text{load}} + T_{\text{sync}} \tag{12}$$

OFDM offers high spectral efficiency, robustness to frequency-selective fading, and ease of implementation using FFT algorithms [5, 7]. However, challenges such as high Peak-to-Average Power Ratio (PAPR) and sensitivity to timing and frequency errors remain [17]. Given these strengths, OFDM is well-suited for UAV communication systems that must operate reliably in dynamic and multipath-prone environments [1, 6, 8]. Wireless communication standards based on OFDM and other technologies are designed for different applications. UAVs benefit from multi-standard support, allowing them to switch between networks based on range, data rate, and environment. Table 1 summarizes key wireless communication standards used in UAV applications, covering use cases from high-speed video streaming and data exchange to low-power sensor transmission and long-distance broadband connectivity [1, 2, 9, 10, 16].

3.3. Fundamentals of OFDM in UAV Communication

In the context of UAV communication, OFDM offers several advantages. It enhances performance in both urban and rural environments by reducing inter-symbol interference and enabling more efficient use of the available spectrum. Key benefits for UAV applications include robust handling of multipath propagation, high spectral efficiency, support for adaptive modulation and coding, and compatibility with a range of wireless standards such as Wi-Fi, LTE, and 5G. Despite these strengths, implementing OFDM in UAV systems presents several challenges. High Doppler shifts caused by UAV mobility can affect synchronization and signal quality. Additionally, power and hardware constraints in lightweight UAV platforms limit the complexity and processing capabilities of communication systems. Furthermore, integration with cognitive and adaptive networking technologies is essential to fully leverage OFDM's flexibility in dynamic environments.

3.4. Multi-Standard Reconfigurable OFDM Transceivers

A multi-standard reconfigurable OFDM transceiver enables UAVs to operate dynamically across wireless networks. These transceivers employ techniques such as FPGA-based partial reconfiguration, software-defined radio (SDR), and cognitive radio technology. FPGA-Based Reconfiguration: FPGA-based transceivers allow UAVs to switch between standards like Wi-Fi, WiMAX, and WRAN with minimal reconfiguration delay, enhancing adaptability [4, 9]. Cognitive Radio for UAVs: Cognitive radios enable UAVs to detect and utilize available spectrum efficiently, improving spectral efficiency and reducing interference [2]. UAVs are used in diverse application environments, such as urban surveillance, rural connectivity, emergency rescue, and military operations. Each environment may rely on a different wireless standard, making it necessary for UAVs to support multiple standards. For instance, UAVs may need to switch between 5G for high-bandwidth

Table 2.

UAV communication standards and associated technical advancements			
Wireless Standard/ Technology	**UAV Use Cases**	**Key Technical Enhancements/ Research Focus**	**References**
Wi-Fi(IEEE 802.11), WLAN	Short-range communication, live video, surveillance, multi-standard reception	SDR, FPGA-based partial reconfiguration, multi-stream synchronization, enhanced synchronization	[4, 9, 10]
LTE/5G/Wi-Fi	High-speed video, control links, urban monitoring, signal processing	OFDM, QAM schemes (16-QAM, 64-QAM), MIMO, Massive MIMO, full-duplex, ML integration, PLS	[1, 5, 6, 10, 13, 16]
NB-IoT/ LoRa	Low-power telemetry, rural/remote sensing	Adaptive modulation, long-range compatibility, low-power design	[2, 10, 14]
WiMAX/WRAN (IEEE 802.16 / 802.22)	Broadband access, rural internet backhaul	SDR-enabled reconfigurable front-end, partial reconfiguration for RAT switching	[4, 9]
mmWave (30–300 GHz)	Ultra-high-speed backhaul, dense urban UAV communication	Beamforming, MIMO, Doppler-division multiplexing, RIS integration, jamming mitigation	[7, 8, 13, 16]
Terahertz (THz)	Next-gen high-throughput UAV links	Ultra-broadband, PLS, THz-aware RF/antenna design, RIS-based optimization	[16, 18]
IM/DD OFDM,OFDM Variants(eU-OFDM,LACO, AVO,ACO, ALACO),OTFS	UAV-based swarm comms, high-mobility links, indoor coverage, delay-Doppler resilience	Zero-padding, DFT-spread OFDM, robust to fading, PAPR reduction, iterative decoding, cluster optimization	[5, 12, 17, 19–21]
FMCW Radar, MIMO Radar, Radar-Assisted Comms	Imaging, mapping, object detection, W-band environmental sensing	Beat frequency division, joint radar-comm, MIMO SAR, real-time W-band processing	[18, 19, 22]
Cognitive Radio (CR), SDR-Based Platforms	Dynamic spectrum access, emergency comms, CR-based UAV flight	AI-based spectrum sensing, adaptive transceivers, energy-efficient SDR, interference mitigation	[2, 6, 15]
Reconfigurable Intelligent Surfaces (RIS)	Smart reflection, enhanced coverage, cooperative UAV relays	Passive beamforming, MIMO/OFDM coordination, RIS-UAV trajectory control	[7, 8, 16, 18]
AI/ML-Driven Techniques	Real-time adaptive comms, energy efficiency	DL-based beamforming, path optimization, spectrum prediction, security enhancement	[2, 6, 10, 15]
Fault-Tolerant/Secure UAV Systems (Cross-Layer Models)	Safety-critical UAV missions, reliable multi-UAV networks	Physical layer security (PLS), encryption, fault-tolerant computing, intrusion prevention, CLR modeling	[1, 3, 11, 15, 16]

video streaming, Wi-Fi for short-range communication, and LoRa or NB-IoT for low-power telemetry. A reconfigurable OFDM transceiver allows this seamless interoperability, enhances mission flexibility, and ensures reliable connectivity under varying network conditions [1, 9, 13].

3.5. Advanced Techniques for UAV OFDM Communication

To further enhance the performance of OFDM-based UAV communication systems, several advanced technologies have been explored:

Reconfigurable Intelligent Surfaces (RIS): RIS technology improves UAV connectivity by intelligently reflecting and steering signals to enhance coverage, manage interference, and reduce energy consumption—particularly in complex or obstructed environments [7].

Terahertz (THz) Communications: Operating at THz frequencies enables ultra-high-speed data transmission, offering significant potential for UAV communication in future-generation networks. This is particularly relevant for applications requiring massive data rates, such as real-time 3D mapping or ultra-HD video streaming[16].

Machine Learning for Adaptive Transceivers: AI-driven techniques, including machine learning algorithms, are increasingly being integrated into UAV communication systems. These approaches enable adaptive transceivers to optimize performance

by predicting channel conditions and dynamically adjusting transmission parameters such as power, modulation, and coding rates in real time [10].

4. Multi-Standard OFDM-UAV Deployment for Various Communication Applications

Recent research from 2015 to 2025 highlights a significant evolution in wireless communication technologies, particularly in UAV-assisted networks (Table 2). Initial efforts [4, 9] focused on enabling multi-standard support through Software Defined Radios (SDRs), optimizing digital front-ends, and improving synchronization for multistream and concurrent receptions. These early contributions laid the foundation for flexible and adaptive architectures for next-generation mobile communications. Progressively, the adoption of various modulation schemes such as OFDM, QAM (including HQAM, RQAM, 16-QAM, 32-XQAM), PSK, and more recently, Orthogonal Time-Frequency Space (OTFS) modulation [1, 5, 10, 12, 17, 19–21] has enabled improved spectral efficiency, resilience to channel impairments, and higher data rates. These schemes have been enhanced through the integration of advanced techniques like DFT-spread OFDM, zero-padding, and efficient FFT/IFFT implementations [16, 20] allowing better performance in high-mobility or fast time-varying environments, such as UAV communications. Technologies such as MIMO, Massive MIMO, NOMA, mmWave, and full-duplex communication have become central to improving system throughput, coverage, and physical layer security in UAV-supported networks [1, 6–8, 13, 14, 16]. Researchers have explored their deployment in diverse environments, integrating features like joint communication and radar sensing, RIS-based beamforming, and Doppler-division multiplexing for enhanced link reliability and reduced latency [7, 16, 18]. Simultaneously, radar-based approaches, especially Frequency-Modulated Continuous Wave (FMCW) and MIMO radar, have been extensively explored for imaging, object detection, and deformation monitoring across W-band frequencies [18, 19, 22]. These techniques support real-time processing and have shown promising results on stationary and moving UAV platforms. In recent years, artificial intelligence, particularly machine learning (ML) and deep learning (DL), has been increasingly used to optimize signal processing and decision-making tasks. Applications include signal detection, proactive spectrum management, channel modeling, and UAV path optimization [2,6,7,10,15]. These advancements contribute to energy-efficient cognitive radio operations and improve the adaptability of UAVs to dynamic environments. Security and reliability have also received notable attention. Several studies [1,3,11,15,16] focus on improving physical layer security (PLS), developing encryption techniques resilient to real-time attacks, and creating fault-tolerant and self-adaptive UAV systems for safety-critical applications. Furthermore, research on cross-layer reliability models and holistic fault monitoring frameworks ensures system robustness across multiple UAV subsystems. Finally, recent efforts incorporate Reconfigurable Intelligent Surfaces (RIS), cooperative multi-UAV deployments, and joint radar-communication architectures to improve connectivity, reduce interference, and extend network coverage [8, 16]. These developments pave the way for efficient UAV-based communication platforms in 6G and beyond, emphasizing security, real-time adaptation, and low-complexity implementation.

5. Future Research Directions

Future research in UAV communication is expected to focus on several promising areas are

6G and Beyond: The integration of UAVs into 6G networks is anticipated to support ultra-reliable low-latency communication (URLLC) and massive machine-type communication (mMTC). These capabilities will enable advanced real-time applications such as autonomous navigation, remote healthcare, and immersive experiences [1,13,16].

Security and Privacy Enhancements: As UAVs become increasingly used in both civilian and defense sectors, secure communication protocols are essential to address potential threats such as cyberattacks, data breaches, and spoofing [3,6,15].

Energy-Efficient Communication: Power efficiency is crucial for UAV missions that require extended flight durations. Ongoing research aims to optimize transceiver hardware, develop energy-aware routing strategies, and utilize AI-driven power management to prolong operational life [10,15].

Interoperability with IoT Devices: With the rapid expansion of smart cities and industrial IoT ecosystems, it is vital to enhance UAV communication frameworks for seamless integration with heterogeneous IoT devices. This will support applications such as large-scale environmental monitoring, infrastructure inspection, and next-generation logistics operations [1,2,18].

6. Conclusion

The emergence of reconfigurable OFDM transceivers marks a pivotal advancement in UAV communication, enabling the flexibility required for seamless multi-standard operations. Technologies such as FPGA-based reconfiguration, cognitive radio, Reconfigurable Intelligent Surfaces (RIS), and terahertz (THz) communication are driving the evolution of UAV networks toward high adaptability, efficiency, and scalability. These innovations improve connectivity and spectral utilization and ensure robust performance in diverse operational scenarios. Future research should continue to address critical challenges such as energy-efficient communication, enhanced physical layer security, and full integration with 6G architectures to fully harness the potential of UAV-assisted wireless communication systems.

References

[1] J. J. Sadique, S. E. Ullah, M. R. Islam, R. Raad, A. Z. Kouzani, and M. P. Mahmud, "Transceiver design for full-duplex uav based zero-padded ofdm system with physical layer security," *IEEE Access*, vol. 9, pp. 59 432–59 445, 2021.

[2] G. M. Dias Santana, R. S. d. Cristo, and K. R. Lucas Jaquie Castelo Branco, "Integrating cognitive radio with unmanned aerial vehicles: An overview," *Sensors*, vol. 21, no. 3, p. 830, 2021.

[3] F. Ahmed and M. Jenihhin, "A survey on uav computing platforms: A hardware reliability perspective," *Sensors*, vol. 22, no. 16, p. 6286, 2022.

[4] T. H. Pham, S. A. Fahmy, and I. V. McLoughlin, "An end-to-end multi-standard ofdm transceiver architecture using fpga partial reconfiguration," *IEEE Access*, vol. 5, pp. 21 002–21 015, 2017.
[5] P. K. Singya, N. Kumar, V. Bhatia, and F. A. Khan, "Performance analysis of ofdm based 3-hop af relaying network over mixed rician/rayleigh fading channels," *AEU-International Journal of Electronics and Communications*, vol. 93, pp. 337–347, 2018.
[6] J. J. Sadique, S. R. Sabuj, S. E. Ullah, S. K. Joarder, and M. Hamamura, "Uav-aided transceiver design for secure downlink ow-dfts-ofdm system: A multi-user mmwave application," *IEEE Access*, vol. 10, pp. 34 577–34 590, 2022.
[7] M. Yuan, H. Wang, H. Yin, and D. He, "Alternating optimization based hybrid transceiver designs for wideband millimeter-wave massive multiuser mimo-ofdm systems," *IEEE Transactions on Wireless Communications*, vol. 22, no. 12, pp. 9201–9217, 2023.
[8] H. Noh, H. Lee, and H. J. Yang, "Ici-robust transceiver design for integration of mimo-ofdm radar and mu-mimo communication," *IEEE Transactions on Vehicular Technology*, vol. 72, no. 1, pp. 821–838, 2022.
[9] S. Díaz, Z. Zhang, T. Hentschel, and G. Fettweis, "A new digital front-end for flexible reception in software defined radio," *Microprocessors and Microsystems*, vol. 39, no. 8, pp. 1262–1272, 2015.
[10] D. Allan, E. Atimati, K. W. Barlee, L. J. Brown, J. Craig, G. Fitzpatrick, J. Goldsmith, A. Maclellan, L. D. McLaughlin, B. McTaggart, *et al.*, *Software Defined Radio with Zynq Ultrascale+ RFSoC*. Glasgow, UK: Strathclyde Academic Media, 2023, vol. 1st.
[11] W. Abdallah, "A physical layer security scheme for 6g wireless networks using post-quantum cryptography," *Computer Communications*, vol. 218, pp. 176–187, 2024.
[12] U. Iqbal, Y. Lee, S. Cho, I.-H. Lee, and H. Jung, "Cooperative transmission of uav swarm using orthogonal time–frequency space modulation," *ICT Express*, vol. 10, no. 6, pp. 1240–1246, 2024.
[13] G. K. Pandey, D. S. Gurjar, H. H. Nguyen, and S. Yadav, "Security threats and mitigation techniques in uav communications: A comprehensive survey," *IEEE Access*, vol. 10, pp. 112 858–112 897, 2022.
[14] M. Omor Faruk, J. Jafor Sadique, K. Cumanan, and S. Enayet Ullah, "Orthogonal variable spreading factor encoded unmanned aerial vehicle-assisted nonorthogonal multiple access system with hybrid physical layer security," *ETRI Journal*, vol. 45, no. 2, pp. 213–225, 2023.
[15] E. E. Elsayed, "Investigations on ofdm uav-based free-space optical transmission system with scintillation mitigation for optical wireless communication-to-ground links in atmospheric turbulence," *Optical and Quantum Electronics*, vol. 56, no. 5, p. 837, 2024.
[16] M. N. Hossain, K. S. Nisar, T. Shimamura, M. R. Islam, S. T. Kamal, and S. E. Ullah, "Transceiver design of a secure multiuser fdss-based dft-spread ofdm system for ris-and uav-assisted thz communications," *IEEE Open Journal of the Communications Society*, 2025.
[17] S. K. Chronopoulos, "Flexible and reconfigurable ofdm implementation in dsp platform for various purposes and applications," *Sensors*, vol. 24, no. 9, p. 2732, 2024.
[18] G. Xu, Y. Chen, A. Ji, B. Zhang, C. Yu, and W. Hong, "3-d high-resolution imaging and array calibration of ground-based millimeter-wave mimo radar," *IEEE Transactions on Microwave Theory and Techniques*, vol. 72, no. 8, pp. 4919–4931, 2024.
[19] S. Y. Jeon, M. H. Ka, S. Shin, M. Kim, S. Kim, S. Kim, J. Kim, A. Dewantari, J. Kim, and H. Chung, "W-band mimo fmcw radar system with simultaneous transmission of orthogonal waveforms for high-resolution imaging," *IEEE Transactions on Microwave Theory and Techniques*, vol. 66, no. 11, pp. 5051–5064, 2018.
[20] R. Bai and S. Hranilovic, "Absolute value layered aco-ofdm for intensity-modulated optical wireless channels," *IEEE Transactions on Communications*, vol. 68, no. 11, pp. 7098–7110, 2020.
[21] Y. Wu, R. Mei, and J. Xu, "Non pilot data-aided carrier and sampling frequency offsets estimation in fast time-varying channel," *Big Data Research*, vol. 36, p. 100461, 2024.
[22] S. Kim, J. Kim, C. Chung, and M.-H. Ka, "Derivation and validation of three-dimensional microwave imaging using a w-band mimo radar," *IEEE Transactions on Geoscience and Remote Sensing*, vol. 60, pp. 1–16, 2022.

Biographies

V. C. Madhavi is currently pursuing her Ph.D. in the Department of Electrical and Electronics Engineering at BITS Pilani, Hyderabad Campus, with a research focus on wireless communication systems, FPGA-based implementation, and software-defined radio (SDR). She received her M.Tech. degree in VLSI and Embedded Systems and her B.Tech. degree in Electronics and Communication Engineering.

Subhendu Kumar Sahoo is a Professor in the Department of EEE at BITS Pilani, Hyderabad Campus. He received his B.E. in Electronics and Telecommunication Engineering from Utkal University, M.E. in Electronic Systems and Communication from REC (now NIT), Rourkela and earned his Ph.D. in VLSI Architecture from BITS-Pilani. His research interests include high-performance arithmetic circuits, VLSI circuits and architectures for DSP applications and low-power circuit design, currently focusing on the development of hardware accelerators and power-efficient design methodologies for next-generation computing platforms. He has published more than 70 peer-reviewed research papers, supervised nine Ph.D. scholars and also executed several funded research projects.

DOI. No. 10.13052/2794-7254.025

Accident Detection and Prevention System Using IoT and VANET

Harsh H. Mangroliya[1,*], *Smit H. Gor*[2], *Christos Politis*[1] *and Rehan Usman*[1]

Abstract: Road accidents are a major global concern, often caused by limited driver awareness and sudden traffic changes. This paper presents an advanced accident detection and prevention system featuring a novel IoT-enabled Onboard Unit (OBU) integrated with a Vehicular Ad-hoc Network (VANET) architecture. The OBU uses ultrasonic sensors and an Arduino-based controller to monitor the proximity and speed of nearby objects, predicting potential collisions and issuing real-time alerts to drivers. Upon detecting a threat or accident, the OBU communicates with Road Side Units (RSUs) to disseminate alerts across the network, enabling timely warnings and emergency response. The system supports both accident prevention and post-accident management through real-time V2V and V2I communication. The research also evaluates network protocols to ensure reliable data exchange in dynamic traffic conditions. This integrated approach aims to reduce accident frequency and severity while improving traffic safety and response efficiency.

Keywords: 802.11p, accident detection and management system, accident prevention, internet of things (IoT), road accidents, vehicular ad-hoc networks (VANET).

1. Introduction

Road accidents remain a major global concern, causing loss of life, injuries, and property damage. Despite the deployment of safety features like airbags and ABS, most existing accident detection systems are reactive, responding only after a collision occurs. They also lack situational awareness and inter-vehicle communication, limiting their effectiveness in dynamic traffic conditions.

To address these limitations, this paper proposes a proactive accident detection and prevention system using Vehicular Ad-hoc Networks (VANETs) and Internet of Things (IoT) technologies. The system focuses on a smart Onboard Unit (OBU) capable of real-time communication with other vehicles and Roadside Units (RSUs). By using ultrasonic sensors and a microcontroller (Arduino), the OBU detects potential collisions and broadcasts alerts through VANET using Dedicated Short Range Communication (DSRC).

[1]Kingston University, London, KT1 2EE, United Kingdom
[2]Surat, Gujarat, India
E-mail: Harsh.Mangroliya07@gmail.com; Smitgor120@gmail.com; C.Politis@kingston.ac.uk; R.Usman@kingston.ac.uk
*Corresponding Author
Manuscript received 06 April 2025, accepted 21 August 2025, and ready for publication 31 December 2025.

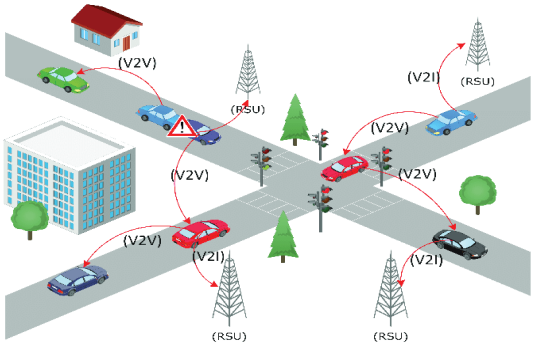

Figure 1.
Communication in VANET.

1.1. Introduction to VANET

Vehicular Ad-hoc Networks (VANET) are a specialized form of Mobile Ad-hoc Networks (MANET) designed for vehicle communication. They enable real-time, decentralized communication between vehicles (V2V) and infrastructure (V2I) using Roadside Units (RSUs). VANET consists of Onboard Units (OBUs) in vehicles, which facilitate communication, gather sensor data, and predict potential accidents to alert drivers. RSUs, placed along roads, relay this information to nearby vehicles, enhancing traffic safety. Communication occurs via Dedicated Short-Range Communication (DSRC) or cellular networks, allowing vehicles to share speed, position, and direction. This improves traffic management and emergency response by providing real-time alerts.

VANET offers several advantages over traditional accident detection systems. It enhances proactive safety by predicting and preventing collisions, ensures network-wide awareness by sharing traffic data, and provides real-time communication for instant alerts, reducing accident risks in high-speed traffic.

1.2. Aims and Objectives

This paper proposes an advanced accident detection and prevention system using IoT and VANET technologies to improve road safety and emergency response. The system features an IoT-based Onboard Unit (OBU) with sensors for real-time collision detection and driver alerts. It facilitates seamless communication between OBUs and Roadside Units (RSUs) to enable fast data transmission

and alert dissemination. RSUs are also designed to notify emergency services and assist traffic management through optimized routing and coordinated post-accident responses, aiming to reduce reaction time and enhance incident handling.

1.3. Proposed System

This project proposes a VANET-based accident detection and prevention system with an advanced OBU that enhances vehicle safety. Using ultrasonic sensors, the OBU detects nearby objects, calculates their speed and trajectory, and alerts drivers of potential collisions. It communicates with RSUs to broadcast accident alerts, preventing multi-vehicle crashes and enabling a swift emergency response. Key features include real-time monitoring with ultrasonic sensors, an Arduino microcontroller for collision prediction, VANET communication for data sharing, and an automated emergency alert system.

1.4. Limitations of Current Research and the Need for Further Improvements

While VANET is a promising solution for accident detection and prevention, it faces challenges such as network congestion, coverage gaps, and security risks. High vehicle connectivity can cause communication delays, while limited RSU deployment, especially in rural areas, reduces effectiveness. Additionally, VANET is vulnerable to hacking and data breaches, posing safety risks. Future research should focus on improving communication reliability, enhancing security, and expanding RSU coverage to ensure a more robust and effective system.

2. Literature Review

Recent advancements in Vehicular Ad Hoc Networks (VANETs) have enabled intelligent, real-time communication between vehicles and infrastructure, supporting applications like accident detection, traffic management, and cybersecurity. This section highlights key technologies and research trends shaping the field.

2.1. Intrusion Detection in VANETs

The decentralized and mobile nature of VANETs makes them vulnerable to cyber threats, requiring specialized Intrusion Detection Systems (IDS). Signature-based IDS matches known attack patterns but lacks adaptability to new threats. Anomaly-based IDS detects unknown attacks by identifying deviations from normal behavior, though they risk false positives due to fluctuating traffic conditions. Specification-based IDSs apply predefined behavioral rules, offering better accuracy but requiring complex rule sets. To enhance efficiency, cooperative and hierarchical IDS architectures distribute detection tasks across vehicles or clusters, improving scalability and resilience against large-scale attacks.

2.2. Trust Management in VANETs

Reliable communication in VANETs depends on trust among participating vehicles and infrastructure. Trust can be infrastructure-based (central authority with digital certificates) or self-organized (behavior-based). However, both are susceptible to attacks like Sybil, where a single node uses multiple identities, or bogus message attacks that spread false data. To counteract this, various trust models have been proposed: entity-based models evaluate the historical behavior of nodes, data-based models assess the credibility of information, and hybrid models combine both to provide a robust framework for secure decision-making.

2.3. Accident Detection and Traffic Management

Accident detection systems in VANETs utilize onboard sensors and roadside infrastructure to identify collisions in real time. IoT-enabled OBUs measure proximity, speed, and impact forces, transmitting alerts to nearby Road Side Units (RSUs) and emergency responders. Frameworks using biomedical and mechanical sensors have been proposed to improve accuracy. Protocols like Traffic-Aware MAC (TA-MAC) and Mobile Edge Computing (MEC) help adapt to traffic density, optimize communication slots, and improve emergency response times. These systems also integrate with intelligent transportation systems (ITS) to adjust traffic signals and prioritize emergency vehicles.

2.4. Routing and Communication Protocols

Routing protocols in VANETs face challenges due to high mobility and changing topologies. Geo-based protocols like GPSR use vehicle location for packet forwarding but struggle in sparse or obstacle-heavy environments. Broadcast-based routing ensures message delivery but risks congestion, especially in dense areas. Cluster-based protocols group vehicles for more structured routing and reduce communication overhead. Selecting the appropriate routing strategy depends on vehicle density, mobility, and application requirements.

2.5. Security and Privacy Challenges

VANETs are exposed to threats like message tampering, impersonation, and denial-of-service (DoS) attacks. Cryptographic techniques such as Public Key Infrastructure (PKI) help secure V2I communication, but are resource-intensive for V2V links. Trust-based models offer lightweight alternatives, evaluating message reliability and sender behavior. However, real-time computation, scalability, and privacy preservation remain ongoing concerns. Reputation systems and pseudonymization techniques can help protect identity and support secure, anonymous communication.

2.6. Emerging Technologies and Future Directions

VANETs are increasingly integrating emerging technologies to enhance functionality. 5G networks offer ultra-low latency and high bandwidth for real-time safety applications. Artificial Intelligence (AI) and Machine Learning (ML) are being applied for dynamic routing, intrusion detection, and accident prediction. Blockchain technology introduces a decentralized trust framework, securing communication and preventing data tampering. Smart contracts automate processes like vehicle authentication and

toll payments, reducing manual intervention. These technologies pave the way for robust, scalable, and secure VANET systems suited for smart cities.

2.7. Summary

VANETs play a critical role in improving road safety, traffic management, and emergency response. Effective accident detection, adaptive routing protocols, and resilient security systems are essential to their success. Emerging technologies like AI, 5G, and blockchain offer promising avenues to overcome existing limitations in scalability, privacy, and trust. Continued research is necessary to address these challenges and unlock the full potential of VANETs in next-generation transportation systems.

3. Methodology and Implementation

3.1. Problem Definition

The development of a Trust and Early Event Prediction Model for accident detection depends on reliable communication between Onboard Units (OBUs) and Road Side Units (RSUs) within a Vehicular Ad-hoc Network (VANET). Efficient OBU-RSU communication is crucial for real-time accident prediction and prevention.

The model analyzes data such as speed, acceleration, and vehicle proximity to detect potential accidents. Its effectiveness hinges on VANET's ability to support timely data exchange between vehicles and infrastructure.

VANET facilitates Vehicle-to-Vehicle (V2V) and Vehicle-to-Infrastructure (V2I) communication, but faces challenges like real-time data transmission, high traffic scalability, and maintaining connectivity. Solutions include enhancing protocols (e.g., DSRC, 5G), developing handover mechanisms, and implementing congestion control to ensure timely and reliable alerts in dense traffic environments.

3.2. Proposed Method for OBU

To create a reliable accident prediction system, various research studies on accident detection in VANETs, early accident detection, and trust management have been reviewed. Based on this research, a method is proposed that utilizes ultrasonic sensors integrated with Arduino-based logic circuits. The system continuously monitors the distance and velocity of nearby vehicles, enabling real-time accident prediction and alert generation. The following is a detailed explanation of the proposed method, including the components, logic, and circuit design.

3.2.1. *System Overview*

Each vehicle is equipped with ultrasonic sensors at both the front and rear. These sensors continuously measure the distance between the vehicle and others in its vicinity, both in front and behind. The data is processed every 0.01 seconds to calculate the relative speed of the vehicles. By comparing this information with a pre-calculated speed limit, potential collisions are predicted, and appropriate alerts are generated for the driver and nearby vehicles.

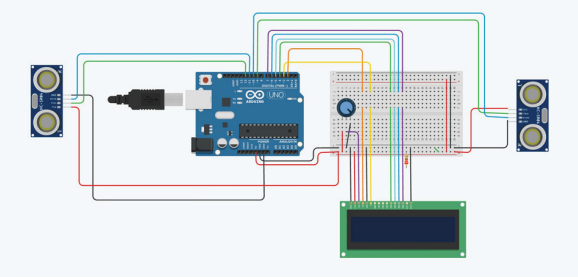

Figure 2.
OBU circuit.

Components:

- **Ultrasonic Sensors:** Measure the distance between vehicles or obstacles within a specific range.
- **Arduino Microcontroller:** Processes sensor data and executes the accident prediction algorithm.
- **RSU (Road Side Unit):** Relays alerts to nearby vehicles and coordinates with other RSUs to notify vehicles across the network.

3.2.2. *Methodology*

Distance and Time Calculation:

Ultrasonic sensors capture the distance between vehicles every 0.01 seconds, and the velocity is calculated using the formula.

$$Speed = \frac{D1 - D2}{T1 - T2}$$

Velocity Threshold Determination:

The speed limit is determined using the braking distance formula:

$$Braking\ Distance = \frac{V^2}{2fg}$$

Here g is gravitational acceleration 9.8 m/s^2. And f is the fraction constant which is 0.7 for average road but can vary according to many factors. So Using this formula we can calculate the maximum speed which will be

$$V = \sqrt{2Dgf}.$$

So for this experiment we have taken the Ultrasonic sensors with the range of 3 meters. The frequency of the Ultrasonic sensors is commonly used at 58 kHz, so by using this frequency we can set it to 11 m range. For this experiment D is 3 m. so calculating speed V will be

$$\begin{aligned} V &= \sqrt{2Dgf} \\ &= \sqrt{2 * 3 * 0.7 * 9.8} \\ &= \sqrt{41.16} \\ &= 6.4156\ \text{m/s} \\ &= 23.09\ \text{km/hr} \end{aligned}$$

This braking distance provides the maximum safe speed limit. If the speed of a vehicle exceeds this threshold, an alert is generated.

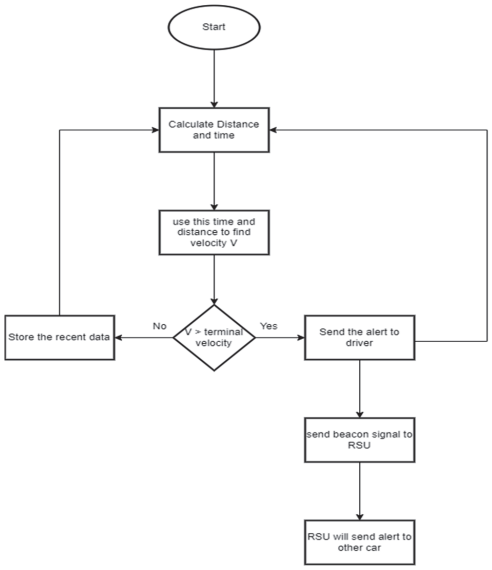

Figure 3.
Flowchart.

Collision Prediction:

If the calculated velocity exceeds the safe speed limit, a potential collision is predicted. The system continuously monitors the data and, when a dangerous situation is detected, sends a warning to the driver.

Alert Generation and Transmission:

Two types of alerts are triggered:

1. A beacon signal sent to the nearest RSU, which further disseminates the alert to surrounding vehicles via the VANET network.
2. An alert to the driver to prompt immediate action.

The RSU receives the beacon signal and sends alerts to all connected nodes, warning other vehicles of potential accident risks.

3.2.3. *Circuit design*

The hardware design employs an Arduino microcontroller connected to ultrasonic sensors and other supporting components:

- **Ultrasonic Sensors:** Positioned at the front and rear of the vehicle to detect the distance to other vehicles or obstacles.
- **Arduino Board:** Processes data from the sensors, calculates the velocity, and compares it to the pre-determined speed limit.
- **LCD Display (Optional):** Used to show real-time distance and speed data for driver awareness.

Process Steps:

1. Ultrasonic sensors gather distance data.
2. The Arduino calculates relative velocities and compares them to the speed limit.
3. If a potential collision is predicted, the system sends alerts to both the driver and the RSU.

3.2.4. *Flowchart*

The system begins by calculating the distance and time interval. Velocity is computed from this information. The calculated velocity is compared to the terminal (safe) velocity. If the velocity exceeds the safe limit, alerts are sent to the driver and a beacon signal is transmitted to the RSU. The RSU then broadcasts alerts to other nearby vehicles within the network to prevent further incidents. If the velocity remains within the safe range, the system stores the most recent data and continues monitoring the vehicle's surroundings.

3.3. Network Simulation

3.3.1. *Accident alert dissemination in VANET using SUMO and OMNeT++/Veins*

This simulation integrates the traffic simulator SUMO with OMNeT++ and the Veins framework to model VANET-based accident alert dissemination. When a vehicle detects an accident, it generates an alert message and broadcasts it to nearby vehicles using Dedicated Short Range Communication (DSRC) based on the IEEE 802.11p standard.

3.3.2. *Traffic and mobility simulation using SUMO*

SUMO, an open-source, highly portable, and widely used microscopic traffic simulator, was used to model the movement of vehicles in a realistic urban road network. Each vehicle was assigned specific routes, generated by a predefined route file (.rou.xml) and the configuration file (.sumocfg). The route file defines the trajectories and behaviours of vehicles on the road network. Vehicles are dynamically created and assigned routes that mimic realistic urban driving conditions. SUMO simulates vehicle mobility based on traffic dynamics, including acceleration, deceleration, and lane changes.

For this simulation, a node representing a vehicle was configured to detect an accident scenario. Upon detecting the accident, the vehicle (or OBU) generates an alert message and disseminates it to nearby vehicles within its communication range. The SUMO

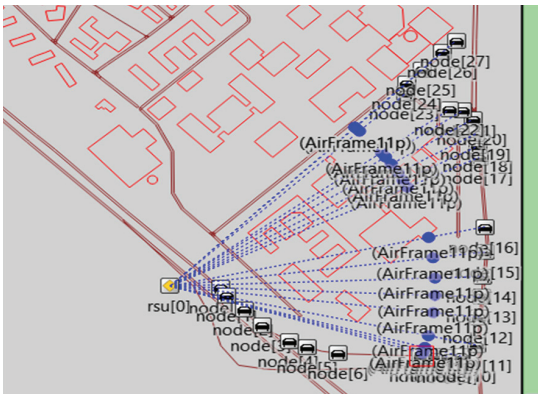

Figure 4.
RSU sending alerts in the network using Airframe.

simulation controls the mobility aspects, ensuring that vehicles follow the assigned routes and interact with each other according to realistic traffic flow patterns.

3.3.3. *VANET communication using OMNeT++ and veins*

OMNeT++ handles the event-driven network simulation, while Veins bridges it with SUMO using the TraCI interface. Vehicle mobility from SUMO is synchronized with OMNeT++ to ensure accurate positioning. Upon accident detection, an AirFrame packet containing the alert message is broadcast using IEEE 802.11p.

802.11p-based DSRC (Dedicated Short Range Communication) offers several key benefits for vehicular networks. It provides low-latency, real-time communication essential for safety-critical applications like collision warnings and emergency alerts. Operating in the 5.9 GHz band, it ensures reliable and interference-free V2V and V2I communication. Designed for high-speed mobility, 802.11p maintains stable connections even in fast-moving traffic. It enables infrastructure-independent communication, making it effective in remote areas without cellular coverage.

Additionally, its standardized protocol promotes interoperability between different vehicle systems, while its proven reliability through extensive real-world testing makes it a strong candidate for large-scale deployment in intelligent transportation systems. Nearby OBUs receive the alert and trigger appropriate responses like deceleration or route changes.

3.3.4. *Security measure*

To secure the accident alert dissemination process in the proposed SUMO–OMNeT++/Veins-based VANET system, public-key cryptography can be employed for both message confidentiality and authentication. Each vehicle (On-Board Unit, OBU) is assigned a public key (Kpub) and a private key (Kpriv). When a vehicle detects an accident, it generates an alert message M. To ensure authentication and integrity, the vehicle creates a digital signature S using its private key:

$$S = Sign(M, Kpriv\_sender)$$

This signature is attached to the message. To maintain confidentiality, especially for sensitive data (e.g., driver ID, location), the alert is encrypted using the public key of the receiving vehicle:

$$C = Encrypt(M \,||\, S,\ Kpub\_receiver)$$

The encrypted message C is then encapsulated in an AirFrame packet and broadcast using IEEE 802.11p through OMNeT++. When a nearby vehicle receives the packet, it uses its private key to decrypt it:

$$M' \,||\, S' = Decrypt(C,\ Kpriv\_receiver)$$

Then, it verifies the signature using the sender's public key to confirm authenticity:

$$Verify(M',\ S',\ Kpub\_sender) = TRUE$$

Only if the signature is valid does the vehicle proceed to process the alert and take action (e.g., slow down or reroute). This integration is implemented in OMNeT++ at the network layer, while SUMO continues to control vehicle mobility. This setup ensures secure, authenticated, and confidential communication between vehicles in real time without compromising simulation fidelity or performance.

3.3.5. *Interaction between SUMO and OMNeT++*

The integration of SUMO with OMNeT++ enables realistic simulation of vehicle mobility and communication. Using the TraCI interface, vehicle positions, speeds, and routes from SUMO are continuously synchronized with OMNeT++, allowing real-time updates that reflect actual traffic dynamics. This ensures accurate modeling of both movement and communication behaviors in a VANET environment. When a vehicle detects a potential accident, it triggers an alert that OMNeT++ broadcasts to nearby vehicles via VANET protocols. Receiving vehicles respond by issuing driver warnings or rerouting to avoid the affected area. This enables rapid, localized decision-making across the network. Together, SUMO and OMNeT++ provide a powerful simulation platform to evaluate the effectiveness of accident alert systems. The setup demonstrates how VANETs can enhance road safety through low-latency communication and dynamic traffic response.

4. Results and Potential Implementation

This section outlines the outcomes of the VANET-based accident detection system, focusing on real-time alerting, network scalability, and potential real-world deployment.

4.1. Real-Time Alert Generation and Driver Notification

The OBU accurately tracked nearby vehicle speeds using ultrasonic sensors and generated alerts when speeds crossed safe thresholds. Alerts were instantly displayed on the driver's interface across various simulated scenarios, significantly improving situational awareness and response time.

4.2. Network Dissemination and System Scalability

Alerts were broadcast to RSUs using IEEE 802.11p-based DSRC. The RSUs relayed messages to nearby OBUs, maintaining consistent performance with minimal latency and packet loss under both light and dense traffic loads. This confirms the system's scalability and effectiveness in real-world deployments.

4.3. Performance Evaluation

The simulation measured key metrics such as alert delivery time, packet delivery ratio (PDR), and system response under varying vehicle densities:

- Average Alert Delivery Time: 75 ms (light traffic), 120 ms (dense traffic).
- Packet Delivery Ratio (PDR): Maintained above 95% in all test scenarios.

- Scalability: System remained responsive up to 200 nodes without major delays.
- Latency: Below 150 ms even in high-load conditions, meeting real-time communication requirements.

These results validate the system's ability to perform reliably in urban environments.

4.4. Industrial Relevance and System Advantages

The system outperforms traditional alert methods like mobile apps or centralized services by enabling decentralized, real-time V2V and V2I communication. Its independence from cellular networks makes it ideal for deployment in both urban and remote areas.

4.5. Implications for Road Safety and Smart Transportation

By reducing driver reaction time, the system can help lower accident rates. When integrated with Intelligent Transportation Systems (ITS), it supports coordinated emergency responses and adaptive traffic control, enhancing overall traffic safety and efficiency.

4.6. Future Enhancements and Applications

Planned improvements include automated braking in autonomous vehicles, machine learning for predictive collision detection, and integration with smart city infrastructure to enable dynamic route control and real-time traffic optimization.

5. Conclusion

This paper presents the design and implementation of an IoT-enabled accident detection and alert system using Vehicular Ad-hoc Networks (VANETs). The On-Board Unit (OBU), built with ultrasonic sensors and an Arduino microcontroller, monitors vehicle proximity, calculates relative speeds, and predicts potential collisions. Leveraging V2V and V2I communication, the system disseminates real-time alerts to nearby vehicles via Road Side Units (RSUs), helping prevent multi-vehicle accidents, particularly in dense traffic.

Using SUMO, OMNeT++, and Veins for simulation, the system demonstrated low-latency communication and high scalability under varying traffic loads. Compared to conventional systems, this decentralized VANET-based approach offers greater reliability, especially where mobile networks are limited. While promising, further improvements are needed to address challenges like signal interference and congestion in high-traffic environments.

References

[1] E. Abinaya and R. Sekar, "An Intelligent Secure Traffic Management System Based On Vanet," IOSR J. Electron. Commun. Eng., vol. 9, no. 1, pp. 15–27, 2014, doi: 10.9790/2834-09121527.

[2] C. Chatrapathi, M. Newlin Rajkumar and V. Venkateshkumar, "VANET based integrated framework for smart accident management system," Proc. IEEE Int. Conf. Soft-Computing Netw. Secur. ICSNS 2015, 2015, doi: 10.1109/ICSNS.2015.7292411.

[3] F. Ahmad, A. Adnane, F. Kurugollu and R. Hussain, "A Comparative Analysis of Trust Models for Safety Applications in IoT-enabled Vehicular Networks," IFIP Wirel. Days, vol. 2019–April, 2019, doi: 10.1109/WD.2019.8734204.

[4] A. M. Kirthima, "IoT Based Accident Detection System in Vanet," vol. 11, no. 7, pp. 100–107, 2020, doi: 10.34218/IJARET.11.7.2020.0.

[5] T. K. Bhatia, R. K. Ramachandran, R. Doss and L. Pan, "A review of simulators used for VANETs: The case-study of vehicular mobility generators," 2020 7th Int. Conf. Signal Process. Integr. Networks, SPIN 2020, pp. 234–239, 2020, doi: 10.1109/SPIN48934.2020.9070933.

[6] N. Chhabra and R. Kumar (2023). A Comprehensive Review of Recent Developments in VANET for Traffic, Safety & Remote Monitoring Applications. Journal of Network and Systems Management.

[7] V. Singh and P. Verma (2023). Smart Accident Detection and Rescue System Using VANET. IEEE Xplore.

[8] P. Gupta and D. Sharma (2023). Simulation of a Vehicular Adhoc Network (VANET) for Mitigating Vehicular Accidents. ResearchGate.

[9] A. Hussain and M. Khan (2023). Advances in Vehicular Ad-Hoc Networks (VANETs): Challenges and Road-map. Open Repository.

Biographies

Harsh H. Mangroliya is a postgraduate from Kingston University, London, United Kingdom, where he earned an MSc in Networking and Information Security with distinction in his dissertation. He completed his B.Tech in Computer Science and Engineering with a specialization in the Internet of Things (IoT) from Vellore Institute of Technology, Vellore, India, also achieving distinction in his dissertation. His research interests include the Internet of Things (IoT), Vehicular Ad Hoc Networks (VANETs), and Network and Information Security. Harsh's academic work

focuses on developing secure and efficient network architectures and exploring innovative approaches to connected systems and data protection.

Smit H. Gor is a software engineer and researcher with interests in backend systems, cloud computing, artificial intelligence, and system optimization. His work focuses on developing efficient and scalable technological solutions while exploring advancements that contribute to modern computing research. He completed his B.Tech in Computer Science and Engineering with a specialization in the Internet of Things (IoT) from Vellore Institute of Technology, Vellore, India. Smit is committed to pursuing innovative research that bridges theoretical understanding with real-world applications.

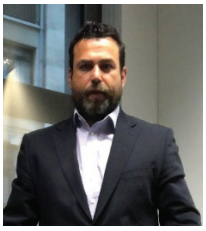

Christos Politis is the Chair of Digital Technologies at **Kingston University London (KU)**, within the **School of Computer Science**. He is a senior member of the **Cyber, Engineering and Digital Technologies KERI**. Upon joining Kingston University, he founded and currently leads the **Wireless Multimedia & Networking (WMN)** research group. His teaching focuses on wireless systems, networks, and protocols.

Before his appointment at Kingston University, **Christos Politis** worked at **Ofcom**, the UK Regulator and Competition Authority, where he served as an **R&D Team Leader**. Earlier in his career, he was a **Postdoctoral Researcher (PDRA)** at the **University of Surrey**, UK, in the **Centre for Communication Systems Research** (now the **Institute for Communication Systems** and **6G Innovation Centre**), where he worked on virtual distributed testbeds. Prior to his academic career, he held engineering positions with **Intracom-Telecom SA** and **Maroussi 2004 SA** in Athens, Greece.

Christos Politis has successfully secured sustained funding from the **EU and UK research and technology frameworks** under the ICT and Security programmes, including **FP5, FP6, FP7, H2020, Horizon Europe, EPSRC,** and **Innovate UK**. He holds **two patents** and has authored **over 200 publications** in international journals and conferences, as well as contributing chapters to **ten books**.

In parallel with his academic work, **Christos Politis** is actively involved in **entrepreneurship and technology innovation**. He is the **Founder and a Director of Ubitech Ltd.**, which has recently launched **UbiTheraPlay**, a gaming platform designed for the **rehabilitation of patients with neuro-disabilities**. He also advises and consults for several **governmental bodies, universities, and commercial organisations** across **Europe, North America, the Middle East, and Asia** – including the **EU, UK, Canada, Greece, Qatar, China,** and **Malaysia** – on research programmes, policies, and strategic portfolios.

Christos Politis holds a **PhD** and **MSc** from the **University of Surrey, UK**, and a **BEng** from the **University of Athens, Greece**, all in **Electrical and Electronic Engineering**. He is a **Senior Member of the IEEE** and a **UK Chartered Engineer**.

Rehan Usman is a Senior Lecturer in Cyber Security at Kingston University London, with a PhD in IT Convergence Engineering and a diverse academic background in telecommunications, project management, and IT. His research focuses on 6G HetNets, medical IoT, cyber security, QoE, and AI in healthcare and smart cities, with over 45 publications to date. He has over a decade of teaching and academic leadership experience and has supervised numerous undergraduate, master's, and PhD students. Dr. Usman has contributed to various IEEE conferences as a session chair, TPC member, and organiser, and currently chairs the Digital Healthcare Vertical Industries Platform (VIP) Working Group at the Wireless World Research Forum (WWRF). He welcomes exceptional PhD applicants with strong research interests.

DOI. No. 10.13052/2794-7254.026

Maximum Ratio Transmission for Pedestrians' Safety at Crosswalks in An Outdoor V2X Environment at 28 GHz

Sai Radha Abhigna Maturi, Hussain Al-Rizzo and Nijas Kunju*

Abstract: Vulnerable Road Users (VRUs) include pedestrians, bicyclists, and motorized two-wheelers operators. According to the World Health Organization's (WHO) 2023 Global Status Report on Road Safety, pedestrians account for 23% of fatalities, or at least 31 deaths every hour. In developed countries, the number of road accidents is significantly declining, but a significant percentage of accidents involving VRUs still remains high. Vehicle-to-everything (V2X) communication is one such safety feature that fosters communication amongst numerous elements on the road for cooperative safety and, consequently, pedestrians. Communication between vehicles and pedestrians (V2P), infrastructure and vehicles (V2I), and vehicles themselves (V2V) is a part of vehicle-to-everything (V2X). Pedestrians carrying mobile devices and wearable technology can depend upon V2X communications to improve their safety and situational awareness. To transmit and receive signals efficiently, this paper compares and evaluates the performance of Linearly Polarized Antenna array (LPA) with and without Maximum Ratio Transmission (MRT) technique in the context of V2P communications. The focus is on the pedestrian's point of view at crosswalks in outdoor V2X scenarios. In conclusion, LPA with MRT technique surpasses in signal reception at pedestrians near crosswalks in a V2X outdoor environment.

Keywords: FR2, LP, MRT, VRU.

1. Introduction

The Governors Highway Safety Association (GHSA) released preliminary data in 2023 showing 7,318 pedestrian traffic fatalities in the United States. According to the report [1], 844 pedestrian fatalities were recorded in the ten most populous U.S. cities. These statistics show that pedestrian deaths occur most frequently in urban areas. Consequently, the safety of pedestrians is an essential consideration in modern transportation systems, especially in urban areas where pedestrian-vehicle interactions are common.

Department of Electrical and Computer Engineering, University of Arkansas at Little Rock, Little Rock, AR 72204, USA
E-mail: smaturi@ualr.edu; Nijas.Kunju@ansys.com; hmalrizzo@ualr.edu
*Corresponding Author
Manuscript received 09 June 2025, accepted 17 December 2025, and ready for publication 31 December 2025.

V2P, which is a subset of V2X, is a general term that refers to the exchange of data between automobiles and pedestrians' wearable technology and smartphones. Real-time alerts to avert collisions are made possible by this technology, which enables the sharing of vital information regarding the position, velocity, and direction of pedestrians and automobiles. To guarantee the prompt delivery of safety- critical signals, V2P communication uses Cellular V2X (C- V2X) or Dedicated Short-Range Communication (DSRC) platforms [2]. The DSRC band ranges from 5.85GHz to 5.925GHz [3]; these platforms leverage low latency and high dependability. Numerous studies have exhibited the efficaciousness of V2P communication in augmenting pedestrian safety [4] and [5]. Moreover, the authors in [6] emphasized the advantages of employing V2P systems to alert pedestrians to oncoming automobiles, thereby decreasing reaction times and enhancing situational awareness. Similarly, [7] remarked on how robust connectivity in different urban areas may be achieved with C- V2X-based V2P communication, which is vital for applications related to pedestrian safety.

V2X operates in two frequency ranges: FR1, which spans from 410 MHz to 7.125 GHz, and FR2, from 24.25 GHz to 52.6 GHz [8]. Specifically, the 28 GHz millimeter-wave (mmWave) band has attracted much interest due to its high data rate capability, improved stability, and low power consumption [9]. Because of its low latency, the mmWave band holds excellent potential for high-level safety applications in V2X communications, such as reducing traffic accidents. This mandate forces the antenna architecture to consider essential design concepts like simplicity, affordability, and miniaturization to guarantee that it satisfies the demands of V2X communications [10] and [11]. Because of this, Microstrip Patch Antennas (MPAs) have become more attractive because of their small size, lightweight, cost- effective production, and ease of assembly [12].

Ansys HFSS is used to produce realistic geometry with intersecting roads that resemble an Outdoor V2X environment. A single MPA is used as a receiving antenna (RX) placed on the hands of four pedestrians carrying smartphones or other devices at the crosswalk. A two-by-two transmitting antenna (TX) array is mounted on the traffic signal. The power density in W/m^2 is computed over a square prediction area of length and width of five meters to see the power distribution at the pedestrians' hand height, roughly equal to one meter. Received power at the pedestrians' RX antenna is computed and compared with and without MRT weights placed at the TX. In summary, LPA targets pedestrians with MRT more successfully than without MRT; according

to the observations, 7dB more power has been received. It should be emphasized that this conclusion is valid only for the specific scenarios and antennas used in this study and, hence, cannot be generalized to other scenarios and/or antenna arrays.

The rest of the paper is organized as follows. The scenario and the solvers utilized for the simulations are covered in detail in Section 2. The TX and RX antenna gain patterns and their reflection coefficients are provided in Section 3. Section 4 discusses the system model and the MRT weights formulation. Section 5 displays the power density maps that illustrate the power distribution around each pedestrian. This can be observed both with and without MRT cases. Section 6 shows received power comparisons. Section 7 stands as the paper's conclusion.

2. Simulation Scenario and Solvers

2.1. Urban V2X Scenario

A four-way intersection used in this paper is depicted in Figure 1, with street length measured as 50 m and four lanes, each 15 m is the width of the road. The following elements are included to make it an appropriate, realistic urban V2X scenario: cars, pedestrians at crosswalks, buildings, trees, and other infrastructure, such as street and traffic lights. All these elements are assigned their respective material assignments, including permittivity and conductivity. The TX antenna is placed on the traffic light facing toward pedestrians 1 and 3, and pedestrians 2 and 4 are placed on the opposite side of the TX antenna. RX antennas are mounted at all four pedestrians. These antennas are assumed to be a part of the wearable gadgets of pedestrians or installed on smartphones. The entire scenario is animated in time for a second (i.e., from 0 to 1 sec) with ten intervals lasting 100 msec. Two cars travel 10 meters in one second at a speed of 1 m/sec. Similarly, all the pedestrians are traveling 11 meters at a speed of one m/sec. For each 100 msec interval, 1 meter is travelled by cars and 0.1 meter by pedestrians.

2.2. Shooting and Bouncing Rays (SBR+) Solver

Ansys HFSS SBR+, an asymptotic high-frequency electromagnetic (EM) simulator [13,14] is used as a solver in our simulations. It models EM interactions in electrically large environments by employing the Shooting and Bouncing Rays (SBR+) method to compute EM solutions rapidly. SBR+ computes installed antenna performance, extended near-field distributions, and far-field radiation patterns for electrically large platforms with minimal computational resources [15]. Antennas operating on large host platforms can experience significant performance degradation due to EM interaction with the host structure. SBR+ facilitates the simulation and study of installed antenna applications, including antennas mounted on buildings or cars and dynamic complex environment scenarios involving several vehicles.

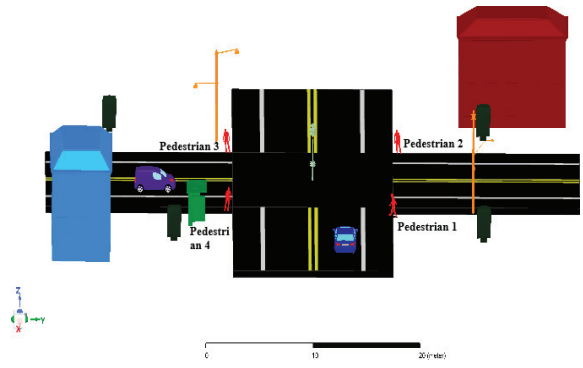

Figure 1.
Realistic urban V2X scenario.

2.3. Parametric Analysis and Optimization

Parametric analysis in Ansys HFSS SBR+ simulates the time-varying scenario for each periodic modification. One or more variables are defined for sweep definitions in the analysis, each specifying a range of variable values. In this case, parametric analysis computes the installed TX and RX antenna interactions concerning the surrounding environment (such as trees, buildings, and lights) for every change and time interval. All the design variations optimetrics instructs the software to solve are specified in parametric configuration. Optimetrics solves the design, calculates the received power (dB), and determines the antenna coupling parameters.

3. Antennas and Gain Plots

3.1. Linearly polarized antenna array

A two-by-two square MPA array with coaxial probe feed [16] is used as an LPA. The design and simulation are conducted using Ansys HFSS Design 2024 R1; the patch antenna resonates at 28 GHz. This antenna is mounted on a Rogers RT-droid 5880 substrate, notable for its dielectric constant of 2.2 and thickness of 0.8 mm. The other design parameters and specifications of the single element are listed in Table 1.

Table 1.

LPA Design parameters for a single element	
Parameter	**Value (mm)**
Length and Width of Substrate	5.4
Length and Width of Top Ground	5.4
Length and Width of Bottom Ground	5.4
Length and Width of Patch	3.1
Coax Feed Length	0.8
Coax Inner Radius	0.1
Patch Spacing	0.625
Radome Height	2
Radome Thickness	0.5
Number of Vias	32
Vias Radius	0.2
Vias Height	0.8
Vias Position	−2.5, −2.5, 0

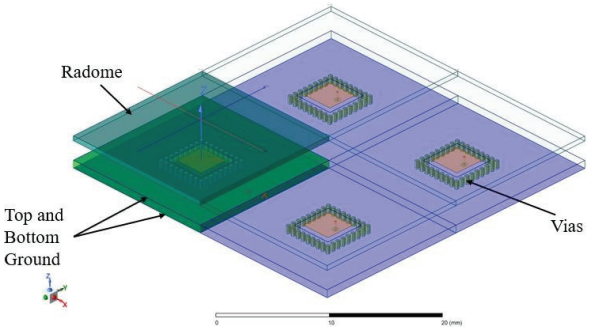

Figure 2.
Two-by-two square patch antenna array at 28 GHz.

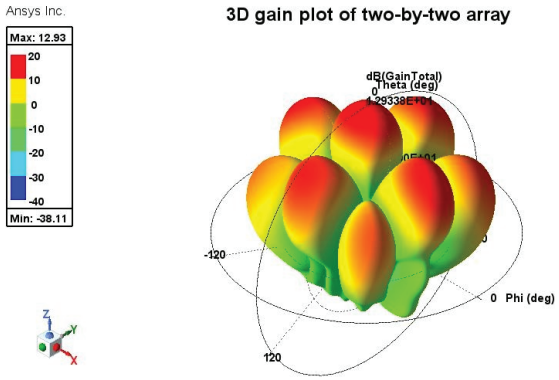

Figure 3.
3-D gain plot of LPA.

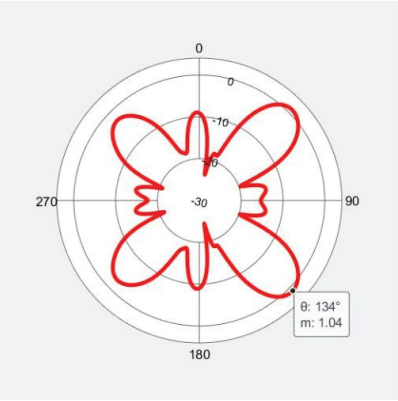

(a)

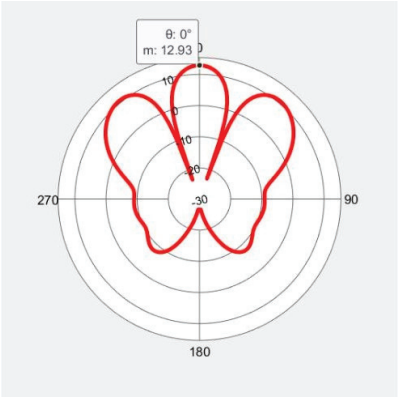

(b)

Figure 4.
2D gain plots of the array (a) Azimuth plane pattern. (b) Elevation plane pattern.

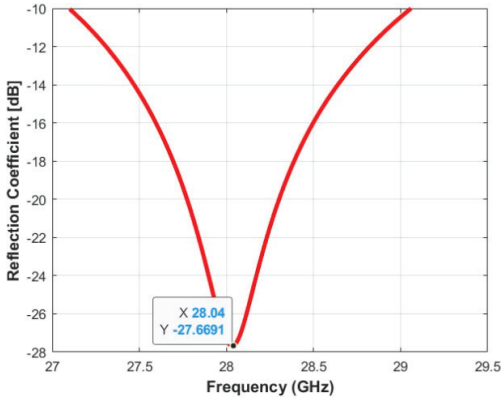

Figure 5.
Reflection coefficient S_{11} of the antenna.

Figure 2 displays the 28 GHz 5G square patch antenna with radome arranged in a two-by-two array [16]. A radome is a protective cover placed over the antenna; its primary purpose is to protect it from environmental factors such as rain, wind, and physical damage. In 5G applications, especially outdoors, the radome is crucial for maintaining consistent performance over time. The antenna has two grounds: one at the top and one at the bottom. These two ground planes in a patch antenna array are essential in offering mechanical support, impedance matching, minimizing surface waves, and controlling operation by providing isolation and shielding. Since the antenna contains multiple layers, vias are essential for interconnecting these layers; they connect the patch or other layers to the ground plane.

3.2. Gain Plots

Figure 3 shows the 3D gain plot of the two-by-two antenna array. The peak gain of the antenna array is 12.93 dB. Figure 4 shows the 2D gain plots of the array for azimuth and (b) elevation planes. The azimuth plane pattern displays the antenna gain in the plane parallel to the ground (XY-plane) when the elevation angle θ is fixed at 90°. It is a polar plot with gain plotted against azimuth angle (φ), which offers details on the antenna's radiation patterns in various azimuthal directions (φ ranging from 0° to 360°). The elevation plane is orthogonal to the ground plane, say either the YZ-plane ($\varphi = 90$ deg) or the XZ-plane ($\varphi = 0°$). Gain versus elevation angle (θ) is plotted in a polar plot to illustrate how the antenna radiates above and below the horizontal plane as the θ changes.

The simulated S_{11} for the proposed antenna, as illustrated in Figure 5 confirms its acceptable performance across a bandwidth

from 27 to 29 GHz. Furthermore, the measured peak minimum value (dip) is approximately −27.6 dB at 28.04 GHz, highlighting the antenna's high efficiency in radiating and receiving electromagnetic signals throughout the frequency range. The antenna's performance highlights its potential for applications requiring high frequency operation and larger bandwidth, particularly in V2X communications where reliable and efficient signal transmission is critical.

4. MRT Beamforming

MRT is a signal processing technique used to increase the performance and reliability of data transmission. Maximal Ratio Combining (MRC) is a traditional antenna diversity technique [18], where the signals from the multiple receive antennas are weighted such that the signal-to-noise ratio (SNR) of their sum is maximized in the absence of interference, or when interference is treated as background noise. MRT is the dual of MRC [19] at the transmitter side, i.e. the transmit antenna weights are matched to channel fading. It is used to direct the transmission in specific directions. This is done by adjusting the phase and amplitude of the signals sent from multiple antennas, which can lead to constructive interference in the desired direction and destructive interference in others. MRT requires knowledge of the Channel State Information (CSI) at the transmitter. The CSI represents the channel properties between each transmitter and receiver antenna pair. The MRT algorithm uses this information to adjust the phase and amplitude of the transmitted signals to maximize the received signal power [19].

The core idea of MRT is to align the transmitted signals from multiple antennas so that they add constructively at the receiver. By knowing the channel, the transmitter can apply complex weights to the signal to compensate for the channel effects, thereby ensuring that the signals combine coherently at the receiver. In our current system one transmitter (TX) with 4 antennas and elements and one receiver (RX) with a single antenna element is present. The formulation of MRT weights for this case as shown below [20].

By concatenating K users, the channel matrix results in

$$H = [h_1\, h_2\, \ldots\, h_K]^T \in C^{K,N} \tag{1}$$

Since the system employs single-antenna users, the received signal for each user k can be stacked in a single received vector.

$$y = H\,x + z \in C^{K,1} \tag{2}$$

where z is the Additive White Gaussian noise (AWGN) at the receiver.

In MRT, the transmitted signals are weighted versions of the original signal s:

$$x = W\,s \in C^{N,1} \tag{3}$$

where $s \in C^{K,1}$ and $W \in C^{N,K}$ are vector of user symbols and precoder matrix respectively.

The precoder matrix can be written as:

$$W = [w_1\, w_2 \ldots w_K]^T \tag{4}$$

w_K are the complex weights applied to the transmitted signal s. The objective is to choose the weights. w_K such that the received signal is maximized. The optimal weights are chosen as

$$w_K = \frac{h_k^*}{\|h\|} \tag{5}$$

h_k^* is the complex conjugate of the channel coefficient h_K.

$\|h\| = \sqrt{\sum_{K=1}^{4} |h_K|^2}$ is the norm of the channel vector.

This choice of weights maximizes the SNR at the receiver. The received signal then becomes:

$$y = \sum_{K=1}^{4} h_K w_K s + n \tag{6}$$

Substituting Equation (5) into Equation (6)

$$y = \frac{1}{\|h\|} \sum_{K=1}^{4} h_K h_k^* s + n \tag{7}$$

Since $h_K h_k^* = \|h\|^2$ the received signal simplifies to:

$$y = \frac{1}{\|h\|} \|h\|^2 s + n \tag{8}$$

$$y = \|h\| s + n \tag{9}$$

This shows that the signal at the receiver is maximized by a factor of $\|h\|$, which is the norm of the channel vector, thus maximizing the SNR at the receiver.

5. Power Distribution Across the Prediction Area

5.1. Without MRT at TX

Without an MRT precoder, the power distribution over a 5 m × 5 m square area with 10 sample points at the 0.8 m pedestrian hand height is simulated. The results are only acquired at three-time intervals rather than eleven (as in the upcoming section) seconds to reduce computation time. To examine the power distributions, beginning, middle, and finishing time intervals – that is, 0 seconds, 0.5 seconds, and 1 second – are taken. The power distribution rectangle contour plots acquired and superimposed at the corresponding pedestrians are displayed in Figures 6, 7, and 8. These graphs give the power density over the region by determining the power transmitted by the TX at each location.

5.2. With MRT at TX

The same procedure was performed when applying the MRT precoder to the TX and observing the plots at these three intervals. Evidently, when the MRT precoder is used, the plots exhibit a higher power density. The highest power distribution for the three-time slots has been observed compared to the scenario in which MRT is not implemented.

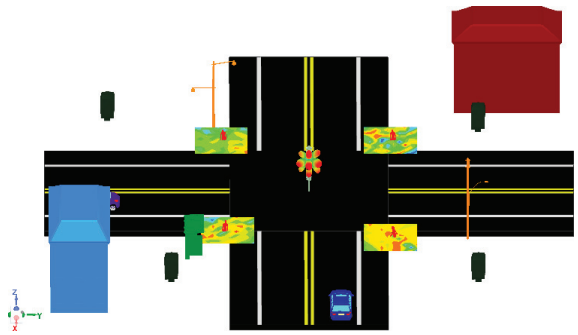

Figure 6.
Power distribution without the usage of an MRT precoder at TX to every pedestrian at interval of 0 sec.

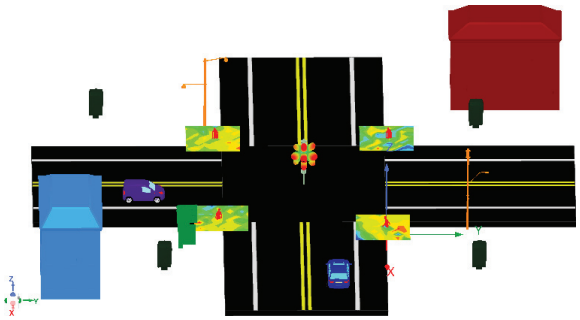

Figure 7.
Power distribution without the usage of an MRT precoder at TX to every pedestrian at interval of 0.5 sec.

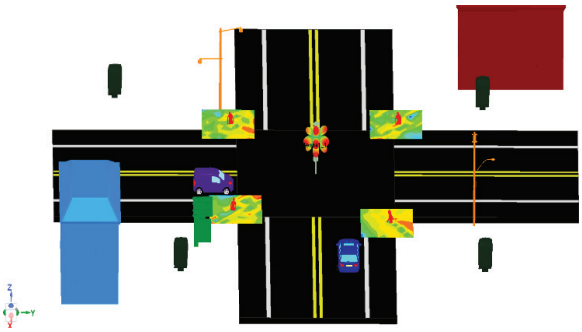

Figure 8.
Power distribution without the usage of an MRT precoder at TX to every pedestrian at interval of one second.

Figure 9.
Power distribution using an MRT precoder at TX to every pedestrian at a time interval of 0 seconds.

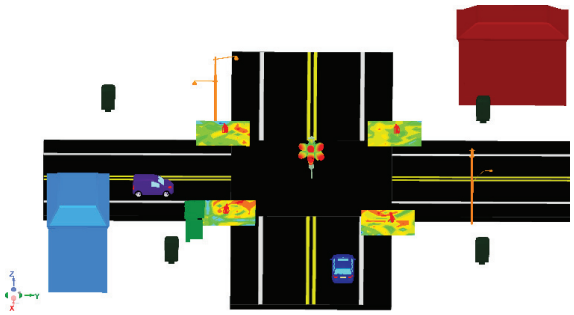

Figure 10.
Power distribution using an MRT precoder at TX to every pedestrian at a time interval of 0.5 seconds.

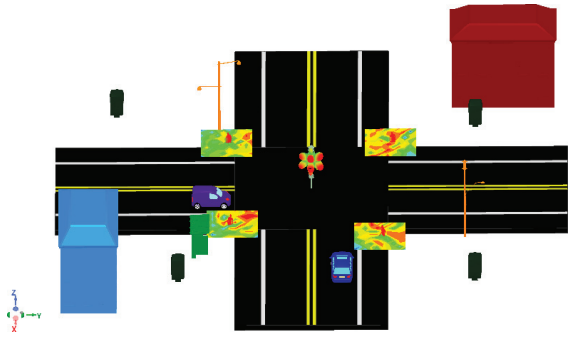

Figure 11.
Power distribution using an MRT precoder at TX to every pedestrian at a time interval of 1 second.

6. Comparison of Received Power with and Without MRT

Received power is determined at each pedestrian location before and after the application of MRT at eleven time slots ranging from 0 to 1 seconds to obtain an accurate measurement with metrics.

Pedestrians 1 and 4 are subject to the MRT algorithm because they face the TX, while pedestrians 2 and 3 are situated behind the TX. By calculating the weights for each pedestrian individually and placing them at the TX antenna, the MRT precoder maximizes the signal transmission to both pedestrians. The simulated received power comparison plots with and without MRT are displayed below in Figures 12 and 13:

Table 2 compares the average received power at pedestrian locations before and after MRT. It clearly shows that, following the MRT application, the average received power for both pedestrians has increased to about 7 dB. MRT guarantees optimal signal

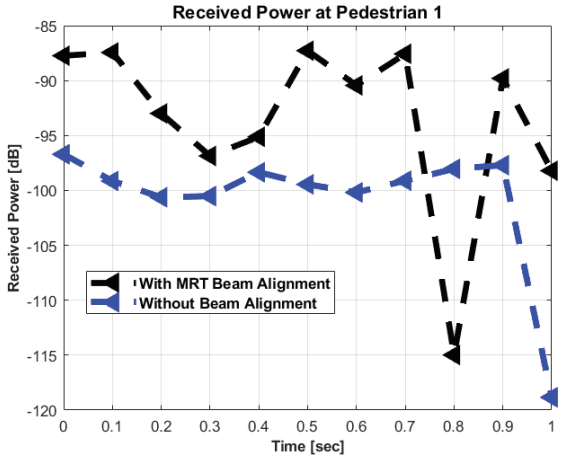

Figure 12.

Comparison of received power values with and without MRT at Pedestrian 1.

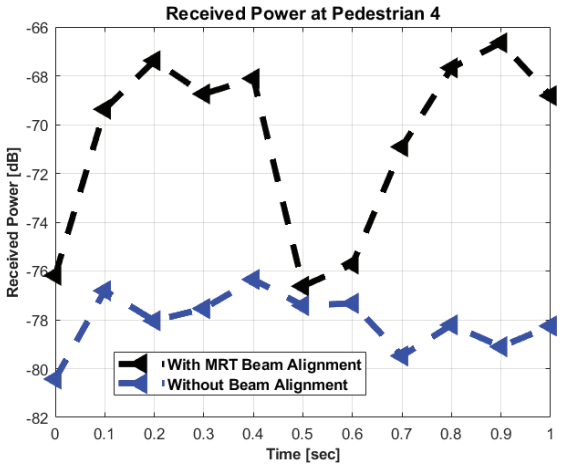

Figure 13.

Comparison of received power values with and without MRT at Pedestrian 4.

Table 2.

Comparison of average received power at pedestrians with and without MRT		
	Pedestrian 1	**Pedestrian 4**
Average power with MRT (dB)	−93.49	−70.56
Average power without MRT (dB)	−100.78	−78.08
Difference value	**7.2**	**7.5**

reception for most temporal instants. Consequently, pedestrians can ensure the best possible signal reception despite reflections and multipath interference by using the MRT.

7. Conclusion

Enhancing signal reception at the pedestrian level is critical for improving the performance and reliability of wireless communication systems, particularly in urban environments where obstacles and multipath effects can degrade signal quality. In an urban V2X environment, this study compared the functionality of MRT signal preprocessing applications at pedestrian crosswalks. The received signal power and power distributions are evaluated with and without MRT. According to this investigation, using MRT has enhanced the signal power reception by an average of 7 dB for pedestrians. And the maximum signal reception is consistently seen across 1 second. Implementing MRT algorithms further improves signal reception by optimizing the transmission power distribution, focusing energy on the desired direction, and enhancing overall signal strength and quality for pedestrians.

References

[1] Spotlight on Highway Safety; Pedestrian Traffic fatalities by State; Technical Report; Governors Highway Safety Association (GHSA) Annual Meeting 2023; Connecting Communities: Putting Vision Zero into Action, New York, NY.

[2] "Connected vehicle safety pilot program," https://www.its.dot.gov/factsheets/pdf/SafetyPilotfinal.pdf.

[3] Xinzhou Wu, Radovan Miucic, Sichao Yang, "Cars Talk to Phones: A DSRC Based Vehicle-Pedestrian Safety System," 2014 IEEE 80th Vehicular Technology Conference (VTC2014-Fall), Vancouver, BC, Canada, 2014, pp. 1–7.

[4] X. Wu, S. Subramanian, R. Guha, R. White, J. Li, K. Lu, A. Bucceri, and T. Zhang, "Vehicular communications using dsrc: challenges, enhancements, and evolution," 2013.

[5] R. Miucic and S. Bai, "Vehicle-to-pedestrian cooperative safety application," accepted for publication at ITS WC 2014.

[6] Sara El Hamdani, Nabil Benamar, Mohamed Younis, "Pedestrian Support in Intelligent Transportation Systems: Challenges, Solutions and Open issues," in Proceedings of the Transportation Research Part C: Emerging Technologies, Volume 121, December 2020, 102856.

[7] P. Li, K. Wu, Y. Cheng, S. T. Parker and D. A. Noyce, "How Does C- V2X Perform in Urban Environments? Results From Real-World Experiments on Urban Arterials," in IEEE Transactions on Intelligent Vehicles, vol. 9, no. 1, pp. 2520–2530, Jan. 2024.

[8] M. Bonato, et al., "Assessment of sar in road-users from 5g-v2x vehicular connectivity based on computational simulations," Sensors, vol. 22, no. 17, p. 6564, Aug. 2022.

[9] T. S. Rappaport, et al., "Millimeter wave mobile communications for 5G cellular: It will work!" IEEE access, vol. 1, pp. 335–349, May. 2013.

[10] C. Kykkotis, P. S. Hall, R. A. Lewis, and A. D. Searle, "Millimetre wave antennas for future vehicle communications," in IEEE 49th Veh. Technol. Conf., vol. 2, pp. 1585–1588, IEEE, May. 1999.

[11] D. Rongas, A. Paraskevopoulos, L. Marantis, and A. G. Kanatas, "An integrated shark-fin reconfigurable antenna for V2X communications," Prog. Electromagn. Res., vol. 100, pp. 1–16, Feb. 2020.

[12] M. U. Khan, M. S. Sharawi, and R. Mittra, "Microstrip patch antenna miniaturisation techniques: a review," IET Microw. Antennas Propag., vol. 9, no. 9, pp. 913–922, Jun. 2015.

[13] ANSYS, Inc. (2018). "ANSYS HFSS SBR+ [White paper]." https://www.ansys.com/content/dam/resource-center/application-brief/ansys-sbr-plus.pdf.

[14] A. P. Sligar, 'Machine learning-based radar perception for autonomous vehicles using full physics simulation,' IEEE Access, vol. 8, pp. 51470–51476, 2020.
[15] ANSYS, Inc. Installed Performance Modeling & Simulation for Antennas "A good antenna, righteously placed..." Advanced Modeling & Simulation (AMS) Seminar Series NASA Ames Research Center, February 18, 2020. https://www.nas.nasa.gov/assets/nas/pdf/ams/2020/AMS_20200218_Carpenter.pdf.
[16] ANSYS, Inc. "How to Design Base Station (or Microcell) Antenna Arrays for 5G Wireless Networks [White paper]." https://www.ansys.com/content/dam/resource-center/application-brief/wp-how-to-design-base-station-or-microcell-antenna-arrays-for-5g-wireless-networks-v2.pdf.
[17] J. Winters, "Optimum combining in digital mobile radio with cochannel interference," IEEE Trans. Veh. Technol., vol. 2, no. 4, pp. 528–539, Aug. 1984.
[18] T. K. Y. Lo, "Maximum ratio transmission," IEEE Trans. Commun., vol. 47, no. 10, pp. 1458–1461, Oct. 1999.
[19] Zhang, Y., Gao, J. and Liu, Y. MRT precoding in downlink multi-user MIMO systems. J Wireless Com Network 2016, 241 (2016).
[20] Zakia, "Maximizing the Sum Rate of Massive MIMO with Rectangular Planar Array and MRT Beamforming," 2019 IEEE 89th Vehicular Technology Conference (VTC2019-Spring), Kuala Lumpur, Malaysia, 2019, pp. 1–5.

Biographies

Sai Radha Abhigna Maturi is PhD Student in the Department of Electrical and Computer Engineering and working as a Graduate Teaching Assistant at University of Arkansas at Little Rock, United States, since August 2022. Completed Master of Technology in Communication and Radar Systems Engineering from Koneru Lakshmaiah Education Foundation, India in May 2020 and received a Silver Medal for academic performance. She published a Journal paper in Acta Geophysica as a main author in her Master's degree as a part of Indian Space Research Organization (ISRO) sponsored project. Her current and previous research areas include Beamforming of Antennas, Massive MIMO, V2X, V2I, V2V, effects of ionosphere on GPS, GNSS.

Hussain Al-Rizzo received his PhD in Electrical and Computer Engineering from the University of New Brunswick, Canada. In 2000, he joined the Systems Engineering Department at the University of Arkansas at Little Rock, where he is currently a Professor of Telecommunication Systems Engineering. He has published over 300 papers in peer-reviewed journals and conference proceedings, two books, eight book chapters, and four patents. His research areas include V2V, V2X, and V2I wireless systems; smart antennas; massive MIMO; flexible RF components and antennas; implantable medical devices; electromagnetic wave scattering by complex objects; design, modeling, and testing of high-power microwave applicators; precipitation effects on GPS; terrestrial and satellite frequency re-use communication systems; field operation of NAVSTAR GPS receivers; data processing and accuracy assessment; and effects of the ionosphere, troposphere, and multipath on code and carrier-beat phase GPS observations.

Nijas Kunju received MSc (2009) and PhD (2015) in Electronics Science from Cochin University of Science and Technology, Cochin, Kerala under supervision of Prof. P Mohanan. He is currently working as Technical Manager at ANSYS Inc. He is specialized in the domain of RF, Antennas, Radar, Signal Integrity, Power Integrity, and Multiphysics simulation. Before he joined ANSYS he was working as Research Consultant in GE Global Research in Bangalore on the area of microwave material sensing for detecting different materials in Crude Oils. He holds 20+ International publications and 20+ national and international conference publications.

DOI. No. 10.13052/2794-7254.027

Channel Modeling using Deep Neural Network with RIS-powered Wireless Communication Systems

Kumud S. Altmayer[1,*], *Ilya Burtakov*[2] *and Hussain Al-Rizzo*[1]

Abstract: This work deals with Reconfigurable Intelligent Surfaces or (also known as Intelligent Reflecting Surfaces) which provide an improvement of performance of wireless communications by utilizing software-controlled meta-surfaces for the reflected signals from the source to destination, especially when the direct path is weak and hence improving the antenna array.

The performance evaluation is done by one of the techniques that utilizes the very high rates and/or large meta-surfaces to outperform the classic method of decode and forward, both in terms of the total transmit power and the energy efficiency. The channel measurements used by classifying them as a function of the frequency band, and usage of deployment scenarios such as indoor/outdoor, and system configuration. So, the 5G and beyond which is 6G use several antennas including the algorithms to make use of signal processing. This improves the antenna array technology.

In the next steps, we work on machine learning-based performance prediction using a deep neural network (DNN) to evaluate the performance of the RIS-aided system in the low-frequency range. This would provide a greater influence of scatterers with a weaker signal attenuation allowing the neural network to pick up a larger number of features, e.g. accurately predicting the energy efficiency (EE), and outage probability (OP).

Keywords: LIS, RIS, 5G, 6G, millimter waves, FR2, Terahertz, MIMO, neural networks.

1. On Reconfigurable Intelligent Surfaces

Reconfigurable Intelligent Surface (RIS) technology is a promising way to improve the performance of wireless communication systems. The RIS is a two-dimensional surface that can be built using electromagnetic meta-materials. Such surfaces have a potential for the capacity improvement and coverage extension as a result of partial control of propagation environment, [4]. Also, "Large" refers to the size of the intelligent surface and the large number of passive elements it contains, while "reconfigurable" highlights its key feature of being programmable to manipulate signals in real-time. Thus, large intelligent surfaces (LIS) and reconfigurable intelligent surfaces (RIS) are two terms for the same technology, with "reconfigurable intelligent surfaces (RIS)" being the more common and modern term.

One should note that for a MIMO channel with no RIS, the throughput is determined by the channel matrix y=Hx. Each element determines signal gain α & β, the phase shifts to the RIS elements, [1]. When one is working on beyond 5G, the advent of electromagnetic components that can shape how they interact with wireless signals enables partial control of the propagation.

2. Mathematical Theory of RIS and Machine Learning Implementation

An RIS is a thin surface composed of N elements, each being a small antenna that receives and passively re-radiates with a configurable time delay. For the narrowband signals, this delay corresponds to a phase shift. Assuming the phase shifts are properly adjusted, the scattered waves add constructively at the receiver. This principle resembles traditional beamforming; each element has a fixed radiation pattern, but the collection of phase shifts determines where constructive interference among the scattered waves occurs. RIS can be modified and is called LIS. In other words, LIS can both generate and reflect electromagnetic waves, while RIS is only used to reflect electromagnetic waves. For machine learning simulations, RIS has been replaced by LIS.

We consider the scattering process with M User elements. The signal received is y and may not be noise free at the multiple R_x antennas together with multiple transmit antennas as follows

$$y = (R\Phi T + H)x + n \tag{1}$$

where $x = [x_1, x_2, \ldots, x_{N_t}]^T$. The noise is $n = \cong \mathcal{C}N(0, \sigma^2)$

It belongs to $\mathbb{C}^{N_t x1}$ for the T_x signal, and y is the R_x signal.

The matrix $\mathcal{H}$ corresponds to the direct connection between T_x and R_x. R is the channel coefficient and the phase shifting is written as below representing the diagonal RIS reflection matrix:

We consider the diagonal matrix Φ from equation (2), that describes the incident signal amplification and phase shift of the each UC. By turning the phase shifts of UCs, the RIS induces some phase between the reflected signals and make them interfere either between the reflected signals and make them interfere either

[1]Department of Systems Engineering, College of Engineering and Information Technology, University of Arkansas at Little Rock, USA
[2]Wireless Networks Lab, Institute for Information Transmission Problems, Russian Academy of Sciences, Moscow, Russia
E-mail: ksaltmayer@ualr.edu; burtakov@wireless.iitp.ru; hmalrizzo@ualr.edu
*Corresponding Author
Manuscript received 10 June 2025, accepted 03 December 2025, and ready for publication 31 December 2025.

constructively so that the desired signal strength increases at the receiver or destructively to mitigate the co-channel interference. The matrix $\mathcal{H}$ corresponds to the direct connection between T_x and R_x. R is the channel coefficient and the phase shifting is written as below representing the diagonal RIS reflection matrix:

$$\Phi = diag(\alpha_1 e^{j\beta_1}, \ldots, \alpha_M e^{j\beta_M}) \tag{2}$$

where each element determines the signal gain of α. The β represent corresponding phase shifts to the UCs. One should note that for a MIMO channel with no RIS, the throughput is determined by the channel matrix $y = Hx$.

In its most simplest form, an RIS can be implemented as a dynamic reflectarray, whose elements are omnidirectional antennas with controllable termination that can be changed dynamically to backscatter and phase shift the incident waveform. A more elaborate implementation would be using a dynamically tunable metasurface, a 2D planar form of metamaterials that has been shown to possess great electromagnetic wave manipulation capabilities. Relying on the metasurface implementation, an RIS element can not only scatter and phase-shift the signal but can also act as an anomalous mirror with a controllable reflection angle and even polarization manipulation abilities.

Now we discuss the main formulas pertaining to the calculation of achievable rate and outage probability by using RIS and machie learning method. There are two approaches from the literature to tackle the problem of optimizing the RIS configuration with limited channel information. The first approach is to forgo channel estimation altogether; instead, the optimization of the RIS can be based on feedback from the receiver. This can be done using a predefined codebook of beam directions; however, the size of the codebook will be proportional to the number of elements.

3. Methods of Channel Modeling Together with Deep Neural Network and RIS

In order to model propagation channels, we are looking for path loss by using RIS-assisted wireless systems. The emitted signal from the transmitter arrives at the receiver as a superposition of multiple signals passing through the channel with RIS and clusters with a controlled feedback link, see Figure 1(a).

The main idea is to consider the statistical properties of scatterers and clusters in the environment. This represents an RIS-aided wireless communication system. We compare the results by mainly using the software QuadriGa with SIMRIS in the MATLAB environment. All these show, how one can model with no limit on the number of antenna elements and a transition between LOS and NLOS scenarios.

3.1. Main Items for Channel Modeling

- LOS and NLOS estimation with scenarios, e.g. UMi (urban microcell), RIS moving with respect to SNR & capacity versus rate is used.
- For beyond 5G, the advent of electromagnetic components can shape interaction with wireless signals along with partial control of the channel propagation [1, 4].
- The frequency range is FR2, 28 GHz covering 5G and 6G and of a channel.

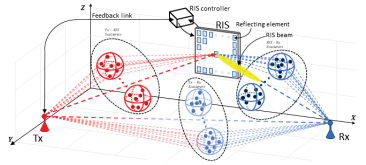

(a) RIS-aided Wireless Communication System

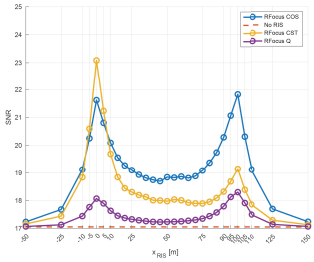

(b) FR2, Teraherz band network & RIS

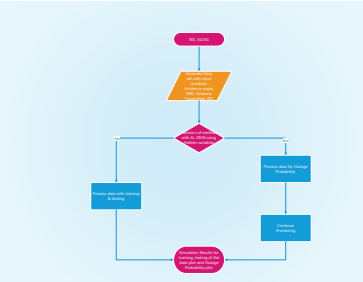

(c) flowchart with DNN

Figure 1.
RIS-simulations.

- A reconfigurable intelligent surface (RIS) is a two-dimensional surface of engineered material with properties not static.
- Input variables: Number of Users, Number of transmit Antennas and Receiving antennas
- Number of RIS elements. In general 30 or 40.
- The downlink bandwidth will be greater than 28-30 GHz, and channel bandwidth is Rayleigh fading
- The model is stationary, and is unsupervised, could be changed to supervised.
- The Optimizer is designed in Matlab with deep learning using the convolutional and deep neural network.
- Number of data symbols as input and the reflection matrix has $\beta = \{0, 1\}$

In Figure 1(b), the RIS position x_{RIS} are varied, and the SNR are measured for COS-UC, Q-UC and CST-UC. RIS is configured by using the ON-OFF algorithm. The powers used are $P_{T_x} = 30$, dBm, and $P_N = -85$, dBm, noise power. $M = \{256, 400\}$, the UCs, and operating frequency is 5.3 GHz. Figure 1(c) and Figure 2(b) provide an idea of the deep neural network implementation. For the validation of CST-UC behaviour, a comparison of free-space scenarios was done by using QRIS with CST-UC and full-wave simulation in CST. It's done by modeling half-wave

Table 1.

Root mean square (RMSE) and DNN performance							
Epoch	**Iteration**	**Time Elapsed**	**Minibatch1**	**Validation1**	**Minibatch2**	**Validation2**	**Base Learning**
1	1	04	142.27	137.37	10120.57	9435.50	$2.1e^{-6}$
4	50	53	55	57.43	1513.89	1655.40	$2.1e^{-6}$
7	100	43	23.30	27.40	271.30	373.80	$2.1e^{-6}$

antenna in CST and then it's imported into QRIS to make the transmitter and receiver behaviour same in both cases.

The R_x power is calculated as below:

$$P_{R_x} = \frac{\lambda^2 P_{T_x} G_{T_x}(\phi_d, \theta_d) G_{R_x}(\phi_a, \theta_a)}{(4\pi)^2 d_{TR}^2} \tag{3}$$

where λ is the wavelength. P_{T_x} is the transmitting power, G_{T_x}, and G_{R_x} are radiation patterns of T_x and R_x respectively. The (ϕ_d, θ_d) and (ϕ_a, θ_a) are the angle of departure and angle of arrival. For the validation, $P_{t_x} = 1$ in Watts both in QRIS and CST. Please see the Figure 2(a).

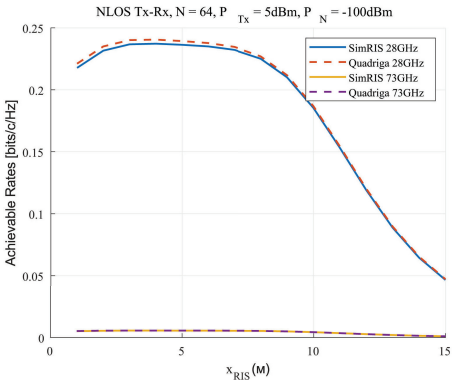

(a) Achievable Rate versus distance

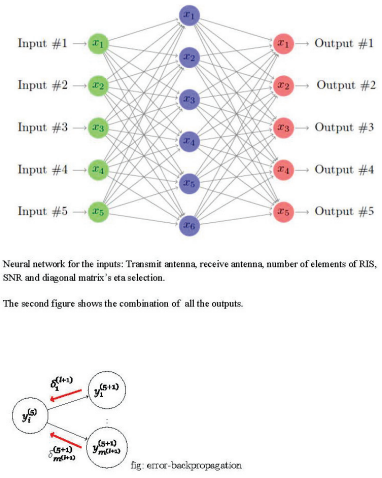

(b) Neural network

Figure 2.
Rates and neural network.

3.2. Simulation with Machine Learning and RIS

To train the network we create different scenarios by using different number of RIS-elements and different number of transit and receive antennas with different number of users, [6]. The physical environment is modeled such that the directions are uniform randomly drawn from the interval $[-\pi, \pi]$. The coefficient β in the diagonal matrix is chosen with permittivity approximately equal to zero. The details of simulations are shown in Table 1.

4. Conclusion & Future Work

Usage of DNNs provides superior estimation accuracy, especially in complex channel conditions used here with typical of millimeter-wave (mmWave) and terahertz (THz) frequencies. The table above shows that the RMSE (Root Mean Square Error) is improved with DNN. RIS approach is used for designing and analyzing RIS-assisted systems, optimizing performance, and understanding of the RIS affect on the overall wireless channel. With no RIS or LIS implies the modeling of the wireless environment which has no additional, programmable element, and uses the traditional channel models that consider only direct or reflected paths between transmitters and receivers, and without the complex phase-shifting and beamforming capabilities of the surface. In this work only one receiver is used and it implies only one user. This work can be extended for several users including obstacles.

Acknowlegement

The author Kumud Singh-Altmayer would like to thank Hitesh Poddar, senior graduate student, New York University for several discussions on millimeter waves.

References

[1] I. Burtakov, A. Kureev, A. Tyarin, E. Khorov, *QRIS: QuadriGa-Based Simulation Platform for Reconfigurable Intelligent Surfaces*, *IEEE Open Access*, vol. 4, 2023.

[2] S. Dorokhin, P. Lysov, V. Lyashev, A. Kunavin1, A. Aderkina1, *RIS-Assisted MIMO Channel Modeling with Spatially Consistent Sparsified Properties*, *Wireless Personal Communications, Springer*, 2024.

[3] Ö. Özdogan, E. Björson, *Deep Learning-based Phase Reconfiguration for Intelligent Reflecting Surfaces*, *arXiv:2009.13988v1*, 2009.

[4] E. Björnson, H. Wymeersch, B. Mattheienen, P. Popovski, L. Sanguinetti, and E. de Carvalho, *Recofigurable Intelligent Surfaces: A Signal Processing Perspective With Wireless Appllications*,*arXiv:2102.00742v2*, 2021.

[5] B. Ozpoyraz, A. T. Dogukan, Y. Gevez,U. Altun, and E. Basar, *Reconfigurable Intelligent Surfaces for Future Wireless Networks: A Channel Modeling Perspective*, *IEEE Open Journal of the Communications Society*, vol. 3, pp. 1749-1809, 2022.

[6] A. Elbir, A. Papazafeiropoulos, P. Kourtessis, and S. Chatzinotas, *Deep Channel Learning For Large Intelligent Surfaces Aided mm-Wave Massive MIMO Systems*, *arXiv:2001.11085v3*, 2020.
[7] R. Faqiri, C. S. Tardiff, G. C. Alexandropoulos, and P. Hougne, *PhysFad: Physics Based End to End Channel Modeling of RIS Parametrized Environments with Adjustable Fading*, *arXiv:2202.02673v1*, 2022.
[8] H. Poddar, S. Ju, D. Shakya and T. S. Rappaport, *A Tutorial on NYUSIM: Sub-Terahertz and Millimeter-Wave Channel Simulator for 5G, 6G and Beyond*, *IEEE Communications Surveys & Tutorials*, December 2023.

Biographies

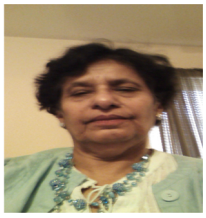

Kumud S. Altmayer did her Ph.D. in Applied Math from Hungarian Academy of Sciences, Budapest, Hungary during 1987. Now, doing research work in the area of channel modeling, signal processing including machine learning with the usage of 5G, and 6G platforms. She completed a master's degree in Electrical Engineering (EE) during the Spring 2024 and she is working on another Ph.D. in Electrical Engineering in a fading channel where the blockage is caused in multipath propagation. The models are designed to develop effective channel prediction with simulation tools.

Ilya Burtakov received the Bachelor degree in applied mathematics and physics from Moscow Institute of Physics and Technology (MIPT) in 2022, and has completed a Master degree in teh year 2024. He joined the Institute for Information Transmission Problems of the Russian Academy of Sciences (IITP RAS) in 2020. His research interests include MIMO, RIS, Channel Estimation, mmWave Communication and prototyping of wireless devices and he is currenty pursuing a Ph.D. degree.

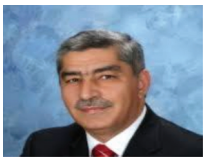

Hussain Al-Rizzo received his Ph.D. in Electrical and Computer Engineering from University of New Brunswick, Canada. In 2000, he joined the Systems Engineering. Department at the University of Arkansas, Little Rock, where he is currently a Professor of Electrical and Computer Engineering. He has published over 300 papers in peer-reviewed journals His publications include journals and conference proceedings, three books, eight book chapters, and four patents. Over the years, he has carried out pioneering research in V2V, V2X, and V2I Wireless Systems; Smart Antennas; Massive MIMO; Flexible RF Components and Antennas; Implantable Medical Devices; Electromagnetic Wave Scattering by Complex Objects; Design, Modelling, and Testing of High-Power Microwave Applicators: Precipitation Effects on Global Positioning System (GPS); Terrestrial and Satellite Frequency Re-Use Communication Systems; Field Operation of NAVSTAR GPS Receivers; Data Processing and Accuracy Assessment; and Effects of the Ionosphere, Troposphere, and Multipath on Code And Carrier-Beat Phase GPS Observations.

Upcoming Events of Interest (Provided by WWRF Members)

Date	Meeting	Location	Theme	WWRF Contact(s)
20 January 2026	WWRF 6G Position Papers Workshop	Online 1300 GMT – https://us02web.zoom.us/j/85983192944?pwd=HVGj6JmUj7NgKuRbulb0BgletXoyzC.1	6G Position Paper	Sudhir Dixit/ Vino Vinodrai/ Hendrik Berndt
Monday March 30–April 1, 2026	WWRF 55	Khalifa University, Abu Dhabi, UAE	TBA	Nigel Jefferies/ Bharat Bhatia/ Sudhir Dixit/Lina Bariah
Septermber 16–17, 2026	WWRF HUDDLE	Istanbul,Türkiye	One Vision – Many Voices	Nigel Jefferies/ Hendrik Berndt/ Vino Vinodrai
27–29 October 2026	WWRF 56	Strathclyde University, Glasgow, UK	TBA	Nigel Jefferies/ Hendrik Berndt/ James Irvine
INVITED AND SPONSORED EVENTS				
Monday, 30 March–Thursday, 2 April, 2026	IEEE International Conference on Machine Learning in Communications and Networking (ICMLCN 2026)	Abu Dhabi, UAE. https://icmlcn2026.ieee-icmlcn.org/	Machine Learning for Communication and Networking (ICMLCN)	Nigel Jefferies/ Hendrik Berndt/ Sudhir Dixit
INTERNATIONAL STANDARDS AND REGULATORY MEETINGS AT WHICH WWRF WILL PARTICIPATE				
Febuary 3–12, 2026	WP5D	Geneva	Meeting 51	Nigel Jefferies/ Bharat Bhatia/Vino Vinodrai
May 5–18, 2026	WP5A & WP5C	Geneva		Nigel Jefferies/ Bharat Bhatia
May 26–June 6, 2026	WP5D	Geneva	Meeting 52	Nigel Jefferies/ Bharat Bhatia/ Vino Vinodrai
November 9–27, 2026	PP-26	Doha, Qatar		Nigel Jefferies/ Bharat Bhatia
November 30–Dec 1, 2026	SG5	Geneva		Nigel Jefferies/ Bharat Bhatia
October 11–18, 2027	Radiocommunication Assembely	Shanghai, China		Nigel Jefferies/ Bharat Bhatia
October 18–November 12, 2027	WRC 2027	Shanghai, China		Nigel Jefferies/ Bharat Bhatia
	CPM 1	Shanghai, China		
19 January–21 January, 2026	FM 56 – Radio Spectrum for Rail	Hybrid/ECO Copenhagen	Spectrum for GSM-R Replacement	Steffen Ring